Functional Characterization of *Minicolumnar* Patterns in the Somatosensory Cortex

Joannellyn Chiu

A dissertation submitted to the faculty of the University of North Carolina at Chapel Hill in partial fulfillment of the requirements for the degree of Doctor of Philosophy in the Department of Biomedical Engineering.

Chapel Hill
2006

Approved by:

Mark A. Tommerdahl, Ph.D.

Robert G. Dennis, Ph.D.

Oleg V. Favorov, Ph.D.

Shawn M. Gomez, Ph.D.

Jeffrey M. Macdonald, Ph. D.

Abstract

Joannellyn Chiu

Functional Characterization of *Minicolumnar* Patterns in the Somatosensory Cortex

(Under the direction of Mark Tommerdahl, PhD)

In the somatosensory cortex, minicolumns have previously been shown to not only be cortical structures, but to be functional entities as well. However, research of their functional role in cortical information processing has been limited. The main focus of the research in this manuscript was to assess and quantify the information processing role of the minicolumn in the evoked cortical response. More specifically, the evoked minicolumnar spatial pattern in SI in a number of stimulus conditions is evaluated. Differences in evoked minicolumnar spatial patterns were examined by evaluation of the change in the stimulus parameters, such as stimulus site location, amplitude, and frequency, needed to evoke a just noticeable difference in the evoked minicolumnar spatial pattern. Through the use of OIS imaging techniques, OIS images for both *in vitro* and *in vivo* assays were collected and analyzed. Data analyses revealed that evoked minicolumnar spatial patterns in SI and the sensorimotor cortical slice do contain information that can be correlated to stimulus conditions, and these evoked minicolumnar patterns are time-dependent, stimulus specific, and reproducible.

Acknowledgment

I would like to thank my family and husband for their constant support and patience, and to give my utmost gratitude to Dr. Tommerdahl for his guidance, invaluable time, and knowledge.

Table of Contents

List of Figures

Chapter 2

Chapter 3

Chapter 4

Chapter 5

List of Abbreviations

SI (Primary somatosensory cortex)
SII (Secondary somatosensory cortex)
RF (Receptive field)
maxRF (Maximum receptitve field)
minRF (Minimum receptive field)
V1 (Primary visual cortex)
IV (Intravenous)
A-P (Anterior-Posterior)
M-L (Medio-Lateral)
ROI (Region of interest)
2-DG (2-deoxyglucose)
OIS (Optical intrinsic signal)
fMRI (Functional magnetic resonance imaging)
MEG (Magnetoencephalography)
EEG (Electroencephalography)
TMS (Transcranial Magnetic Stimulation)
CNS (Central nervous system)
CS (Central sulcus)
WM (White matter)
NMDA (N-methyl-D-aspartic acid)
Ach (Acetylcholine)
Hz (Hertz)
n (number of subjects)
DFT (Discrete Fourier Transform)
2-D (2-Dimensional)
3-D (3-Dimensional)
K+ (Potassium ion)
[K+] (Potassium ion concentration)
NaCl (Sodium Chloride)
mm (millimeters)
µm (micrometers)
nm (nanometers)
sec (seconds)
msec (milliseconds)
hr (hour)
kg (kilogram)
IACUC (Institutional Animal Care and Use Committee)
USPHS (United States Public Health Service**)**
NIH (National Institutes of Health)

Chapter 1 - Overview

This chapter provides a brief introduction and history on cortical minicolumns. The idea of minicolumns was first introduced by Mountcastle in 1969. However, in 1993, through 2-DG experiments, Tommerdahl *et al.* were the first to show that minicolumns were not just cortical structures, but were functional entities as well. Chapter 1 explains what prompted the proposed research and the methods by which further characterization minicolumnar function could be assessed quantitatively.

Introduction

Much of the early research pertaining to cortical information processing, in general, and somatosensory information processing, in particular, was initially guided by the outstanding work of Mountcastle and colleagues in 1969. Through the use of single electrode recording in SI cortex, Mountcastle postulated both the macrocolumn and the minicolumn, functional structures which numerous researchers routinely have used, and still use, in their working hypotheses. However, only a limited number of researchers have presented findings on the nature of the SI population response in terms of patterns of columnar activation.

A minicolumn is a radial cord of cells ~30-50μm in diameter. Sensory stimuli activate local groupings of minicolumns (called “macrocolumns”) which are approximately 300-600μm in size. There are approximately 40-80 minicolumns in a

macrocolumn. Favorov and colleagues have demonstrated that a honeycomb-like pattern ("mosaic") made up of discrete place-defined macrocolumns – "segregates"– in the region of cat and monkey somatosensory cortex which receives input from forelimb skin, also proposed that discrete place-defined macrocolumns are a common mode of topographic organization throughout somatosensory cortex (Favorov *et al.*,1990, 1994a, 1994b). Within such discrete macrocolumns, moving from one minicolumn to the next results in a shift in the receptive fields (RFs), displaying local RF diversity without yielding any overall RF shift across the entire macrocolumn. Only at a border separating adjacent macrocolumns do RFs shift en masse in a single step to a new skin position. Using 2-DG data, Tommerdahl *et al.* have also shown that minicolumns are not just structures in the cortex, but are functional entities (Tommerdahl *et al.*, 1993). However, research to further understand the functional significance and contributions of minicolumns to perceived stimuli in SI has been limited. From Tommerdahl *et al.*'s 2-DG experiment, two questions arose, 1) Can a local group of SI minicolumns express a large range of unique activity patterns which are mutually independent of each other? and 2) Are minicolumnar activity patterns stimulus specific? Therefore, the main objective of the performed *in vitro* and *in vivo* experiments was aimed to answer these questions, and also to determine how minicolumnar patterns contribute to perceived stimuli by attempting to further characterize minicolumnar function.

In order to quantitatively characterize the effects of repetitive stimulation on the spatio-temporal patterns of response in SI cortex, *in vitro* experiments were performed to determine the dependence of minicolumnar activity on cortical connectivity. These *In vitro* studies showed that minicolumnar patterns are a function of cortico-cortico

interactions rather than a function of peripheral receptor activation. Even though sensorimotor cortical slice experiments allow for analysis of all cortical layers, the applied stimuli is un-natural and does not allow for understanding of how the cortex responds to stimuli when all of the cortical connections are still in tact. Therefore, in order to better assess the response to natural stimuli, the evoked spatio-temporal patterns in SI were also examined through *in vivo* experiments.

Optical intrinsic signal (OIS) imaging was utilized in a number of *in vivo* experiments in order to assess minicolumn activity evoked by a number of different stimulus conditions. Although OIS imaging is capable of imaging only the upper cortical layers, layers II/III, it has an advantage over *in vitro* experimentation in that all the cortical connections are still in tact. Previous data examined the changes in evoked patterns of the population response to flutter stimuli in area 3b of the SI cortex, but a more in depth study of these evoked macrocolumnar and minicolumnar patterns have not yet been performed. In order to characterize the evoked spatio-temporal patterns of activity within the responding SI region, OIS images were collected and analyzed using techniques that were able to quantify the differences in the evoked patterns, such as spatial frequency analysis. Additionally, variations within different modes of stimulation, such as stimulus duration, stimulus location, and pre-exposure to a skin stimulus were applied to examine how evoked minicolumnar patterns differed with changes in the stimulus parameters.

Chapter 2

Minicolumnar patterns in the sensorimotor cortical slice

Prior *in vitro* sensorimotor cortical slice experiments show that minicolumnar function remains in tact even when long-range cortical connections had been severed. This chapter gives a detailed explanation of minicolumnar function and minicolumnar properties. It also explains how cortical processing is modular on at least two different scales, macrocolumnar and minicolumnar. A major portion of this chapter has been published, and can be found in "Minicolumnar patterns in the global cortical response to sensory stimulation" in the text "*Neocortical modularity and the cell minicolumn*" (M. Casanova, editor, 2005).

Introduction

In 1978 Mountcastle (Edelman and Mountcastle, 1978) hypothesized that the smallest functional unit of neocortical organization (the "minicolumn") is a radial cord of cells about 30-50μm in diameter, and that sensory stimuli activate local groupings of minicolumns (called "macrocolumns"). This hypothesis subsequently received support from multiple lines of experimental evidence, leading to its substantial elaboration.

Structurally, minicolumns are attributable to the radially-oriented cords of neuronal cell bodies evident in Nissl-stained sections of cerebral cortex. It is likely that

they also are related to ontogenetic columns (Rakic, 1988) and to the radially-oriented modules defined by the clustering of the apical dendrites of pyramidal neurons (Peters and Yilmaz, 1993). Among the various elements of neocortical microarchitecture, *spiny-stellate* cells and *double-bouquet* cells (Jones, 1975, 1981; Lund, 1984) are most directly relevant to Mountcastle's concept of the minicolumn. Spiny-stellates are excitatory intrinsic cells that are especially prominent in layer 4 of primary sensory cortex. They are the major recipients of thalamocortical connections and, in turn, they (especially the star pyramid subclass of spiny-stellates) distribute afferent input radially to cells in other layers. Double-bouquet cells are GABAergic cells whose somas and dendritic trees are confined to the superficial layers. The axons of double-bouquet cells descend in tight 50μm diameter bundles across layers 3 and 4 and into layer 5, making synapses along the way on the distal dendrites of pyramidal and spiny-stellate cells, but avoiding the main shaft of apical dendrites (Jones, 1975, 1981; DeFelipe, 1989, 1992). Because the double-bouquet cells are more likely to inhibit cells in adjacent minicolumns rather than in their own, they offer a mechanism by which a minicolumn can inhibit its immediate neighbors.

Overall, the detailed features of primary sensory cortical microarchitecture are clearly suggestive of a <u>structural</u> substrate for the minicolumns hypothesized by Mountcastle. But it remains unproven that these structurally-defined units act as <u>functional</u> entities – that is, that there is a minicolumnar dimension to primary sensory cortical information processing and representation. In this paper we review some of the experimental evidence that supports the proposal that primary sensory cortical information processing and representation exhibits a minicolumnar nature, and consider

the possible functional utility of this dimension of the primary sensory cortical response to natural stimulation of peripheral receptors.

Minicolumnar Receptive Field Organization

Receptive field (RF) mapping studies carried out in primary somatosensory cortex (SI) of cats and monkeys obtained experimental evidence that strongly supports Mountcastle's minicolumnar hypothesis (Favorov and Whitsel, 1988a; Favorov and Diamond, 1990). These studies found that the receptive fields (RFs) of neurons within fine (~50μm in diameter) radial cords are very similar in size, shape, and position on the skin. In contrast, the same studies found that neurons located in adjacent minicolumns typically have RFs that differ significantly in size and shape, and frequently overlap only minimally on the skin (on average, RFs of neurons in adjacent minicolumns overlap by only 22% in cat, and 28% in macaque monkey). Comparable results have been reported in the primary auditory and visual cortical areas of cat and monkey (Abeles and Goldstein, 1970; Hubel and Wiesel, 1974; Albus, 1975). These findings are schematically summarized in Figure 1.

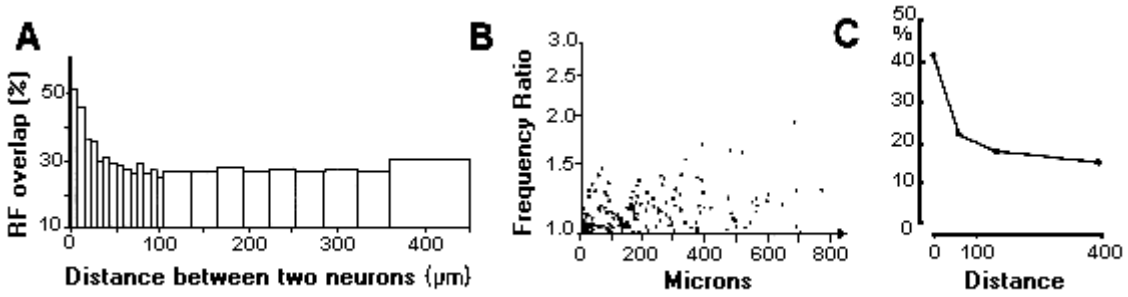

Figure 1. RF similarity as a function of the tangential distance separating neurons in primary sensory cortex. The plots show that neurons that are near neighbors in the tangential plane of the cortex have very similar RF properties, and that similarity declines with increasing distance. The decline in RF similarity with increasing tangential separation has two distinct phases: In the first phase, at separations less than 50μm, average RF similarity declines very quickly with distance; in the second phase, at separations greater than 50μm the rate of decline is much slower. In contrast, neurons with very similar RFs are found at much greater separations in the radial dimesion of sensory cortex – a finding that suggests the presence of radially-oriented strands of cells, <50μm in diameter, within each there is relatively limited RF diversity (see Favorov and Whitsel, 1988a; Favorov and Diamond, 1990 for in-depth discussion). **(A)** Ordinate indicates the average degree of RF overlap of pairs of neurons in somatosensory cortex (reproduced with modifications; from Favorov and Whitsel, 1988a). **(B)** Ordinate indicates the ratio of optimal stimulus frequencies of pairs of cells in auditory cortex (higher frequency/lower frequency; reproduced with permission; from Abeles and Goldstein, 1970). **(C)** The ordinate is the frequency of encountering 2 visual cortical neurons with optimal stimulus orientations differing by less than 7.5^{o} (reproduced with modifications; from Albus, 1975).

Most of the experimental literature that has addressed the topographical organization within the primary somatosensory, visual, auditory, and motor cortical areas (and association cortex as well) at high resolution shows that while neighboring neurons exhibit a remarkable uniformity from the standpoint of some RF property (e.g., stimulus orientation in visual cortex), they tend to differ prominently in other properties (for review see Favorov and Kelly, 1996). In fact, when sensory cortical neuron RF dimensions are considered *in toto*, neighboring neurons typically have little in common – that is, a stimulus optimal for one cell frequently activates its neighbor much less

effectively. The studies reviewed above (Favorov and Whitsel, 1988a; Favorov and Diamond, 1990; Abeles and Goldstein, 1970; Hubel and Wiesel, 1974; Albus, 1975; Merzenich *et al.*, 1981) suggest, however, that this prominent diversity in the receptive field properties of neurons located in the same locale in sensory cortex is constrained substantially in the radial dimension – that is, cells that occupy the same radially-oriented minicolumn have very similar RF properties. In other words, the tendency for the RF properties among neighboring sensory cortical neurons to be different is mainly attributable to the diverse RF properties of neurons that occupy neighboring minicolumns. Figure 2 illustrates the minicolumnar organization of single neuron RF properties that published studies have identified within cat and monkey primary sensory cortex.

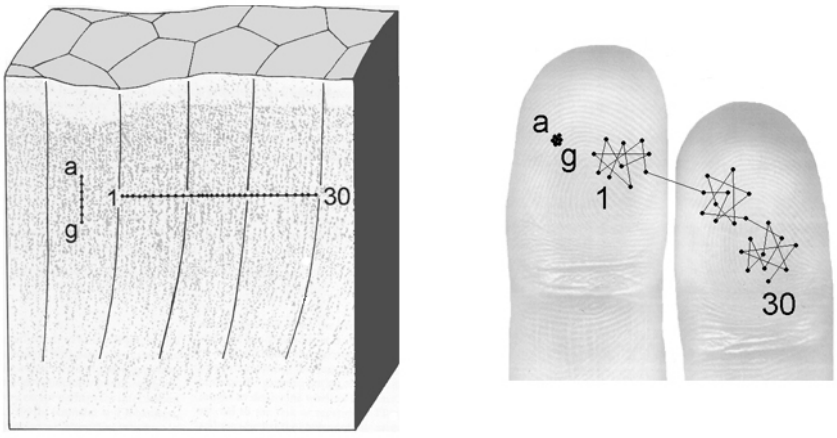

Figure 2. Summary of minicolumnar RF organization in SI somatosensory cortex. **Left:** Drawing of cross-section of Nissl-stained cortical tissue showing darkly-stained cell bodies organized in radially oriented cords, interpreted as minicolumns. Filled circles labeled *a-g* - sequence of neurons located within a single minicolumn; *1-30* - sequence of neurons located in series of adjacent minicolumns. **Right:** Sequences of RF centers (connected dots) mapped by neuron sequences *a-g* and *1-30*. Note that RF centers for SI neurons that occupy the same minicolumn stay close together, whereas the RF centers for pairs of neurons located in neighboring minicolumns shift back and forth over large distances, and occupy totally non-overlapping skin regions when the pair of neurons occupies different SI macrocolumns. Based on Favorov and Whitsel (1988a), and Favorov and Diamond (1990).

Model of Minicolumnar RF Formation

The predominance of radially-oriented intrinsic connectivity within cerebral cortex clearly predicts that cells lying in a particular minicolumn will have very similar RFs. But why are the RFs of neurons in adjacent minicolumns so different? Favorov and Kelly (Favorov and Kelly, 1994a; 1994b) suggested in a modeling study that during perinatal development minicolumns might actively drive their neighbors to establish afferent connections with different, only partially overlapping sets of thalamic neurons. This might be accomplished via the lateral inhibitory interactions among adjacent minicolumns expressed via the connectivity attributable to double-bouquet cells. In the model of Favorov and Kelly (1994a; 1994b shown schematically in Figure 3) each minicolumn is driven during self-organization of the network by inhibitory interactions with adjacent minicolumns (mediated by double-bouquet cells) to acquire a set of afferent (thalamic) connections *different* from those of its immediate neighbors. On the other hand, each minicolumn also is driven by excitatory interactions with neurons in a larger circle of neighboring minicolumns (mediated by spiny-stellate cells) to make its set of afferent connections *similar* to theirs. According to this model these opposing pressures are satisfied by the achievement (during early development) of a permuted arrangement of the minicolumns in the macrocolumn. To achieve this arrangement the RFs of adjacent minicolumns in the macrocolumn move farther apart, and at the same time the RFs of the entire macrocolumn are prevented from diverging too widely. In this way the model of Favorov and Kelly (Favorov and Kelly, 1994a; 1994b) generates complex patterns of RFs across the macrocolumn similar to those observed experimentally in microelectrode

penetrations through SI cortex in adult subjects (Favorov and Diamond, 1990; Favorov and Kelly, 1994a, 1994b).

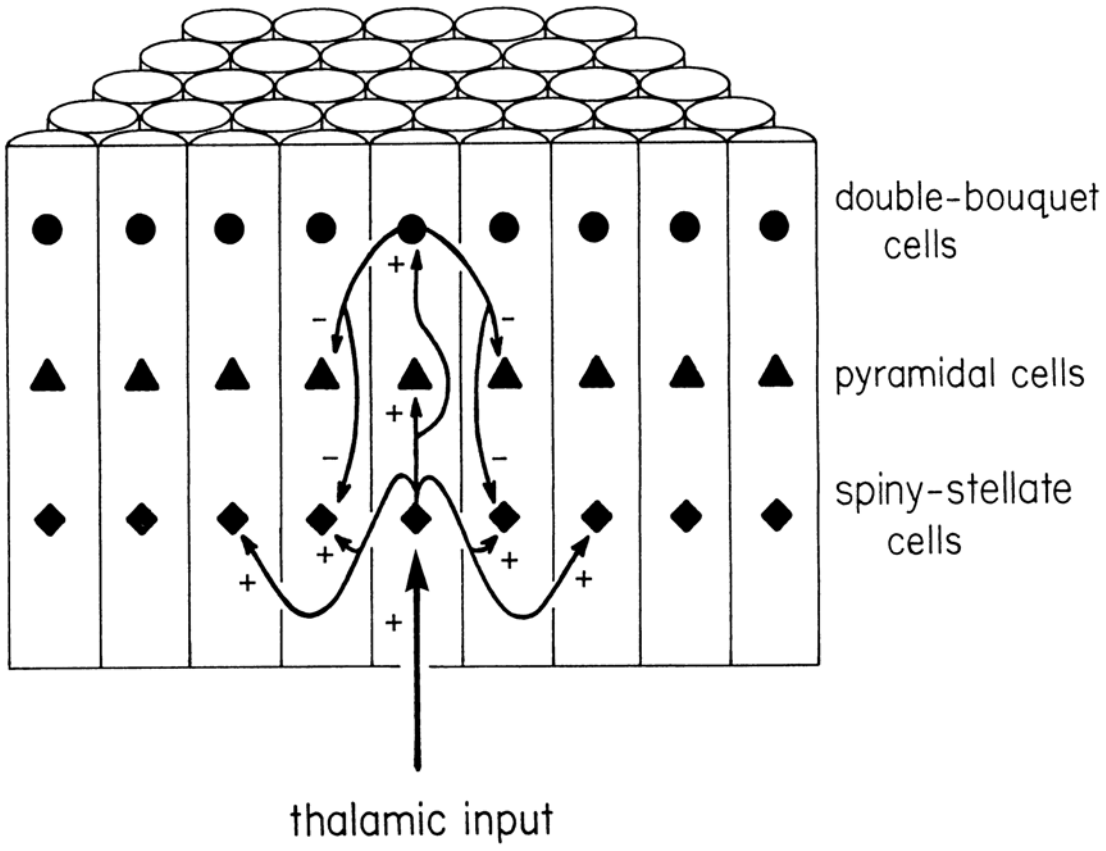

Figure 3. Pattern of minicolumnar connections (modified from Favorov and Kelly (1994a)). Shown is a section across an idealized cortical region, represented as a tightly packed field of cylinder-shaped minicolumns, each containing one representative spiny stellate, pyramidal, and double bouquet cells. Afferent, intra-minicolumnar, and local inter-minicolumnar connections are shown for one minicolumn.

In Vivo Stimulus-Evoked Minicolumnar Activity Patterns

Because of the prominent differences in RF properties that exist among neighboring minicolumns in sensory cortex in adults, even the simplest sensory stimulus should evoke a spatially complex minicolumnar pattern of activity in the engaged cortical

region – such a pattern consisting of a patchwork of active and inactive minicolumns (Favorov and Kelly, 1994b). This expectation is in accord with experimental observations obtained in high-resolution 2-deoxyglucose (2-DG) metabolic studies of mouse (barrel field) and monkey SI (Tommerdahl *et al.*, 1987, 1993; McCasland and Woolsey, 1988). Those studies revealed not only that the distribution of stimulus-evoked 2-DG labeling in somatosensory cortex is modular on a macrocolumnar scale, but is highly non-uniform within such a macrocolumnar module. Analysis of the spatial distribution of activity within the characteristic column-shaped patches of 2-DG label evoked in primary somatosensory cortex by natural skin stimuli suggested that such patches are made up of groupings of highly active minicolumns interdigitated with less active minicolumns. The experimental evidence that led the authors to propose this concept is summarized in Figure 4.

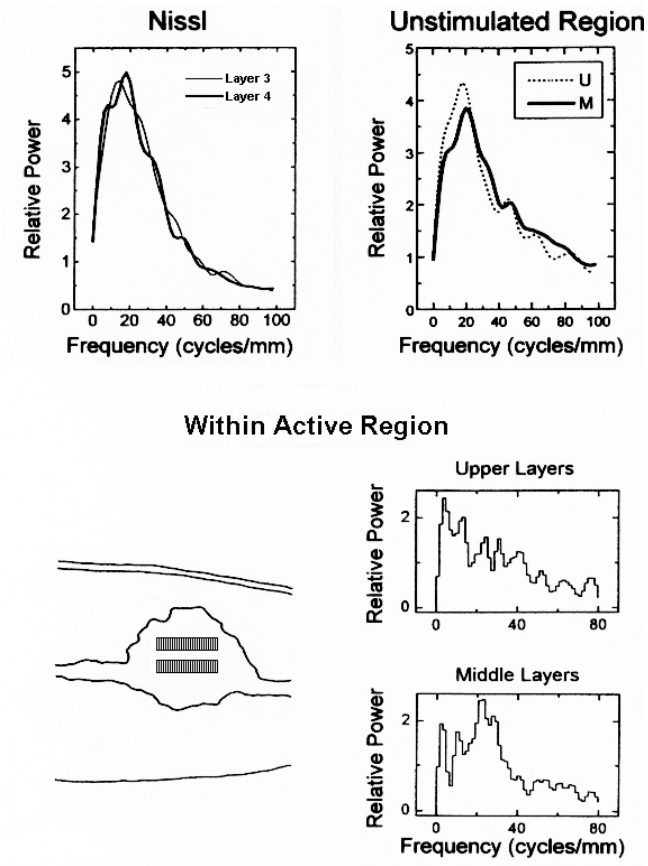

Figure 4. Minicolumnar pattern of stimulus-evoked activation in monkey SI cortex: Spatial frequency analysis of stimulus-evoked 2-DG labeling (modified from Tommerdahl *et al.*, 1993). Discrete Fourier transforms were computed across linear, tangentially-oriented sectors of middle and upper cortical layers, and plotted as periodograms. **Top-left:** Average periodograms for optical density data sampled from Nissl-stained sections of SI cortex. Note that distribution of spatial frequencies is the same in the upper and middle layers, and that the radial striation of Nissl-stained sections is reflected by the prominent peak near the minicolumnar frequency of 20 cycles/mm. **Top-right:** Average periodograms of 2-DG labeling in an unstimulated region of SI. Note close similarity of periodograms for 2-DG labeling to those obtained from Nissl-stained sections: both demonstrate prominent minicolumnar periodicity of 20 cycles/mm. **Bottom:** Outline of a patch of above-background 2-DG labeling in a section through stimulus-activated SI region. Fourier transforms were computed across the two rectangular regions and plotted as periodograms on the right. Note that the periodogram of the middle layers is similar to those obtained from both the unstimulated region and the Nissl-stained sections, in that its peak is near to the minicolumnar frequency. In contrast, in the upper-layer periodogram the peak is prominently shifted to lower spatial frequencies, indicating that in the upper layers the activated SI column consists of interdigitated radial strands of elevated and near-background 2-DG labeling. This outcome suggests that neighboring minicolumns were differentially activated by the stimuli that were used.

More recently our laboratory has employed a very different imaging modality to continue our investigation of the response of primary somatosensory cortex at the minicolumnar level of resolution – in these studies we used near-infrared (830 nm) imaging of the optical intrinsic signal (OIS) evoked by mechanical stimulation of the skin (Tommerdahl *et al.*, 1999, 2002). The spatial resolution of this imaging method is fine enough to enable direct visualization of stimulus-evoked patterns of active/inactive minicolumns in local cortical territories viewed from above. An example of such a minicolumnar activity pattern within SI cortex of the cat is shown in Figure 5.

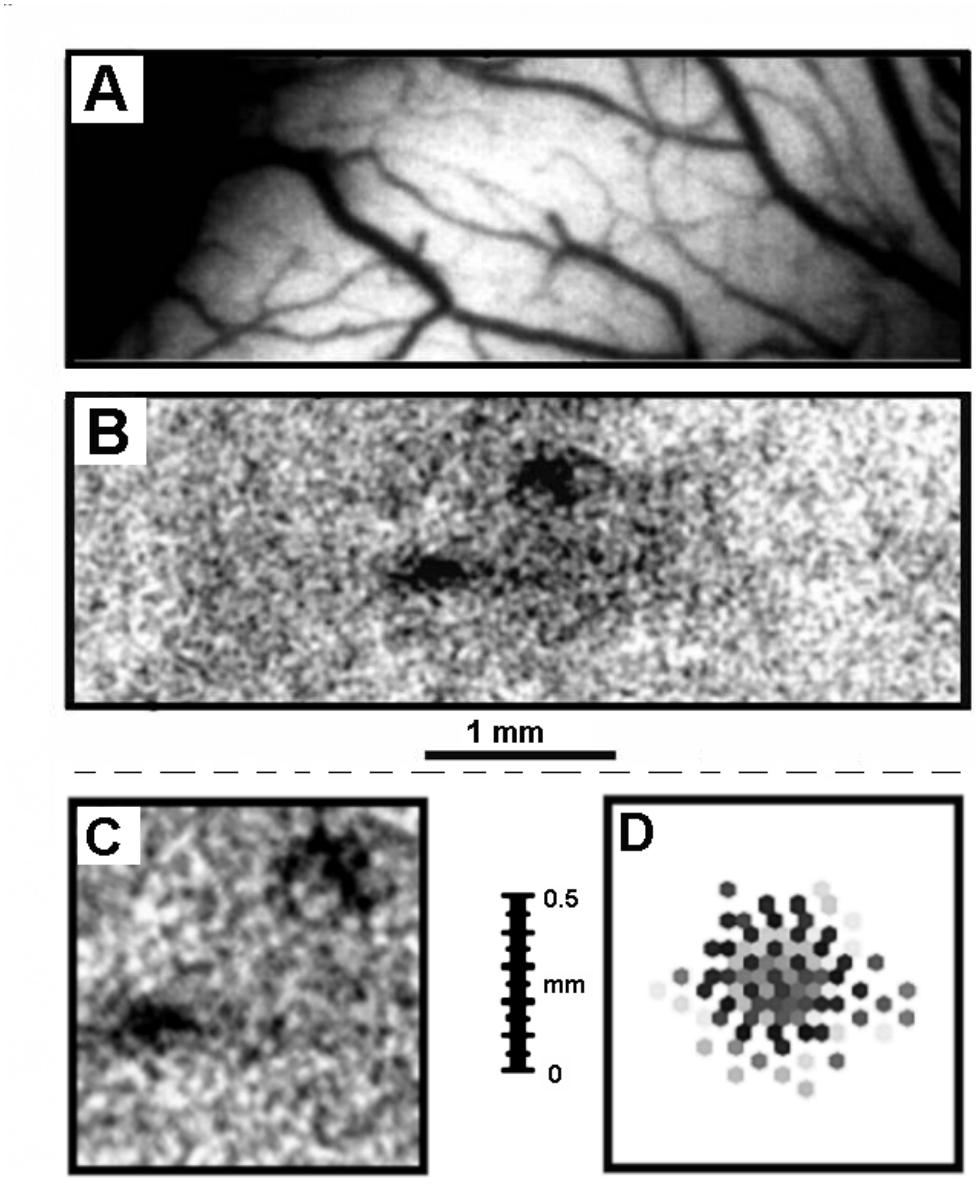

Figure 5. Minicolumnar pattern of activation in cat SI cortex: OIS imaging of the stimulus-evoked intrinsic signal (**B** & **C**) and modeling prediction (**D**). The response in B and C was evoked by 400 μm amplitude 25 Hz vibrotactile stimulation of the ulnar eminence on a contralateral foreleg. Image in B shows two activated cortical regions, the bottom one in area 3b, top one in area 3a. Upon closer inspection shown in C, each active region appears to consist of a patchwork of minicolumn-sized spots. Note that the spots tend to be organized in short parallel strings, and that orientation of the strings varies across the activated region. Image in D was generated by the minicolumnar model of Favorov and Kelly (1994a, 1994b). It shows a spatial pattern of active minicolumns, driven by a punctate stimulus. This model-generated pattern is similar to the one on the left in that minicolumns activated by the stimulus are also organized in short parallel strings which run in different directions in different parts of the pattern.

The optical intrinsic signal (OIS) is an activity-dependent change in the light scattering properties of neural tissue. Although both the OIS evoked in cortical tissue by natural stimulation and the OIS evoked in a cortical slice by electrical stimulation co-localize with stimulus-evoked neuronal activity, and increase in magnitude with increasing stimulus intensity, the OIS recorded *in vivo* or *in vitro* is primarily non-neuronal in origin. That is, the OIS mainly reflects the changes in the extracellular space and cell swelling attributable to glia and neurons. Specifically, repetitive activity in a neuronal population leads to a local excess of potassium and glutamate in the extracellular space that, after a brief delay, is restored to normal by the surrounding glia. The movement of potassium from the extracellular space into glial cells (via ion pumps, transporters and channels), is accompanied by glial uptake of water and swelling. The resultant decrease in extracellular space causes the stimulus-activated region in a brain slice to increase its light transmittance, and the stimulus-activated region in the cortex of an intact subject to undergo an increase in light absorbance. Since the glial swelling that results from uptake of the activity-related excesses in extracellular potassium and glutamate are highly correlated with the degree and spatial extent of neuronal activity, the change in light transmittance *in vitro* can be used to characterize the spatial characteristics of the distributed response of the neocortical slice to controlled afferent drive, and the increase in absorbance observed *in vivo* can be used to evaluate the spatially distributed response of the intact sensory cortex to natural skin stimulation.

In Vitro Stimulus-Evoked Minicolumnar Activity Patterns

Optical imaging has been used extensively to study the global patterns of response to natural tactile stimulation (Tommerdahl *et al.*, 1999, 2002; Chen *et al.*, 2003; Shoham and Grinvald, 2001). However, only a few studies have evaluated the minicolumnar patterns of activity evoked by skin stimulation (e.g., Figure 5). I*n vitro* studies of the sensory cortical response to controlled afferent drive at the minicolumnar level of resolution are also relatively rare, but the few studied of this type that have been carried out have provided observations that make it evident that the column-shaped SI response evoked by stimulation at layer VI/WM border is not spatially homogenous (Figure 6). Instead, spatial frequency analysis revealed that although all minicolumns are activated at the level of the cortex at which most direct thalamocortical afferents terminate (i.e., layer IV), at more superficial levels (in layers II-III) activated groupings of minicolumns in the responding macrocolumn are separated from one another by less active minicolumns (Khon *et al.*, 1997).

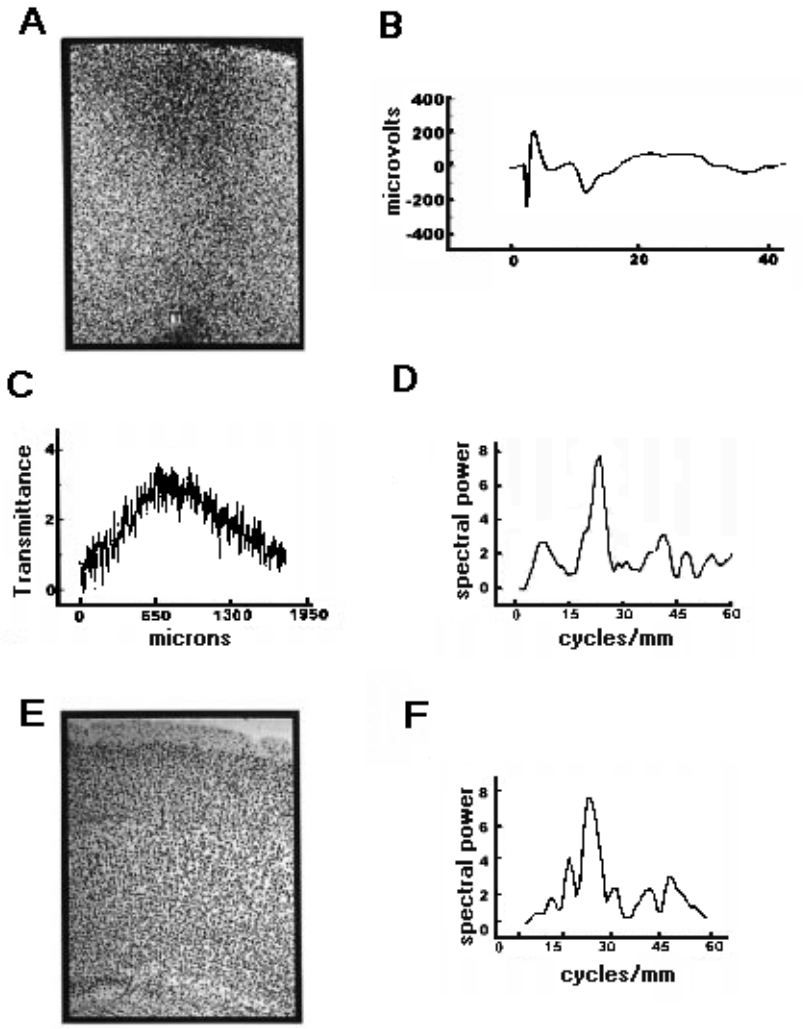

Figure 6. Measures of OIS minicolumnar SI activity patterns *in vitro* in rat somatosensory cortical slice preparation. **(A)** Image of column-shaped OIS evoked by a threshold pulse stimulus delivered to the layer VI/WM junction. **(B)** Evoked potential evoked from the same layer VI/WM locus by single pulse at same intensity. **(**C**)** Spatial intensity histogram obtained by averaging all pixel values sampled radially across middle layers. **(D)** Power spectrum of the spatial intensity histogram in C. Note a prominent peak at approximately minicolumnar frequency of 24 cycles/mm, or 42 μm period, as well as a second peak at ~8 cycles/mm. **(E)** Image of a Nissl-stained section from the same slice that yielded the OIS response in A. **(F)** Power spectrum of the distribution of optical densities in layer IV of the Nissl-stained section. Note the presence of a peak at the minicolumnar frequency, but not at the frequency of ~8 cycles/mm. This difference in power spectra of OIS and Nissl images suggests that the stimulus activated the cortical macrocolumn non-uniformly, preferentially driving on average every third minicolumn.

The above-described spatial variations in OIS intensity indicate the presence of a repeating radially-oriented structure within layer IV of the responding column with a center-to-center spacing equal to that of the cortical minicolumn. That these spatial variations correspond to activated minicolumns is supported by the observation that no change in spatial frequency occurred in the radial direction**.** More recently, we have investigated the patterns of SI minicolumnar activation detected under different stimulus conditions *in vitro*. Figure 7 exemplifies the influence of increasing stimulus intensity of electrical stimulation in the sensorimotor cortical slice on the spectral content of the stimulus evoked OIS.

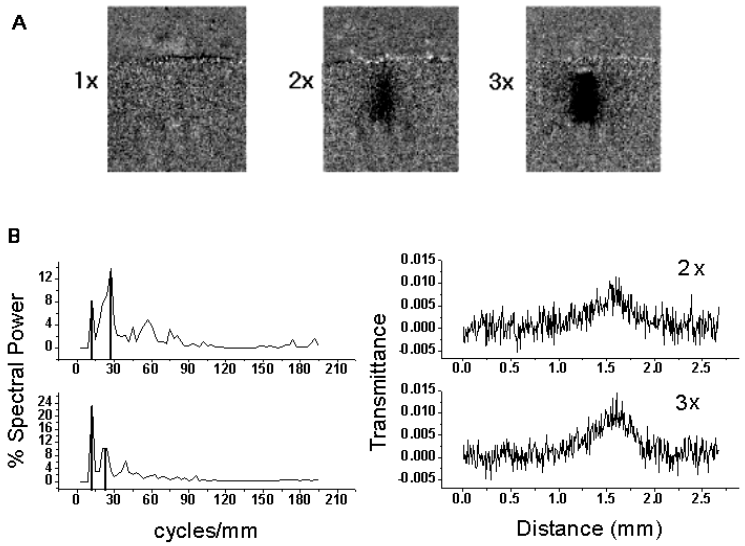

Figure 7. Stimulus intensity influences the pattern of minicolumnar activity within the responding SI macrocolumn. **A**: 3 OIS images obtained in response to 3 different intensities of stimulation (1x, 2x and 3x threshold) delivered to the layer VI/WM junction. **B**: **Left column:** Power spectra of OIS activity across the columnar response evoked by stimuli of two different intensities (2x and 3x threshold). **Right Column:** Histograms showing spatial distribution of the response at each stimulus intensity. Note that at both stimulus intensities the spectrum contains two peaks – one at the minicolumnar frequency of 25 cycles/mm, or 40 μm period, the other at 13 cycles/mm, or 80μm period. However, the relative powers of these two peaks change with stimulus intensity, with 13 cycles/mm frequency growing in power at stronger stimulus.

While prominent power is observed at the minicolumnar spatial frequency (~25 cycles/mm) when using relatively low intensities of layer VI/WM stimulation, a consistent leftward shift in the power spectrum occurs when higher intensities of stimulation are used. We interpret this enhanced low-frequency component at higher intensities of stimulation to be a result of increased local lateral interactions among minicolumns, resulting in significant numbers of minicolumns becoming inhibited, or "turned off," by their neighbors.

We also have initiated an examination of the patterns of SI minicolumnar activity evoked by multi-site afferent drive more representative of the spatially distributed input patterns evoked *in vivo* by natural skin stimuli. Figure 8 demonstrates a method which provides detailed information about this more complex, but probably much more realistic pattern of afferent drive. Arrays consisting of 3-5 electrodes placed at the layer VI/WM junction were used to deliver input to the SI slice. In the example shown in Figure 8, the stimulus intensity in the central electrode was maintained at threshold while the intensity at the 2 electrodes positioned to either side of the central electrode were systematically modified.

While the observations obtained to date in our *in vitro* studies are preliminary, they clearly indicate that competitive (inhibitory) minicolumnar interactions leading to a "checkerboard-like" interleaved pattern of local groupings of activated and non-activated minicolumns occurs under 2 conditions: (1) when the afferent drive evoked by a single electrode placed at VI/WM border is strong; and (2) when the minicolumns within a large cortical territory receive simultaneous, equal-intensity (suprathreshold) afferent drives from a linear array of layer VI/WM sites. On the other hand, when the afferent drive

provided at the same multiple layer VI/WM sites is unequal (for example, the 4x-1x-4x condition in Figure 8) activity in the minicolumns within the weakly-driven macrocolumn is suppressed by lateral inhibitory influences arising in the neighboring, more strongly activated macrocolumns.

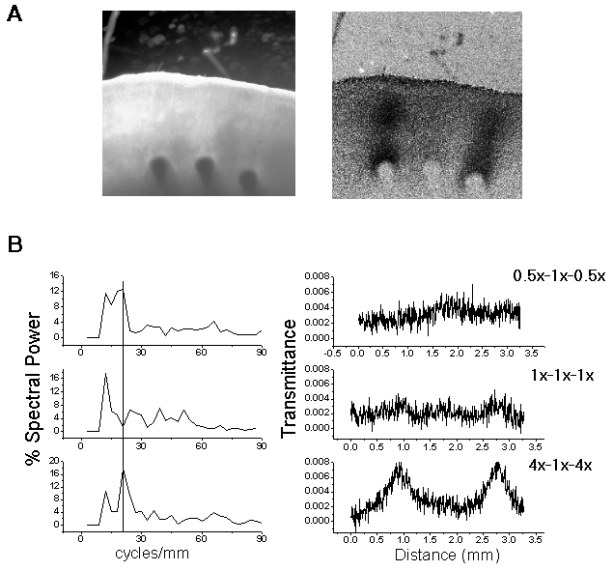

Figure 8. Lateral influence of adjacent cortical territories on stimulus-evoked minicolumnar activity patterns. In this experiment, threshold for each stimulating electrode was set independently. Responses shown in this figure were those obtained when stimuli of the indicated intensities (1x = threshold) were delivered at each of the electrodes simultaneously. **(A) Left panel:** Image of a neocortical slice with 3 stimulating bipolar electrodes located at layer VI/white matter border. **Right panel:** OIS image evoked by all three stimulating electrodes simultaneously. For this particular response the stimulus condition used was 4x threshold intensity at the left electrode, 1x threshold at the central electrode, and 4x threshold at the right electrode (denoted by 4x-1x-4x). **(B)** Stimulus conditions are denoted at far right. **Right column:** Spatial intensity histograms obtained by sampling OIS data tangentially across the region of slice activated by the three electrodes**. Left column:** Power spectra of the spatial intensity histograms sampled above the central stimulating electrode. Note the presence of a peak at the minicolumnar frequency of ~21 cycles/mm (48 μm period) under 0.5x-1x-0.5x and 4x-1x-4x stimulus conditions, and another peak at lower spatial frequency of 12 cycles/mm (83 μm period) under all three stimulus conditions. The relative magnitudes of these two peaks vary depending on the stimulus conditions. In particular, the minicolumnar frequency peak completely disappears when a larger cortical region is driven by the stimulus (1x-1x-1x), even though the stimulus intensity here is near threshold, which in the case of single-electrode stimulation produces a prominent peak at the minicolumnar frequency (see for example Figure 7).

Discussion

What picture of sensory information processing in somatosensory cortex has emerged from the studies reviewed in this paper? Most fundamentally, it is apparent that cortical processing is modular on at least two different scales, macrocolumnar and minicolumnar.

With regard to macrocolumns, according to Favorov *et al.* (Favorov and Whitsel, 1988a; Favorov and Diamond, 1990; Tommerdahl *et al.*, 1987), the mystacial vibrissa region of rodent somatosensory cortex is not unique in being organized as a mosaic of discrete macrocolumns; i.e., barrel-based columns. Favorov and colleagues demonstrated a similar honeycomb-like pattern made up of discrete place-defined macrocolumns – "segregates" – in the region of cat and monkey somatosensory cortex that receives input from forelimb skin, and proposed that discrete place-defined macrocolumns are a common mode of topographic organization throughout somatosensory cortex. Within such discrete macrocolumns, as one move from one minicolumn to the next, the RFs of neurons shift back and forth on the skin, displaying local RF diversity without yielding any overall RF shift across the entire macrocolumn. Only at a border separating adjacent macrocolumns do RFs shift en masse in a single step to a new skin position (see Figure 2 for a graphic illustration).

The studies of Pearson *et al.* (1987), Montague *et al.*. (1991), Senft and Woolsey (1991), and Xing and Gerstein (1996) suggest that such discrete macrocolumns – either barrels or segregates – emerge during perinatal development when small (0.3-0.5 mm diameter) cortical regions become innervated each by a selected group of thalamic neurons, sharing similar RFs, whose axons all terminate extensively throughout the

territory of that macrocolumn. Within a macrocolumn, according to Favorov and Kelly (1994a), thalamocortical axons do not connect to all the minicolumns uniformly, but connect selectively so that each minicolumn receives afferent connections from a unique subset of the thalamic neurons projecting to that macrocolumn. The differences in afferent inputs to neighboring minicolumns in a macrocolumn are further amplified by lateral inhibitory interactions among adjacent minicolumns. As a result, in response to a tactile stimulus (even a simple punctate stimulus), an activated macrocolumn generates a complex, spatially heterogeneous pattern of activity that consists of active minicolumns interdigitated throughout the macrocolumn with much less active minicolumns. Furthermore, tactile stimuli, even the most spatially restricted ones, usually activate not a single macrocolumn but a local group of macrocolumns (Tommerdahl *et al.*, 1993). Each macrocolumn in such an active group generates its own pattern of minicolumnar activation. Thus, the SI response to a skin stimulus takes the form of a patchwork of active minicolumns that extends across multiple macrocolumns (as illustrated in Figure 5). The Favorov and Kelly model predicts that the richly-detailed spatiointensive minicolumnar patterns evoked by tactile stimuli should be very stimulus-specific, exhibiting exquisite sensitivity to stimulus location, shape, and temporal characteristics (such as direction of motion for moving stimuli). One demonstration of such sensitivity is provided in Figure 9.

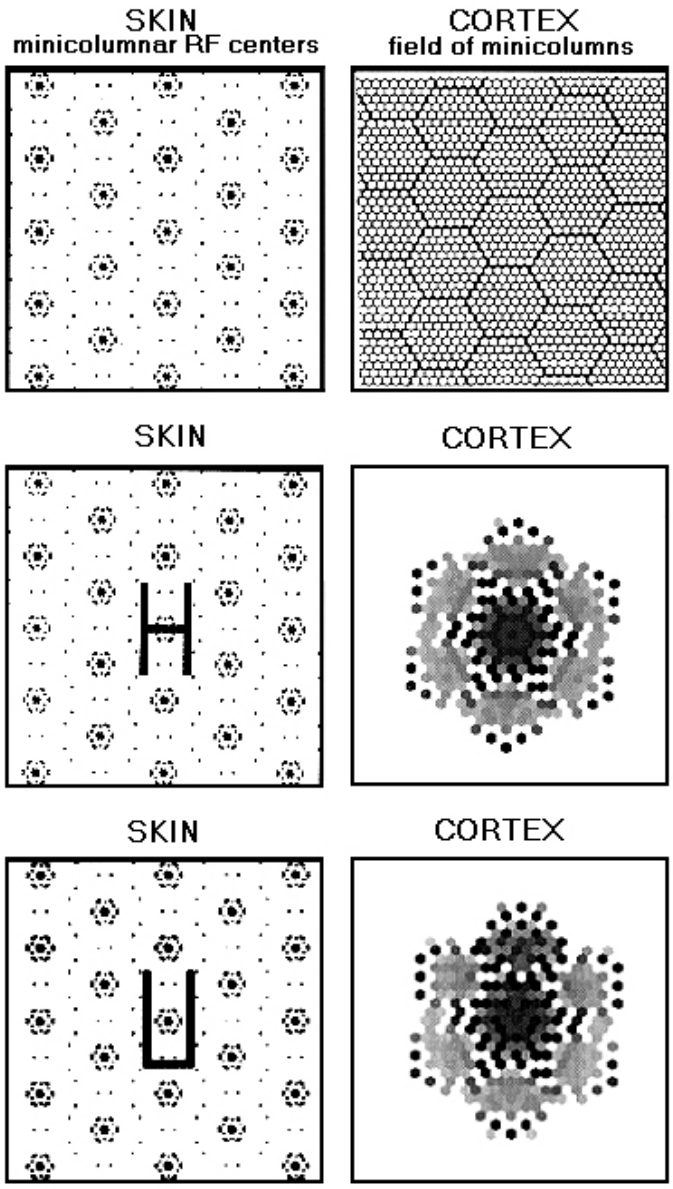

Figure 9. Minicolumnar activity patterns generated by Favorov and Kelly (1994a, 1994b) model in response to spatially detailed stimulus patterns in a shape of letters H and U. **Top row:** on the right, the field of minicolumns (small hexagons) organized into larger groups, macrocolumns (large hexagons). On the left, locations on the model skin of the RF centers (dots) of the minicolumns shown in the right panel. **Middle row:** on the left, the shape and location on the skin of the stimulus pattern. On the right, the pattern of activities evoked by the stimulus in the minicolumns (activity level is grayscale-coded from white – no activity – to black – maximal activity). **Bottom row:** minicolumnar response pattern evoked by another stimulus. Note the prominent differences in spatial details of the two minicolumnar activity patterns *throughout* the activated cortical field, despite the fact that the two stimuli were quite similar to each other (the change from H to U is merely a small downward shift of the horizontal bar).

In conclusion, while the subject of the existence and functional significance of minicolumns has received relatively little experimental exploration, primarily due to profound technological difficulties associated with addressing it, the combination of experimental and modeling studies reviewed in this paper suggest that cortical networks respond to sensory stimulation with spatially complex patterns of differentially activated minicolumns. An intriguing possibility is that such spatial patterns of activities among minicolumns in an activated cortical field might function to encode highly detailed information about stimulus properties such as, for example, its location, motion, and various spatiotemporal features.

Chapter 3

Amplitude dependent minicolumnar spatial patterns of response in SI cortex

As shown in chapter 2, minicolumnar function mostly relies on cortico-cortico interactions, rather than from receptor/afferent inputs. Even though all layers of the cortex can be analyzed using the sensorimotor cortical slice, *in vitro*, however, connections are severed, and it is difficult to fully assess cortico-cortico interactions. Stimuli applied to the slice is also very un-natural. The main idea is that changes in stimulus parameters, such as stimulus intensity, will yield changes in the stimulus evoked spatio-temporal patterns in SI. A major portion of chapter 3 has been published, and can be found in "Stimulus-dependent spatial patterns of response" in *BMC Neuroscience* (Chiu *et al*., 2005).

Chapter Abstract

Background: Recently we reported that vibrotactile flutter stimulation of a skin locus at different amplitudes evokes an optical response confined to the same local region of the primary somatosensory cortex (SI), where its overall magnitude varies proportionally to the flutter amplitude. In this report, we characterize the impact of the flutter amplitude on the spatial patterns of activity evoked within the responding SI region.

Results: In order to characterize the spatial pattern of activity within the responding SI region, images of the flutter-evoked SI optical response were segmented and analyzed with spatial frequency analysis. The analysis revealed that: (1) dominant spatial frequencies in the optical intrinsic signal emerge within the responding SI region within 3-5sec of stimulus onset; (2) the stimulus-evoked activity is spatially organized in a form of several roughly parallel, anterior-posteriorly extended waves, spaced 0.4-0.5 mm apart; (3) the waves themselves exhibit spatial periodicities along their long axis; and (4) depending on the flutter stimulus amplitude, these periodicities can range from fine 0.15mm "ripples" at 50μm amplitude to well-developed 0.5mm fluctuations at the amplitude of 400μm.

Conclusions: The observed spatiointensive fractionation on a sub-macrocolumnar scale of the SI response to skin stimulation might be the product of local competitive interactions within the stimulus-activated SI region and may be a feature that could yield novel insights into the functional interactions that take place in SI cortex.

Background

Afferent projections from skin to primary somatosensory cortex (SI) are well known to form a fine map of the body surface in SI. In this map, a skin locus provides afferent input to an extensive cortical region in SI (Favorov and Whitsel, 1988a; Favorov and Whitsel, 1988b). In particular, the direct connectivity between somatosensory thalamus and SI cortex is now recognized to be much more spatially distributed than previously believed (e.g., in primates the ventrobasal thalamic region which receives its input from a single digit projects to an extensive, 20mm^2 sector of SI cortex – (Rausell *et*

al., 1998; Jones, 2000)). The intrinsic SI excitatory connections link not only neighboring but also widely separated regions of somatosensory cortex (Burton and Fabri, 1995). These connections ensure that many members of widely distributed neuronal populations interact extensively within milliseconds after the onset of stimulus-evoked thalamocortical drive. Thus it is not surprising to find that the processing of even a very local skin stimulus is associated with SI activation over several sq. millimeters of cortical area, as revealed, for example, with optical imaging techniques (Tommerdahl *et al*., 1998; Tommerdahl *et al*., 1999a; Chen *et al*., 2001; Shoham and Grinvald, 2001; Tommerdahl *et al*., 2002).

Such spatially extensive cortical regions are not functionally homogeneous. For example, using Optical Intrinsic Signal (OIS) imaging in near-infrared (830nm) range, we find that in squirrel monkeys a small-diameter stimulus probe oscillating on the skin at 25Hz activates more than 3 mm^2 of cortical territory in area 3b of SI (Tommerdahl *et al*., 1998; Tommerdahl *et al*., 1999a; Tommerdahl *et al*., 2002). Such a territory can contain as many as 20 place-defined cortical columns ("segregates"; (Favorov and Diamond, 1990)) organized into 4-6 alternating rapidly- and slowly-adapting submodality bands (Sur *et al*., 1984). Chen *et al*. (Chen *et al*., 2001) reported that the relative magnitudes of optical response in local, 0.2-0.4mm wide, SI regions changes when the frequency of the stimulating probe is changed from simple taps to 25Hz to 200Hz (thus preferentially activating different submodalities of skin mechanoreceptors). And on even finer spatial scale SI might be organized in ~50μm-diameter functionally distinct minicolumns (Tommerdahl *et al*., 1987; Favorov and Whitsel, 1988a; Favorov and

Diamond, 1990; Tommerdahl *et al*., 1993; Kohn *et al*., 1997; Buxhoeveden *et al*., 2000; Tommerdahl *et al*., 2004).

Together these considerations suggest that the spatial pattern of activity evoked in SI by even the smallest stimuli might be structurally more complex than a typically envisioned basic bell-shaped pattern. A closer inspection of such patterns might reveal certain spatial formations within them with significant functional implications. Recently, we investigated the response of SI cortex to varying amplitudes of flutter stimulation. Regardless of the amplitude of stimulation (in the range of 50 to 400 μm), we found that the spatial extent of the response of SI cortex remained the same (Simons *et al*., 2005). Instead, the actuated cortical region exhibits increases in its magnitude of neuronal response proportional to the intensity of stimulation (Sheth *et al*., 1998; Chen *et al*., 2003; Simons *et al*., 2005). One feature of particular interest in our study was that the activity patterns evoked within these spatially delineated regions, when viewed at high resolution, appeared to develop in an orderly manner dependent on stimulus amplitude. The purpose of this study was to determine if those patterns are indeed systematic, and if so, to characterize them quantitatively.

Methods

All methods and procedures are consistent with USPHS policies and guidelines on animal care and welfare in biomedical research, and were reviewed and approved in advance by an institutional animal use committee (IACUC). Experiments were conducted in 5 squirrel monkeys. Surgical procedures were carried out under deep general anesthesia (1-4% halothane in a 50/50 mixture of oxygen and nitrous oxide).

After induction of anesthesia the trachea was intubated to facilitate positive pressure ventilation and delivery of the gaseous general anesthetic. A catheter was inserted into a branch of the femoral vein of the hindlimb ipsilateral to the hemisphere to be imaged, allowing intravenous (IV) administration of drugs and fluids (5% dextrose and 0.9% NaCl). Methylprednisolone sodium succinate (20 mg/kg) and gentamicin sulfate (2.5 mg/kg) were injected intramuscularly to lessen the probability of halothane-induced cerebral edema and prevent bacterial septicemia, respectively.

A 1.5cm diameter opening in the skull exposed the forelimb region of SI cortex. A recording chamber was positioned over the opening and cemented to the skull with dental acrylic. The chamber was filled with artificial cerebrospinal fluid, the dura mater overlying SI cortex incised and removed, and all wound margins outside the chamber dressed with long-lasting local anesthetic in oil (Cetacaine). All skin and muscle incisions were closed with sutures and bandaged.

After the completion of all surgical procedures subjects were immobilized with Norcuron (vercuronium bromide; 0.5mg/kg loading dose; 0. 25-0.5 mg/kg/hr maintenance dose) and ventilated with a gas mixture (a 50/50 mix of oxygen and nitrous oxide; supplemented with 0.5-1.0% halothane). At these concentrations and under normocapnic conditions, halothane has no effect on brain energy metabolism (Fujibayashi *et al*., 1994; Hess *et al*., 2000), and only minor effects on cerebrovascular regulation (Burdett *et al*., 1995). Ventilator rate and volume were adjusted to maintain end-tidal CO_2 between 3.0-4.0%. EEG and cardiovascular signs (EEG slow wave content; EKG and heart rate) were monitored continuously, and the anesthetic gas mixture adjusted intermittently to maintain values and reactivity to skin stimuli consistent with

light general anesthesia. Rectal temperature was maintained (using a heating pad) at 37.5°C.

The recording chamber was filled with artificial cerebrospinal fluid and hydraulically sealed using a clear glass plate. Vibrotactile stimuli were delivered to selected loci on the hand using a servocontrolled vibrotactile stimulator (Chubbuck, 1966), capable of delivering precisely controlled sinusoidal vertical skin displacement stimuli. The stimulator made contact with the skin via a cylindrical 2mm-diameter Delrin probe. All sinusoidal vibrotactile stimuli were superimposed on a static displacement ("pedestal") of 500μm. Identical parameters of stimulation were used at each skin site that was studied: frequency of vibration 25Hz (in the flutter range), stimulus duration 7sec, and interstimulus interval 60sec. Different peak-to-peak amplitudes of flutter stimulation (0, 50, 100, 200 and 400μm) were interleaved on a trial-by-trial basis.

The optical imaging system consisted of a computer-interfaced CCD camera, light source, guide and filters required for near-infrared (830nm) illumination of the cortical surface, a focusing device, and a recording chamber capped by an optical window (for additional methodological details see (Tommerdahl, 1999a, 1999b). Images of the exposed cortical surface were acquired 200ms before stimulus onset ("reference" or "prestimulus" images) and continuously thereafter ("poststimulus" images; at a resolution of one image/s) for 15s following stimulus onset. Exposure time was 200ms. Light absorbance images were generated by subtracting each prestimulus (reference) image from a poststimulus image and subsequently dividing by the reference image. Absorbance images obtained in this way typically show regions in which light absorption increases and other regions in which absorption decreases in response to skin stimulation.

These regions, respectively, have been shown to correspond to regions in which neuronal activity increases and decreases in response to sensory stimulation ((Grinvald, 1985; Grinvald *et al*., 1991; Grinvald *et al*., 1994; Tommerdahl *et al*., 1996; Tommerdahl *et al*., 1998); for review see (Ebner and Chen, 1995)). Stimulus-evoked OIS responses of SI were displayed as either grayscale images or 3-D surface plots. To reduce amount of noise in these displays, the images were smoothed using a 3x3 pixel boxcar filter.

Cortical images were taken at light/time exposures that place the region of interest in the middle of the range of the recorded pixel values. Histogram analysis was used during experimental setup to make sure to avoid any nonlinearities that may arise from overexposure. In some of the experiments the camera was rotated by 90˚ relative to the SI orientation to better capture the responding cortical field. These rotations did not have any noticeable effect on spectral power distributions along the anterior-posterior and medial-lateral cortical dimensions.

The spatial organization of the stimulus-related light absorbance changes in SI was evaluated using linear image segmentation. This involved segmentation of the relevant region of the image into a linear series of bins and computation of the average absorbance value of the pixels in each bin. The sequence of average absorbance values obtained in this way was plotted as a function of distance (mm) along the cortical path traced by the central points of the series of bins – yielding an absorbance *vs.* distance plot (thus forming a spatial histogram). Power spectra of the spatial histograms were then computed using Discrete Fourier Transform (DFT) algorithm and plotted as a periodogram. Fourier analysis was always performed on raw, unfiltered images.

At the end of the experiment the subject was euthanized by overdose of pentobarbital (50 mg/kg/IV), followed by intracardial perfusion with saline and 10% formalin.

Results

Figure 1 illustrates the basic method that we used to examine and compare the absorbance patterns evoked by different amplitudes of flutter stimulation. Panel A shows the cortical field (SI cortex of squirrel monkey) that was imaged. Panels B and C are the light absorbance images evoked in this subject by low-amplitude (50μm) and high-amplitude (400μm) flutter stimulation of the same spot on the thenar eminence. The responses to both stimuli occupy the same approximately circular, 2mm-diameter cortical region. The stimulus-evoked activity in the central 2 x 2 mm sector of this responding region was plotted as a 3-dimensional surface map (Panels D and E) to facilitate the view of the evoked patterns of response. In order to quantify this pattern, the pattern was segmented along the cortical anterior-posterior axis and the medial-lateral axis (segmentation orientations indicated by Panels F and G) and generated spatial histograms (Panels H, I, L and M). These histograms hint at a spatial pattern that could have some underlying spatial frequency. To observe their spatial frequency composition, the power spectra of these spatial histograms are plotted in Panels J, K, N and O. The periodograms in these panels reveal major differences in the spatial organization of the SI responses to the 50μm and 400μm stimuli when segmented in the anterior-posterior dimension. That is, the SI response to the higher-amplitude stimulus is greatly dominated by lower spatial frequencies between 1.5-2.5 cycles/mm, whereas in the SI response to the weaker stimulus the relative power in these frequencies is greatly reduced and greater power is

present at spatial frequencies between 5.5-9 cycles/mm. In contrast, when segmented in the medial-lateral dimension (Panels N and O), there is no shift in the power spectra between the low and high amplitude responses. The medial-lateral power spectra are clearly dominated by the low spatial frequencies around 1.5-2.5 cycles/mm.

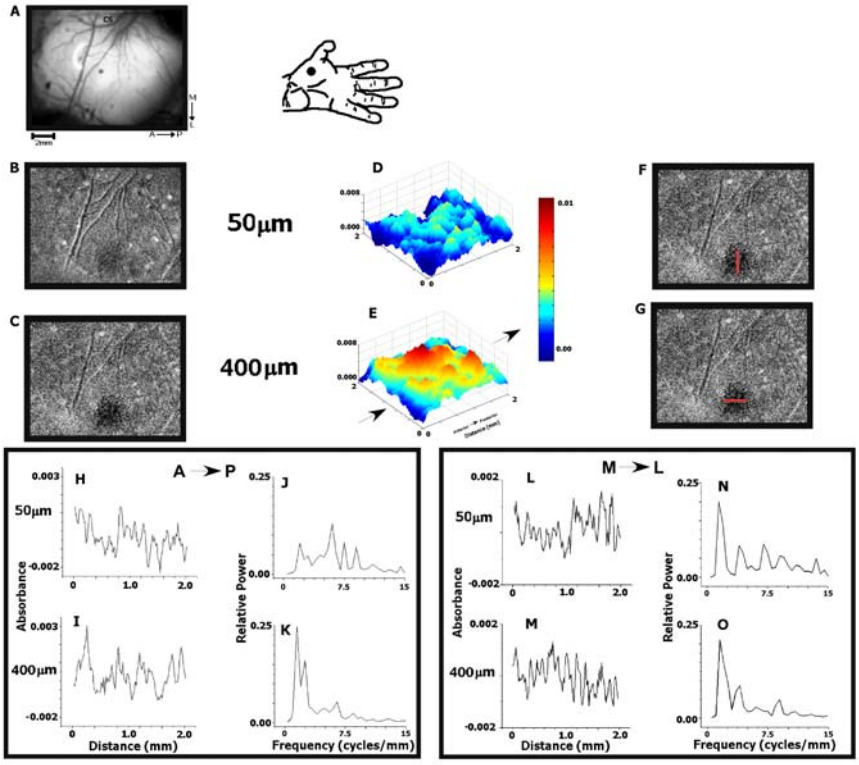

Figure 1. Comparison of SI cortical responses evoked by low- and high-amplitude 25Hz flutter stimuli. **A:** View of the somatosensory cortex with the lateral end of the central sulcus (CS) at the top. Stimulus location is shown on the hand figurine. **B:** Optical response of the SI to the low-amplitude (50µm peak-to-peak) flutter. Shown is the light absorbance image ([poststimulus image – prestimulus image]/prestimulus image) averaged across 20 stimulus trials, and in each trial across 3 poststimulus images taken during the 5-7 sec interval of continuous stimulation. Increased light absorbance is indicated by darker shading. **C:** Optical response of SI to the high-amplitude (400µm) flutter. **D & E:** Magnified 3-D surface maps of OIS magnitude in the responding cortical region. **F & G**: Orientation of segmentation in the M-L dimension (F) and the A-P dimension (G). **H, I, L & M**: Spatiointensive histograms generated via segmentation of areas indicated in F & G for two different stimulus conditions. **J, K, N & O:** Periodograms showing the spatial frequency composition of the spatiointensive histograms. Note change in the power spectra with the change in stimulus amplitude in data sampled in the A-P orientation, but not in the M-L orientation.

Comparable results were obtained from the 4 other subjects, (3 subjects shown Fig. 2). Viewing the 3-D activity maps (Figure 2, second-left column), it is evident that the low amplitude stimulus evokes a pattern with a much higher spatial frequency than that evoked by the higher amplitude stimulus. The third column also shows that in each subject there was a shift of the most prominent frequency band of the OIS power spectrum from ~7.5 cycles/mm to ~2 cycles/mm as the stimulus amplitude was increased from 50μm to 400μm, when the stimulus-evoked activity was sampled in the anterior-posterior dimension. In the medial-lateral dimension (Figure 2, right column), no such shift in the power spectra was observed. Low frequencies around 2-2.5 cycles/mm dominate all of these spectra.

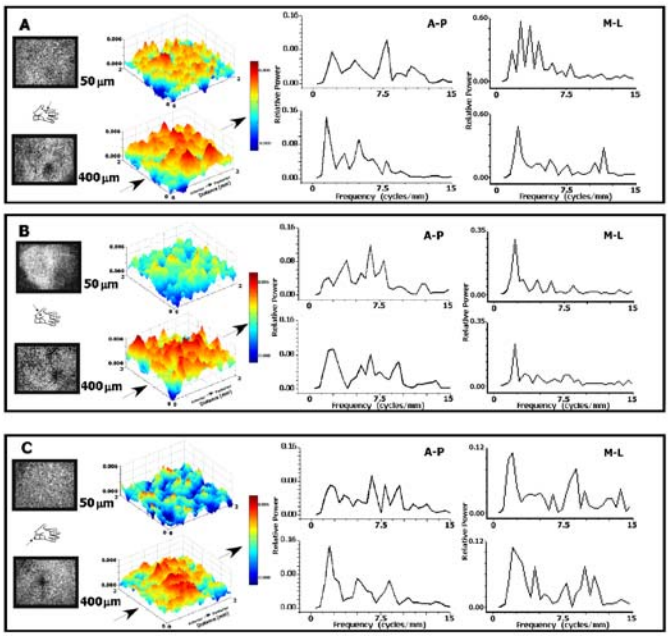

Figure 2. Comparison of SI cortical responses evoked by low- and high-amplitude 25Hz flutter stimuli in three additional subjects. Shown for each subject (A-C) are: (1) the stimulus location on the hand, (2) the average light absorbance images of the cortical optical response to the 50μm- and 400μm-amplitude stimuli, (3) the magnified 3-D activity maps of the region sampled, and (4) the power spectra of the OIS responses. All subjects exhibited similar differences between their low and high stimulus amplitude power spectra.

Figure 3 illustrates results obtained in a more detailed examination of the effect of increased amplitude of flutter stimulation on the spatial organization of the OIS response pattern. Figure 3A shows the SI optical responses, obtained in the same experiment, to five different stimulus amplitudes ranging from 0 (control) to 400μm. 3-D surface maps of the central 2 x 2 mm activated cortical region are displayed in Figure 3B. The power spectra of the responses sampled in the anterior-posterior dimension (Fig. 3C) show that in the absence of flutter (0μm stimulus amplitude) the distribution of power at different spatial frequencies is relatively uniform, with the most dominant frequency at 6.5 cycles/mm. With increments in stimulus amplitude, however, the relative power in the spectral distribution shifts towards lower spatial frequencies. In the case of the medial-lateral dimension (Figure 3D), the power spectra remain essentially constant, with an exception of the no-stimulus control, and there does not appear to be a shift in the distribution of the power with increasing the amplitude of stimulation.

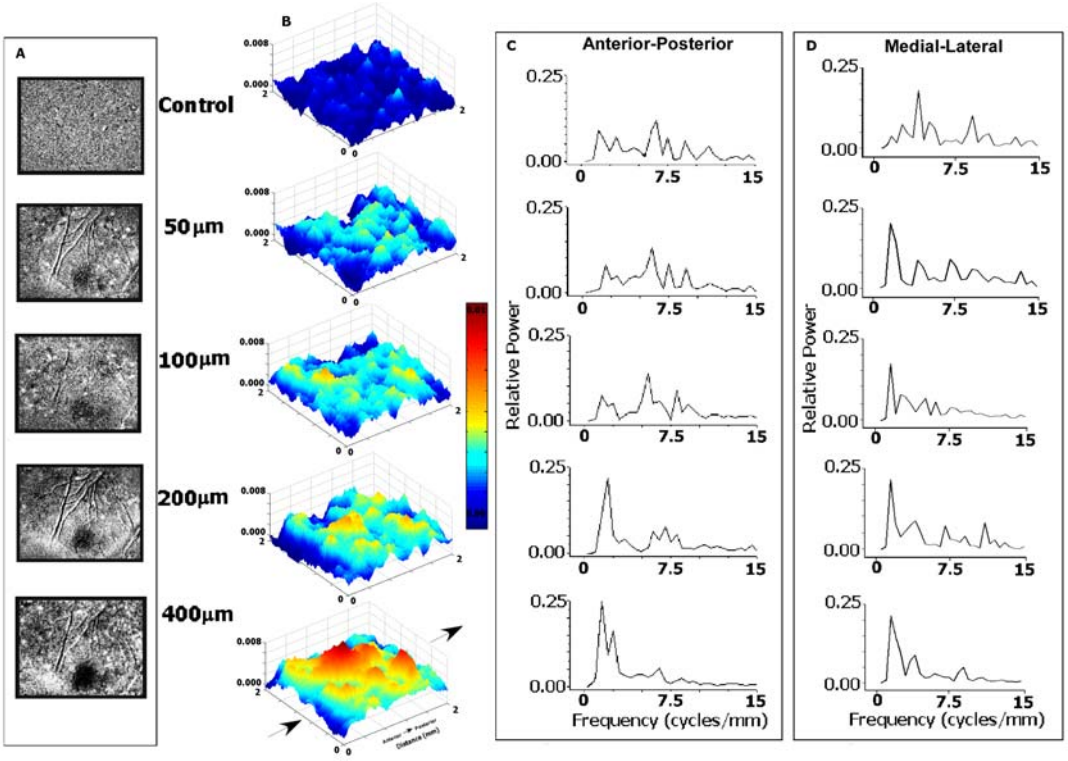

Figure 3. Comparison of SI optical responses evoked at different stimulus amplitudes (0, 50, 100, 200, and 400µm) in an exemplary experiment. **A:** Average light absorbance images for each of the stimulus amplitudes (20 trials, 3 poststimulus images per trial). **B**: 3-D activity maps of the responding cortical region. **C & D:** Power spectra measured for each stimulus amplitude in the two dimensions sampled. With an increase in stimulus amplitude, the spectral power shifts to lower spatial frequencies for the data sampled in the A-P dimension, but not in the M-L dimension.

This effect of stimulus amplitude on the distribution of spatial frequencies in the OIS response along the anterior-posterior dimension is highly reproducible across all subjects. Figure 4A shows the average across-subject (n=5) power spectra, obtained in response to flutter stimuli delivered at 5 different amplitudes. The 6-9.5 cycles/mm frequency band, which is most prominent in the absence of stimulation (control; 0µm amplitude), loses relative power as stimulus amplitude is increased (Fig. 4B top). In contrast, relative power at 1.5-3 cycles/mm grows as stimulus amplitude is increased, and

at the highest amplitude used (400μm) it greatly dominates the power spectrum (Fig. 4B bottom). Overall, the OIS power spectrum appears to respond to an increase in stimulus amplitude by a shift of the relative power towards lower frequencies. This tendency is expressed more clearly in Figure 5, where the highest-power frequency (Fig. 5A; or, inversely, in Fig. 5B, the highest-power period) is plotted as a function of the stimulus amplitude.

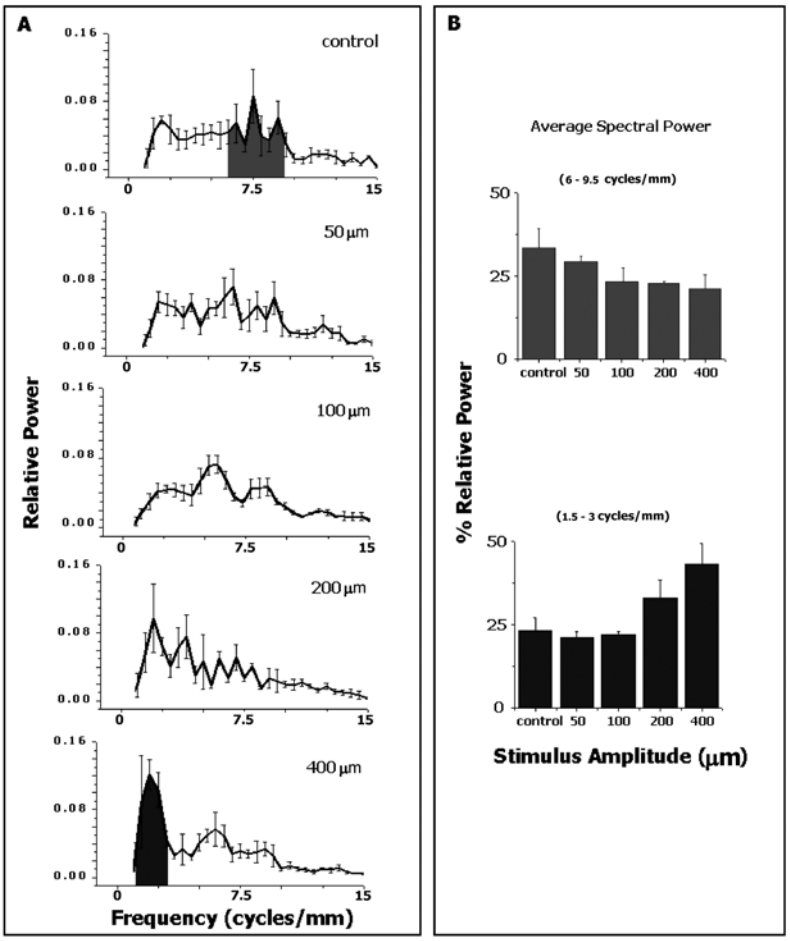

Figure 4. Across-subject reproducibility of the effect of flutter stimulus amplitude on the power spectra of the data sampled in the A-P dimension. **A:** Average periodograms of the OIS responses of 5 subjects to 5 different stimulus amplitudes. **B:** Average relative power in the 6-9.5 cycles/mm and 1.5-3 cycles/mm frequency bands plotted as a function of the stimulus amplitude. As the stimulus amplitude increases, the spectral power shifts progressively to lower spatial frequencies.

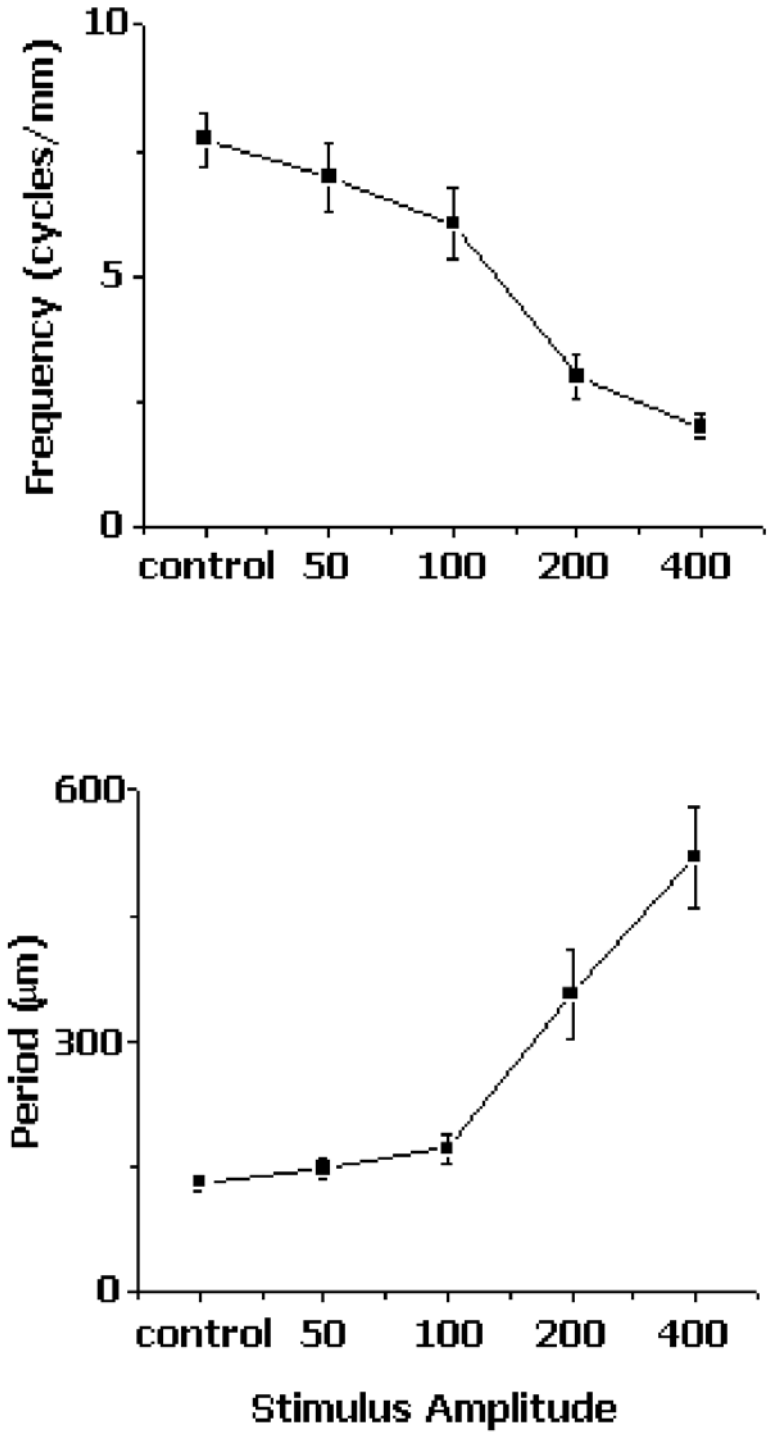

Figure 5. Dependence of the position of the largest spectral peak in OIS periodograms on the stimulus amplitude. The frequency (**A**) and the period (**B**) of the largest spectral peak (average of 5 subjects – see Figure 4) are plotted as a function of the stimulus amplitude. The peak frequency/period shifts across the power spectrum with a change of stimulus amplitude.

Stimulus *duration* appears to alter the spatial organization of SI optical response to flutter in a manner similar to the alteration that accompanies an increase in stimulus amplitude. Figure 6 displays the temporal evolution of the responses evoked by four different amplitudes. In each case, the pattern of absorbance evoked by the flutter stimulus appears to become more organized and periodic with time after the stimulus onset. In other words, with increasing stimulus duration, the local aggregates of above background absorbance tend to form larger clusters – which would lead to higher periodic values (lower spatial frequencies). The spatial frequency changes with stimulus duration were quantified in a manner similar to those that were used to quantify the spatial frequency characteristics that changed with stimulus amplitude. To give a representative example, Figure 7 shows the temporal evolution of the SI response of a subject to a 400μm-amplitude flutter stimulus. The images in Figure 7A were obtained 1sec prior to stimulus onset (control), as well as at 1, 3, 5, and 7sec after the onset of continuous skin flutter stimulation. The power spectra obtained from these images (Fig. 7B) show a systematic leftward shift of the dominant frequencies with increasing time after stimulus onset, from ~6.5 cycles/mm prior to stimulation, to ~2 cycles/mm after 7sec of continuous stimulation. The plots in Figure 7C show that the 6-9.5 cycles/mm frequency band, which is dominant in the resting state, loses relative power after onset of stimulation, and during this same time relative power within 1.5-3 cycles/mm frequency band also becomes maximal.

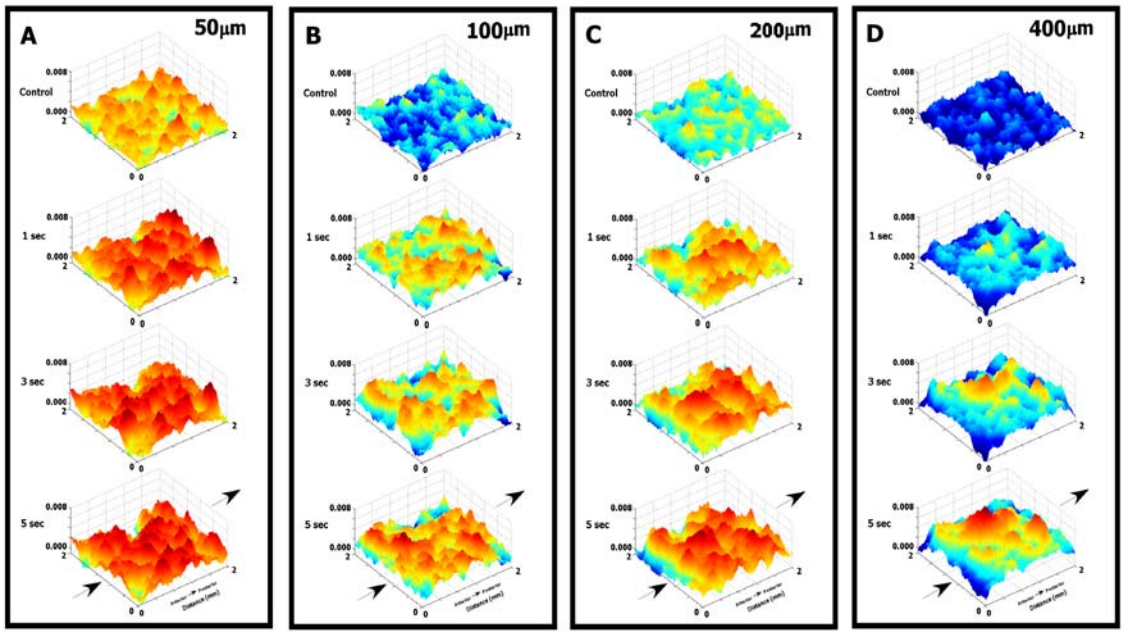

Figure 6. Comparison of temporal development of cortical patterns of absorbance evoked by different amplitudes of flutter vibration. 3-D activity maps of the same cortical region (of the same subject) are plotted at -1 (control), 1, 3 and 5 secs after the stimulus onset for amplitudes of 50, 100, 200 and 400µm (Panels A, B, C, & D respectively; in all panels, color-scales are normalized by their maxima). Note the difference in the progression of the pattern development evoked by the different stimulus amplitudes.

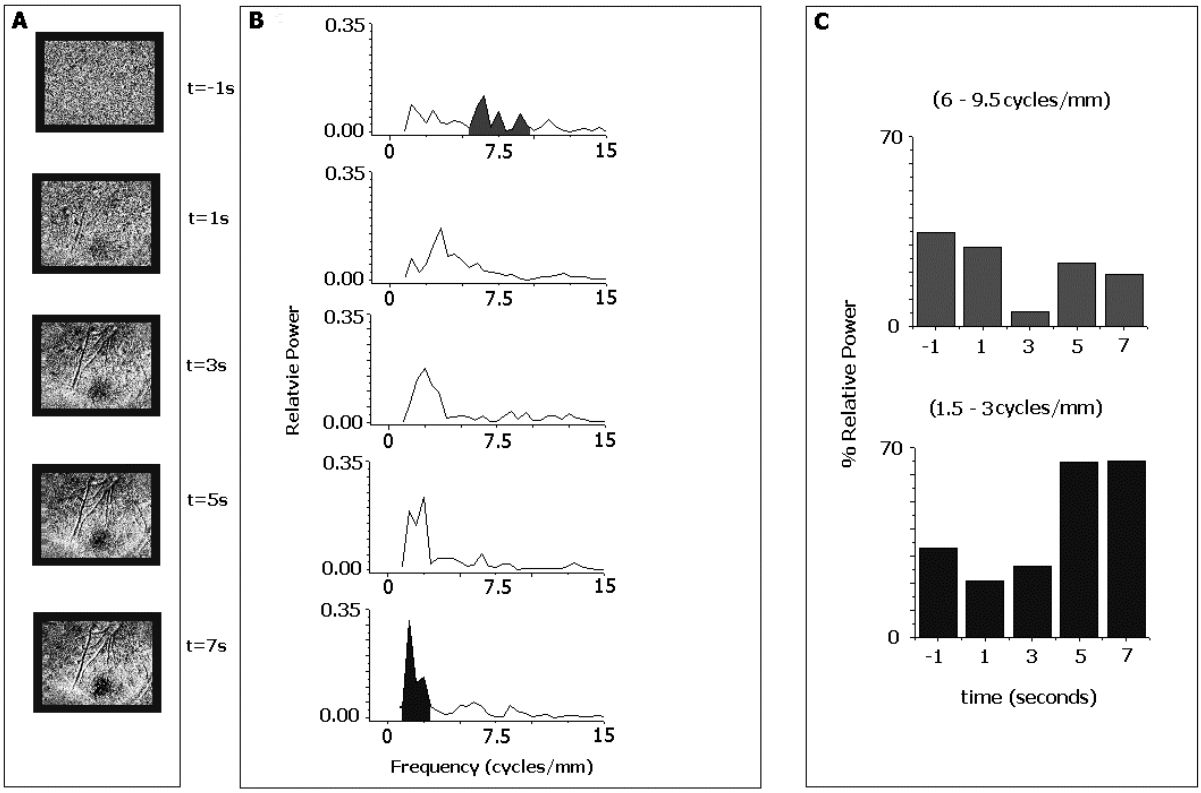

Figure 7. Temporal development of power spectra in response to a 400μm-amplitude flutter stimulus. **A**: Light absorbance images obtained at selected times before and during flutter stimulation. **B**: Power spectra of OIS activity sampled in the anterior-posterior dimension across the activated cortical region. With increasing stimulus duration, the most prominent frequency band in the power spectra shifts to the left relative to the pre-stimulus condition. **C:** Temporal shift in relative power in the 6-9.5 cycles/mm band (top) and in the 1.5-3 cycles/mm band (bottom). As stimulus duration increases, the relative power decreases in the 6-9.5 cycles/mm band, but increases in the 1.5-3 cycles/mm band.

Figure 8 summarizes the temporal development of OIS response patterns by plotting the highest-power spatial frequency in the anterior-posterior dimension (averaged across 5 subjects) at different times after stimulus onset. Two plots are shown for comparison: the first for 400μm-amplitude stimuli, the second for 50μm-amplitude stimuli. These plots make it evident that during continuous flutter stimulation: (1) the

spectral power of the response migrates towards lower frequencies with increasing time after stimulus onset – indicating that SI optical response pattern undergoes a gradual spatial reorganization; and (2) the higher the stimulus amplitude, the faster the shift of spectral power towards lower frequencies.

Figure 8C plots the magnitude of OIS response to the 50μm- and 400μm-amplitude stimuli as a function of time after the stimulus onset, showing that during the time when the dominant spatial frequency migrates across the power spectrum, the OIS also grows overall in its magnitude. The concurrency of these changes raises a parsimonious possibility that OIS periodicity is a direct function of the OIS magnitude (and thereby only an indirect function – via their control of the OIS magnitude – of the stimulus strength and duration). To evaluate this possibility, Figure 8D plots the highest-power spatial frequency at any given time (taken from Figure 8A plot) as a function of the overall OIS magnitude at that time (taken from the Figure 8C plot). As the Figure 8D plot shows, the relationship between OIS magnitude and periodicity obtained with the 50μm-amplitude stimuli appears to be different from the relationship obtained with the 400μm stimuli, suggesting that OIS periodicity cannot be explained simply by the overall OIS magnitude.

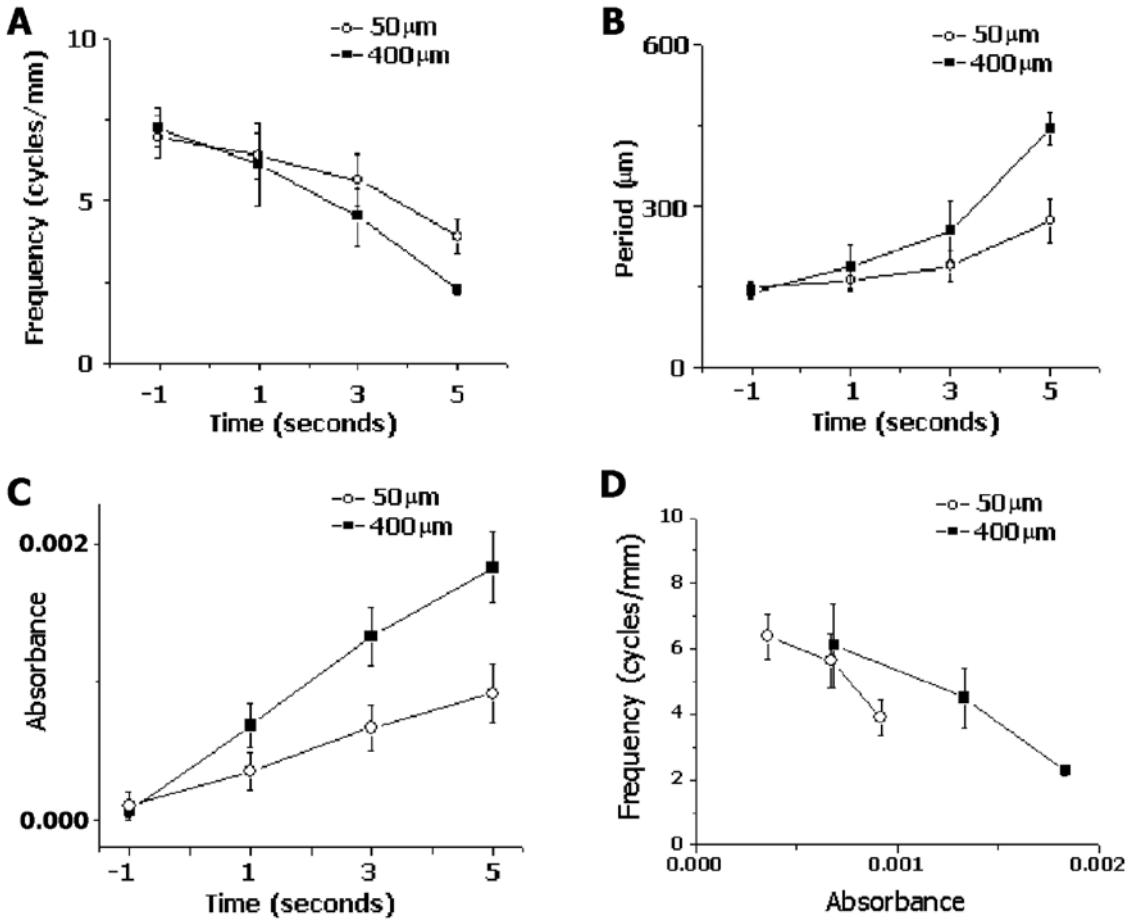

Figure 8. Temporal shift of the position of the largest spectral peak in the anterior-posterior OIS periodograms and its dependence on stimulus amplitude. The frequency (**A**) and the period (**B**) of the largest spectral peak (average of 5 subjects) are plotted as a function of time since the stimulus onset. Two plots are shown, for 50μm-amplitude and 400μm-amplitude stimuli. With increasing stimulus duration, the peak frequency/period shifts across the power spectrum, at a rate dependent on the stimulus amplitude. **C:** Average magnitude of OIS in the segmented region as a function of time after stimulus onset. The dominance of lower spatial frequencies develops in time in parallel with an overall growth of the OIS response to the stimulus. **D:** The frequency of the largest spectral peak plotted as a function of the average magnitude of OIS in the sequential region. The relationship between the largest spectral peak and overall OIS magnitude varies depending on the stimulus amplitude.

Discussion

Spatial frequency analysis revealed that the SI response to flutter stimulation produces systematic, spatially periodic fluctuations in the magnitude of the OIS within the responding SI region. In the absence of stimulation – the control condition – the power spectra have a small prevalence of spatial periodicities in the range of 0.1-0.14mm. In contrast, in the presence of a prominent flutter stimulus spatial periodicities in the range of 0.4-0.6mm dominate the stimulus-activated SI region.

Visual inspection of the 3-D activity plots (Figures 1, 2, 3, 6), together with the results of spectral analyses performed along the anterior-posterior and medial-lateral cortical dimensions, point to a substantial tendency of the stimulus-evoked activity to take a form of a pattern of roughly parallel elongated waves oriented in the anterior-posterior direction. These waves have a medio-lateral spacing of 0.4-0.5mm between their crests. This tendency is already well developed in response to a relatively weak, 50μm-amplitude flutter. At such weaker stimuli, each anterior-posteriorly oriented wave has a pattern of fine "ripples" along its long axis, with the dominant spatial periodicities in the neighborhood of 0.15-0.2mm – values close to those characteristic of the OIS in the no-stimulus condition. Stronger stimuli lead to an emergence of larger spatial periodicities in the anterior-posterior dimension, up to 0.6mm. Such a stimulus amplitude-dependent shift towards larger spatial periodicities suggests that the spatial pattern of SI response to flutter stimulation undergoes substantial reorganization in response to changes in stimulus amplitude/intensity. That is, the stronger (200-400μm amplitude) stimuli have an effect of restructuring the anterior-posteriorly oriented waves

by replacing the high-frequency ripples along their crests with more prominent *ca.* 0.5mm periodic fluctuations.

Such a reorganization of stimulus-evoked OIS spatial patterns apparently also occurs across time. That is, flutter stimulus-evoked OIS patterns in the anterior-posterior dimension develop gradually from the resting state – dominated by high spatial frequencies – through a series of states characterized by progressively lower spatial frequencies. Thus, the spatial organization of the patterned response evoked in SI by a flutter stimulus varies with both stimulus strength and stimulus duration.

In interpreting the outcomes of our spatial frequency analyses, it is important that it be recognized that they were performed not on the SI neuroelectrical responses to flutter stimulation, but on SI *optical* responses to such stimulation. It now is well established that cortical neuroelectrical activity is positively and strongly correlated with the local increase in cortical tissue light absorbance (Grinvald *et al*., 1988; Lieke *et al*., 1989; Bonhoeffer and Grinvald, 1996; Shmuel and Grinvald, 1996; Tommerdahl *et al*., 1996; Grinvald *et al*., 1999; Tommerdahl *et al*., 1999a; Tommerdahl *et al*., 2002). Although highly correlated with neuroelectrical activity, however, the OIS is not a direct reflection of either neuronal spike discharge activity or, more generally, the local voltage changes evoked by a sensory stimulus. Notably, it has a much slower onset and decay than the neuroelectrical responses of cortical cells. The intrinsic signal detected using the near-infrared light ("IR imaging") is relatively independent of changes in blood flow (Haglund *et al*., 1992; Ba *et al*., 2002). The optical signal observed under near-infrared light reflects a variety of factors but, most significantly, change (shrinkage) in the volume of the extracellular fluid compartment attributable to the glial swelling due to stimulus-

evoked changes in extracellular [K+] and/or neurotransmitter release (Cohen, 1973; Lieke *et al*., 1989; MacVicar and Hochman, 1991). In view of these complex origins of the near-infrared OIS, it remains to be determined whether the observed stimulus-dependent periodicities reflect the spatial organization of stimulus-evoked neuroelectrical activity. Alternatively, the observed OIS periodicities might reflect the spatial organization of the cortical glial reaction to local neuroelectrical activity, or SI microvascular responses (Woolsey *et al*., 1996), which become more prominent with increases in both stimulus strength and duration.

If the observed stimulus-dependent OIS periodicities were to reflect neuroelectrical activity patterns, how well would they fit with the known features of SI functional organization? In particular, a macrocolumnar functional organization has been well documented in SI cortex. Receptive field-mapping techniques have revealed that SI cortex is partitioned into ~0.5mm-wide submodality- and place-defined columns (Powell and Mountcastle, 1959b; Sretavan and Dykes, 1983; Sur *et al*., 1984; Favorov and Whitsel, 1988a; Favorov and Whitsel, 1988b; Favorov and Diamond, 1990). These topographic entities, repeating every 0.5mm, might indeed be responsible for the prominent 0.5mm periodicity in SI OIS stimulus-evoked activity patterns. If the spatial OIS periodicities were due to selective modulation of entire macrocolumns (in other words, due to SI response fractionation on the macrocolumnar scale), then the observed OIS periodicities would be at least double the size of macrocolumns. Since this is not the case, and the OIS periodicities approximate the size of macrocolumns, the fractionation of the SI response would appear to take place on the submacrocolumnar scale, with flutter stimuli preferentially activating only a subsector of each macrocolumn in the SI

region engaged by the stimulus. Such preferentially activated subsectors would then form a roughly periodic pattern across the responding SI region. In support of this proposal, Chen *et al.* (Chen *et al*., 2001) have reported that single skin taps, 25Hz flutter, and 200Hz vibration (stimulus conditions that allow preferential activation of the different classes of skin mechanoreceptors) were associated with preferential activation of different 0.25mm-diameter regions within the responding SI territory. The small size of these regions suggests that they should occupy only a subsector of a typical submodality column, rather than a whole column (Sur *et al*., 1984).

Whether or not the 0.5mm periodicities in OIS stimulus-response patterns in SI owe their existence to submodality- and/or place-defined macrocolumns, the fact remains that a flutter stimulus activates multiple cortical loci, separated from each other by less active loci. Such a locally selective distribution of activity in SI is suggestive of the presence in SI functional architecture of a mapping factor in addition to submodality and place on the skin – a factor specific to some yet to be explored attribute(s) of mechanical skin stimulation. Similarly, Bruno and colleagues recently demonstrated that individual barrels in rat SI contain minicolumns of neurons preferring the same whisker deflection angle and that these angular tuning domains could be the result of convergent inputs from thalamocortical cells with corresponding angular preferences (Bruno *et al*., 2003). It is possible that upon further investigation, the spatial activity patterns evoked in SI cortex, such as the amplitude-dependent patterns described in this report, will also be found to be submodality-dependent as well.

Finally, considering that spatial periodicities in SI OIS response patterns emerge gradually, and evolve with time after the stimulus onset, the fine sculpting of the SI

response might be the result of a network-level neurocomputational process that involves competitive and cooperative interactions among local neuronal aggregates. That is, SI sensitivity to the stimulus attribute(s) responsible for the observed fractionation of activity within the responding SI region might be an emergent property of the SI network (i.e., a product of network-level computation), rather than a simple outcome of selective convergence of thalamocortical afferents on SI neurons.

Observations of the spatial patterns of SI cortical response within an activated region, such as those evoked by flutter stimulation of the skin, suggest that evoked cortical activity within such a territory is not evenly distributed. Furthermore, the cortical activity patterns change in a manner that appears to be dependent upon stimulus conditions. The observed spatiointensive fractionation on a sub-macrocolumnar scale of the SI response to skin stimulation might be the product of local competitive interactions within the stimulus-activated SI region, and as such can lead to new insights about the functional interactions that take place in the SI cortex.

Chapter 4

Chapter four is divided into four sections, all of which assess the effects of changes in stimulus parameters on the evoked minicolumnar patterns.

Section I:

Part A: Effects of Changes in Stimulus Position on Minicolumnar Patterns Using Single Point Stimulus Modality

Part B: Effects of Changes in Stimulus Position on Minicolumnar Patterns using Two Point Stimulus Modality

Section II: Effects of Stimulus Duration on Minicolumnar Patterns

Section III: Different Modes of Long Duration Stimuli will evoke different but reproducible Cortical Response Patterns.

Section IV: Effects of pre-exposure to a skin stimulus on the minicolumnar pattern of a subsequent skin stimulus

Introduction

In order to characterize the differences between cortical patterns of activity evoked by different conditions of skin stimulation, a number of different stimulus conditions will be investigated. Differences in stimulus site position, stimulus duration, as well as pre-exposure to a stimulus, has been altered in order to determine the baseline quantitative differences in the cortical response to repetitive stimulation. The goal was to determine the minimum change in stimulus parameters that evokes a just noticeable difference (jnd) in the evoked cortical response between different stimulus parameters. For example, a flutter stimulus will be delivered at a specific frequency and amplitude at a particular skin site. Separate comparisons will be made with incremental changes in frequency (5 Hz) as well as stimulus site position (2 mm distance from previous stimulus site. A baseline stimulus (200 μm peak to peak, 25 Hz) delivered to a particular "fixed" stimulus site, will serve as the comparator in order to visually and quantifiably determine which of the changes in the stimulus parameters evoked a jnd cortical response from the comparator stimulus.

Comparison of previous 2-DG experiments and receptive field mapping experiments gave the first evidence of a time-dependent process involved in the formation of somatosensory cortical activity patterns (Whitsel and Juliano, 1984; Juliano and Whitsel, 1987; Tommerdahl, 1989). The discrepancy between the metabolic mapping results and the neurophysiological results led Whitsel and co-workers to conduct a series of experiments investigating the response of SI cortex to repetitive stimulation and the possible role that cortical dynamics played in SI pattern formation. Repetitive tactile stimuli led to prominent changes in single neuron response (Diamond *et al*., 1986; Whitsel

and Kelly, 1988; Whitsel *et al*., 1989), and the global cortical neuroelectrical response to the same tactile stimulus was shown to change quickly and systematically when a stimulus was applied repetitively. Additionally, the strip-like patterns that characterized cortical 2-DG maps were postulated to be a reflection of the end result of the repetitive stimulus (Whitsel *et al*., 1989).

The view of SI activity pattern formation in previous studies (Whitsel and Kelly, 1988; Whitsel *et al*., 1989; Whitsel and Franzen, 1989) revealed that the initial cortical response to a somatic stimulus is not the selective activation of a relatively few, highly tuned neurons, but rather a complex spatio-intensive pattern of activity involving very large numbers of neurons. It involves broadly-tuned neurons that respond in some fashion to many different tactile stimuli, but with repetitive stimulation, this extensive and less differentiated initial activity pattern becomes rapidly sculpted by a dynamic cortical inhibitory mechanism into a more stimulus-specific spatiotemporal pattern or "signature", consisting of multiple, complexly arrayed (in the form of strips) columnar assemblies. In this manner, the somatosensory cortex appears to synthesize, over time, a unique and statistically reliable response (a spatiointensive activity pattern) out of the activity of extremely large numbers of broadly-tuned, individually unreliable elements. In a review article on neural coding, Doetsch states that a specific stimulus is encoded by a unique spatiotemporal pattern, and intensity changes mainly showed an increase in magnitude of that unique spatiotemporal pattern (Doetsch, 2000).

Repetitive stimuli trigger input-specific, time-dependent pericolumnar lateral inhibitory interactions in the somatosensory cortex (Mountcastle, 1978, 1984, 1988). The differential activation of neighboring segregates by a peripheral stimulus increases the

extracellular K+ levels in neighboring segregates to an extent approximately proportional to their evoked activity levels (for definition of "segregates" see Favorov, 1994. Due to the suggested action of the elevated extracellular K+ level on cortical NMDA receptors, subsequent stimuli lead to increasingly discrepant activity levels between neighboring segregates, causing the extracellular K+ level in a particular segregate to become progressively more elevated relative to that of its neighboring segregates. Because elevated levels of extracellular K+ interfere with presynaptic autoregulation of Ach release (Meyer and Otero, 1985), neighboring segregates are less effective. Ach release can also persist (Metherate *et al*., 1988a, 1988b; Schwindt *et al*., 1988b), repetitive stimulus leads to a "piling up" of the effect of Ach release, enhancing the local contrast in the stimulus-evoked activity pattern, which culminates in a strip-like columnar activation pattern that is more focused than that achieved by the same repetitive stimulus in the absence of cholinergic drive. Through this mechanism, the non-topographically projecting nucleus basalis cholinergic neuron modulatory system is able to exert a highly selective spatial pattern of excitatory influences which is in perfect registration with the complex strip-like activity pattern evoked by the topographically organized thalamocortical pathways to SI.

In the 1990's, Tommerdahl and co-workers began to implement the method of optical intrinsic signal (OIS) imaging in their study of SI cortical response (Tommerdahl *et al*., 1996). Their reason for switching to this method, from that of 2-DG metabolic mapping, was to make observations about the time course of the response of SI cortex to repetitive stimuli that had been predicted by their previous studies. One interesting difference between Tommerdahl and colleagues and their approach to OIS imaging from the majority of other workers in the imaging field was that they chose to study the

response of SI cortex at the wavelength of 830 nm (most of the published literature shows investigators using wavelengths in the range of 560-660 nm). The reason for this choice of wavelength was that, even though the magnitude of the response is much less in this range than in the lower range, is that it was predicted to be a better indicator of the status of the NMDA receptor system – the system which Whitsel and co-workers predicted to play a prominent role in the sculpting of cortical activity patterns via repetitive stimulation. OIS imaging had the distinct advantage over 2-DG metabolic mapping method, in that it could be used to map the global *temporal* response of the somatosensory cortex, with the disadvantage of only imaging the upper cortical layers. Another advantage of the method (over 2-DG metabolic mapping) is that it allows for imaging multiple images of the response of the same cortical region to the same or to different stimuli in the same subject. The cortical intrinsic signal is relatively independent of blood flow changes (Haglund *et al*., 1992), reflects changes in the volume of the extracellular fluid compartment attributable to stimulus-evoked changes in extracellular K+ and/or neurotransmitter release (Cohen, 1973; Lieke *et al*., 1989), attenuated in a does-dependent manner by cortical NMDA receptor block (Haglund *et al*., 1992), and the signal is not a direct reflection of either neuronal spike discharge activity or, more generally, the local cortical voltage changes evoked by a sensory stimulus (the intrinsic signal has a much slower onset and decay than the neuroelectrical responses of single neurons or neuron populations).

In psychophysical studies, adaptation to vibration enhances the ability for humans to discriminate from two slightly different test stimuli (Delemos and Hollins, 1996). Delemos *et al*. (1996), suspected that, under optimal conditions of adaptation, the test

stimuli differing slightly in amplitude became perceptually more distinct due to physiological events underlying the sensory experiences within the CNS, and that this adaptation is stimulus specific. The extent of threshold elevation also relies on the relationship between the vibrotactile frequencies of the adapting and test stimulus (Wedell and Cummings, 1938). Hollins *et al* (Hollins *et al*., 1990) found that for a 10Hz adapting stimulus, the threshold is elevated only by activation of non-Pacinian receptors, therefore cross-adaptation does not exist between non-Pacinian and Pacinian channels (Verrillo and Gescheider, 1977; Gescheider *et al*., 1979). However, Tommerdahl *et al* recently found that RA and PC channels interact, where the concurrent PC input spatially sharpens or "funnels" the SI cortical response to skin flutter stimulation (Tommerdahl *et al*, 2005a, 2005c). O'Mara *et al*. (O'Mara, 1988) concluded that vibrotactile adaptation was more of a central process instead of "failure" of cutaneous afferents. Adaptation was also determined to depend on the temporal summation of action potentials, and that this temporal patterning in the CNS directly reflects the nature of the peripheral stimulus (Hollins *et al*., 1990). This chapter will try to assess the changes in spatiotemporal patterns of SI cortical response evoked by repetitive stimulation parallel (or correlate to) the improvements in sensory discrimination that result from adaptation.

Repetitive stimulation leads to adaptation, not only in the somatosensory cortex, but in the visual and auditory cortex as well. When adaptation occurs, neuronal responsiveness and sensitivity of the activated cortical population decreases in respect to the adapting stimuli. Reduction in the coding redundancy in the cortical neuronal population allows for recent sensory history to reduce of the number of neurons that must be recruited to solve a particular processing task (Barlow, 1990; Muller *et al*., 1999). This

reduction in neuronal recruitment would reduce metabolic cost associated with information processing (Laughlin *et al*., 1998). In a model of the visual cortex, immediately after stimulus onset, strong periodic neuronal excitation is robust, which leads to enhanced competition for activity between cortical columns of different orientation preferences in the visual cortex, (Adorjan *et al*., 2002). After a period of time, the strength of the recurrent excitation decreases due to spike-frequency adaptation of the excitatory neurons. In VI, cells strongly driven by the adapter experiences a reduction in the strength of recurrent excitation (Kohn and Movshon, 2004). Furthermore, in the auditory cortex, Lu *et al*. (Lu *et al*., 1992) studied echoic memory where subjects compared the loudness between two auditory stimuli. They found that the performance depended on the time interval between the presentation of the two stimuli, and the loudness match was best for shorter intervals.

In Abbott and Nelsons review of synaptic plasticity (Abbott and Nelson, 2000), they emphasize that there are many forms of synaptic plasticity across different regions and even across layers within one region of the brain which are essential to learning and memory. Using OIS and extracellular recordings, Schuett *et al* (Schuett *et al*., 2001) demonstrated that synaptic inputs were responsible for plasticity (tuning curves shift towards paired orientation resulting in increase in signal strength and increase in cortical area to the preferred orientation) in V1 neurons. This was prominent in the supra and infragranular layers where inputs from other cortical cells predominate. However, plasticity was not found in layer IV, where input from the thalamus is prominent.

Dragoi *et al* (Dragoi *et al*., 2001) demonstrated through neuronal recordings in V1, that during adaptation, a neuron's response/stability depends on the structure of the

neighboring neurons, ie. if the neuron is surrounded by neurons that have broad orientation distributions, then the change in orientation tuning and firing rates are more robust or less stable. They have also reported that adaptation induced effects are maximal at pinwheel centers, where neurons with different orientation preferences are close in proximity (Sur *et al*., 2002). In the somatosensory cortex, the neurons in area 3b/1, could be similar to neurons located at pinwheel centers found in V1. After adapting to a specific stimulus, the introduction of a novel stimulus could evoke robust changes in the pattern or activation, where there is this "pooling of inputs" from neurons that are more sensitive to respond to the novel stimulus versus the adapting stimulus.

Thalamocortical interactions are found to be important in sensory adaptation. In the rat whisker barrel cortex, (Moore *et al*., 1999; Castro-Alamancos, 2004; Moore, 2004) cortical adaptation was measured during different behavioral states, and found that increases in thalamocortical firing can result in adaptation (enhanced cortical inhibition), allowing for finer discrimination of spatiotemporal patterns of stimulation. As the animal learns a task and becomes more proficient, sensory adaptation enhances and the animal becomes less alert. Ghazanfar *et al* (Ghazanfar *et al*., 2001) examined the role of corticothalamic feedback, and found that integration and transmission of tactile information to the thalamus is dependent on the state of the SI cortex.

Section I Part A

Effects of Changes in Stimulus Position on Minicolumnar Patterns Using Single Point Stimulus Modality

Previously, it has been proven that the pattern of cortical response is an emergent property, and these patterns are not only stimulus specific, but time dependent as well. Tactile stimuli activate not a single macrocolumn, but a local group of macrocolumns. Each macrocolumn in an active group generates its own pattern of minicolumnar activation. Therefore, the SI response to a skin stimulus is a "patchwork" of active minicolumns that extends across multiple macrocolumns. It was also widely believed that changes in stimulus parameters will not yield changes in stimulus. However, analyses of recent data have shown that changes in minicolumnar patterns occurred when the stimulus position changed.

Favorov (1990) found using both maximal receptive field (maxRF) mapping and minimal receptive field mapping (minRF) that each "segregate" or macrocolumn has a similar central locus in its RF. Therefore, no matter where the stimulus position is, as long as they share a common central locus, the same group of macrocolumns will be activated. The only differentiating factor that portrays the shift in the stimulus parameter (ie. position) will be in its stimulus evoked minicolumnar patterns.

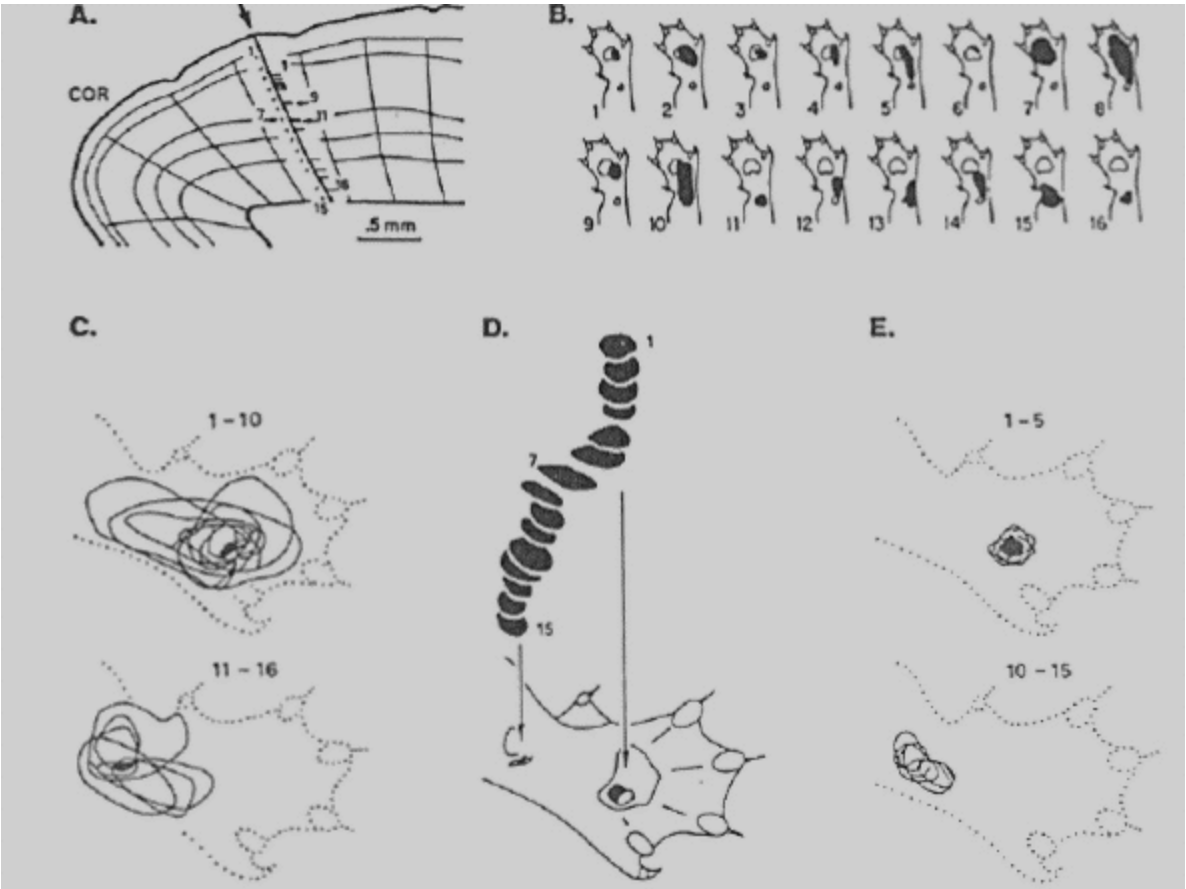

Figure 6. Typical near-radial penetration of cat SI in which both max- and minRF data were collected. This penetration crossed a boundary separating two segregates. The different central tendencies of maxRFs of neurons 1-10 and 11-16 are shown in panel C. The different central tendencies of minRFs 1-5 and 10-15 are shown in panel E. Relative positions of the skin loci shared in common by RFs making up each of the four groups are shown in panel D.

Favorov, OV. In: Information Processing in the Somatosensory System: Chapter 16 (Franzen and Westman), Macmillan Press, London, 1990.

The OIS images shown in figure 1, reveal that even though the stimulus position shifts to a distance of 6mm from the first stimulus position (first three images), the evoked spatial global pattern at 5 seconds after stimulus onset is similar. Notice that the contour lines encompassing the ROI for the first three images in the lower panel are similar in shape. The black regions in the lower panel of images also show where evoked

spatial responses from stimulation at the first three stimulus positions overlap. Notice the significant overlap in the activated group of macrocolumns. However, once the stimulus position is far enough in distance from the first stimulus position, a shift it the evoked spatial global pattern occurs significantly, shown in far right images of Figure 1.

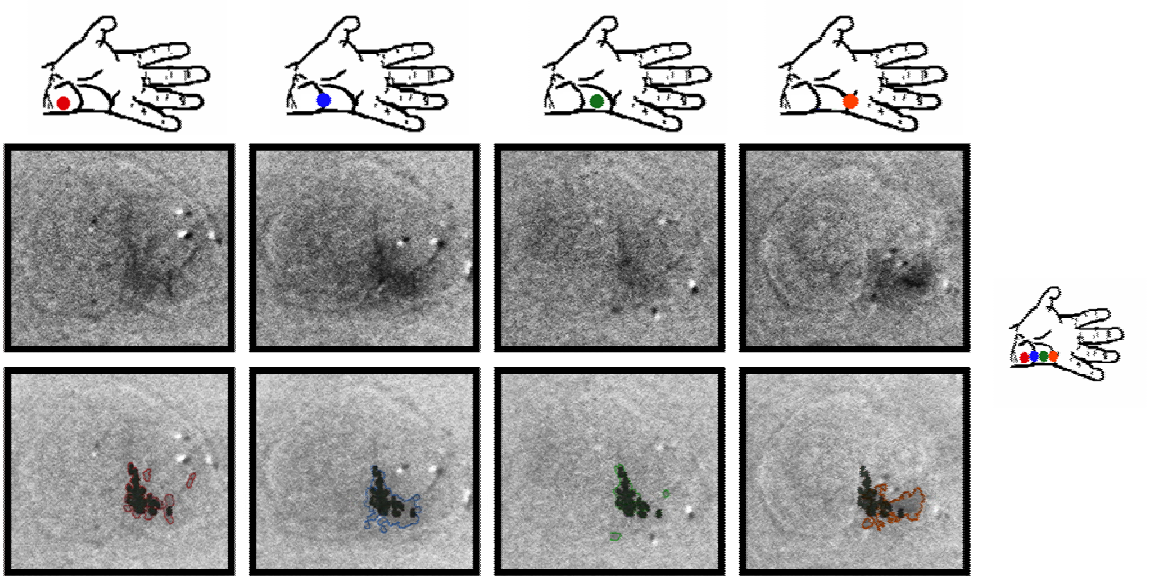

Figure 1. The OIS responses above were evoked by a 25Hz200µm 5sec flutter stimulus at varying stimulus positions. The stimulus probe (2mm in diameter) was initially located on the hypothenar, and was moved ~2mm towards ID5 for each subsequent stimulus condition. Images above are OIS images at each stimulus position. Each image is boxed in its respective color according to its stimulus position shown on the figurine to the right (stimulus position is indicated on the figurine with a colored dot). The contour lines encompassing the ROI in the second row of OIS images outlines the pattern of the evoked response. The black region in the bottom panel of images indicates where the ROI from the first three stimulus positions overlap.

Figure 2 shows enlarged OIS images (3x3mm) of the ROIs taken from figure 1 for each stimulus position, respectively. A more in depth study of the evoked macrocolumnar patterns reveal that within the evoked global spatial pattern, there are discrete activated regions that are unique for each stimulus position. Adjacent stimulus

positions also show to have more discrete regions that tend to be similar. These discrete regions reflect changes in minicolumnar patterns as the stimulus position shifted away from the hypothenar towards ID5 in 2mm increments. The first three stimulus positions evoked responses in the same group of segregates that had overlapping receptive fields and similar response characteristics. However, the evoked minicolumnar patterns differ significantly, and the difference in the minicolumnar patterns increase as the distance between the stimulus positions increase. The last stimulus position evoked both macrocolumnar and minicolumnar patterns that were grossly different from the response evoked at the first three stimulus position. At this stimulus position, the skin position no longer shares the "common skin locus" that was found in the first three stimulus positions.

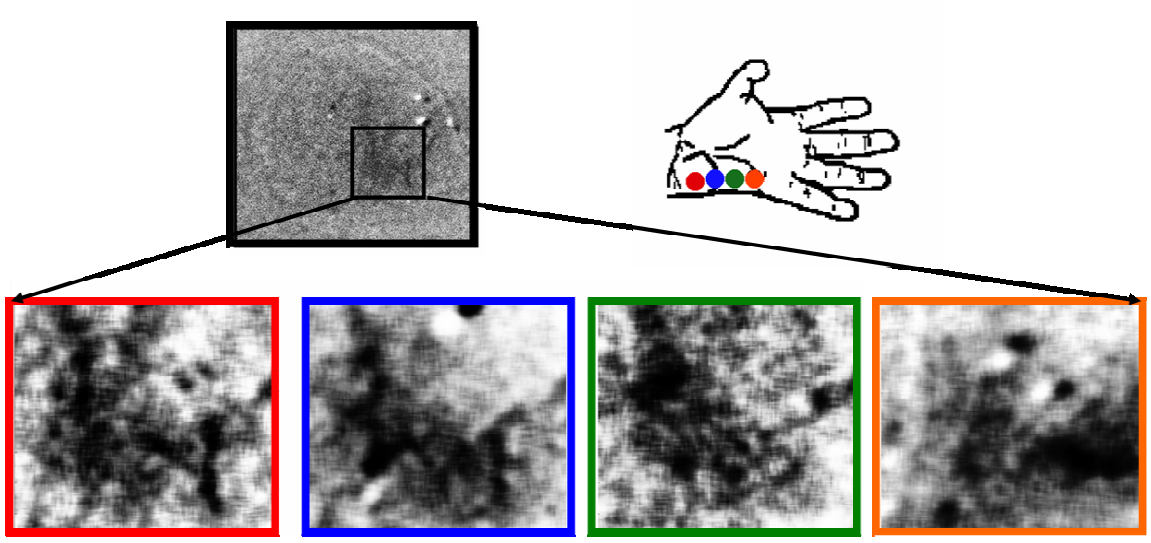

Figure 2. Enlarge images of the ROI evoked from vibrotactile flutter stimulation (25Hz 200μm) at varying stimulus positions. Notice that the evoked minicolumnar patterns are different at all stimulus positions. However, the larger the separation between the stimulus positions, the greater the differences found in the evoked minicolumnar patterns. Notice that the evoked minicolumnar patterns of the first two stimulus positions are more similar than the evoked minicolumnar patterns of the first and third stimulus positions, even though the global spatial patterns were similar. The last stimulus position evoked a minicolumnar pattern response that was significantly different from the response evoked from the other stimulus positions.

Section I Part B

Effects of Changes in Stimulus Position on Minicolumnar Patterns using Two Point Stimulus Modality

In the previous section, the same groups of macrocolumns were activated regardless of stimulus position, as long as the activated groups of macrocolumns shared a similar "central skin locus". Even though the stimulus evoked similar macrocolumnar patterns, the minicolumnar patterns were proven to be different at each stimulus site. To further assess the effects of changes in stimulus position on minicolumnar patterns, the effects of a second stimulus was applied at various distances from the first stimulus (2, 5, 8, 11, and 14mm) towards the hypothenar. The first stimulus site fixed on the thenar. Both stimuli consisted of a 25Hz 200μm vibrotactile flutter stimulus, and were applied simultaneously for 5 seconds. Patterns observed in the ROI of the fixed stimulus were analyzed.

Results show that when both stimulus positions share the same central skin locus, similar to the single point stimulus protocol, the same groups of macrocolumns are activated. When the stimulus probes are close together (2 and 5mm) the perceptual sensation is that the probes feel "stronger". Notice that in figure 3, the magnitude of the evoked response is greater when both probes are applied to the skin in comparison to the evoked response of the single point. Closer scrutiny of the evoked spatial patterns at 2 and 5mm separations reveal that the evoked minicolumnar patterns also differ. There are macrocolumns that are more strongly activated in one region of the pattern for the 2mm separation compared to the 5mm separation, and vice versa. When the stimulus probes

are 8 and 11mm apart, the macrocolumnar response changes dramatically. However, the evoked macrocolumnar patterns when the probe separation is 8 and 11mm are similar, differing only in the evoked minicolumnar patterns. The reason is that the second stimulus probe at these two skin positions, share a common central locus, therefore evoking the same groups of macrocolumns differentially. Then the same groups of macrocolumns activated by the second stimulus will have similar effects on the macrocolumnar pattern evoked by the first stimulus. Notice that the same region of the macrocolumnar pattern evoked by the first stimulus is driven down when the probes are 8 and 11mm apart, and the response in the other regions increase due to a decrease in local inhibition. When the two probes are 14mm apart, the second stimulus probe no longer has a great effect on the evoked macrocolumnar pattern of the first stimulus. Lateral inhibition decreases, and the evoked spatial response pattern begins to resemble the evoked macrocolumnar pattern of the single point stimulus.

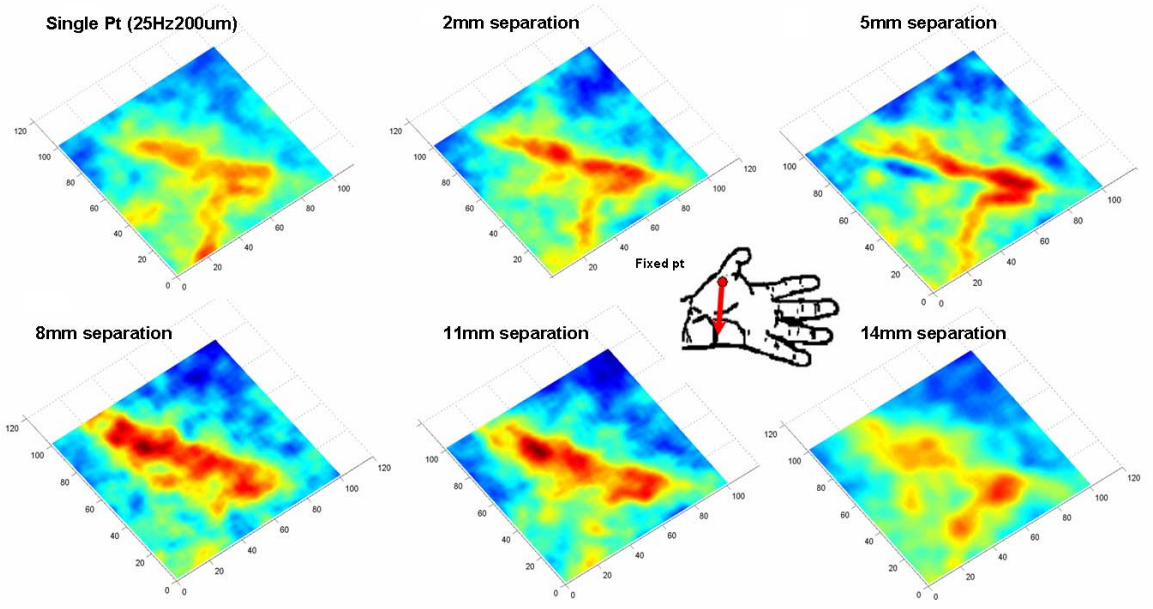

Figure 3. For all images, the 2x2mm ROI analyzed is the ROI that was evoked by the first stimulus. Both stimuli were 25Hz 200µm vibrotactile flutter stimuli, and both stimulus probes were applied simultaneously for 5sec. The fixed stimulus point position was at the thenar, and the second stimulus probe was moved 2, 5, 8, 11, and 14mm apart from the first stimulus position towards the hypothenar. Notice that the evoked spatial pattern is similar when the two stimuli are less that 5mm in separation. Note that the magnitude of the evoked response increases at all separations in comparison to the single point stimulus. However, at 8mm & 11mm separation, the evoked spatial pattern is significantly different from the spatial pattern evoked by a single stimulus. When the two stimuli are 14mm apart, notice that the evoked spatial pattern begins to resemble the spatial pattern evoked by a single stimulus.

Section II

Effects of Stimulus Duration on Minicolumnar Patterns

The differences between SI cortical response patterns evoked by short (less than 750 msec) and long (5 sec) stimulus duration flutter was examined and characterized. Preliminary findings suggested that for a given stimulus, the pattern of cortical response is an emergent property, and these patterns are not only stimulus specific, but time

dependent as well (Chiu *et al*, 2005). It was found that a long duration stimulus (5 sec) evoked an SI cortical pattern that was very different in its spatial organization after 3-5 seconds than a short duration (1 sec) stimulus. Although the peak response of the optical intrinsic signal (OIS) to a short duration stimulus is typically between 2.5 and 4 seconds after stimulus onset, the pattern of SI cortical response evoked by the short stimulus was very different from that evoked by the longer stimulus – even though the magnitudes of the response to the different stimuli are very similar (between 2.5 and 4 seconds after stimulus onset).

Additionally, in order to determine the effects of repetitive stimulation on the evoked minicolumnar patterns of SI cortical response, the effects of short duration stimulus (0.5sec) was compared with the effects of longer stimulus durations (1, 2, and 5sec). Tommerdahl *et al* (1999) have already shown that even for very different stimulus conditions (25Hz and 200Hz), regardless of the stimulus duration or amplitude, the earlier evoked spatial response patterns (<1sec after stimulus onset) were similar in nature, but the characteristics of the evoked spatial response patterns begin to differ and become more defined later on in the time course of the response (>1sec). Current findings show that short duration (0.5sec) vibrotactile flutter stimuli failed to produce a cortical response pattern that was as distinctly spatially organized as the patterns evoked by longer duration stimuli (>750msec). Cortical activation evoked by short duration stimuli was also more evenly distributed in the ROI.

Figure 4 compares the spatio- temporal response patterns evoked by a long duration (5sec) and short duration (0.5sec) with a 200 microns 25Hz flutter vibrotactile stimulus applied on the thenar eminence. OIS images with 2x2mm boxels surrounding

the ROI for both short (0.5sec) and long (5sec) duration stimuli are shown at the top of the image. Left and right panels are enlarged images of the surface plots of the 2x2mm ROI region for short and long duration stimulus, respectively, from 1-5 seconds after stimulus onset. For the long duration evoked cortical response (right panel), an organized spatial response pattern is already emergent at 1 second after stimulus onset, and the same groups of macrocolumns that is activated even at 1 sec after stimulus onset, only becomes more distinct over the course of the stimulus. The magnitude of response in the groups of activated macrocolumns also increase over time, while the magnitude of response in the regions surrounding these activated groups decrease. However, with the short duration stimulus (left panel), there is no noticeable organization in the spatial response. Even at 1 sec after stimulus onset, there is no emergent organized spatial pattern for the short duration stimulus that is seen at 1 sec after stimulus onset for the long duration stimulus. There is never a detectable, reproducible, or an organized spatial pattern of activation or "fixed" pattern of response seen in short duration stimuli. In fact, in short duration stimuli, over time the response of the activated region actually goes below the initial activity of that area.

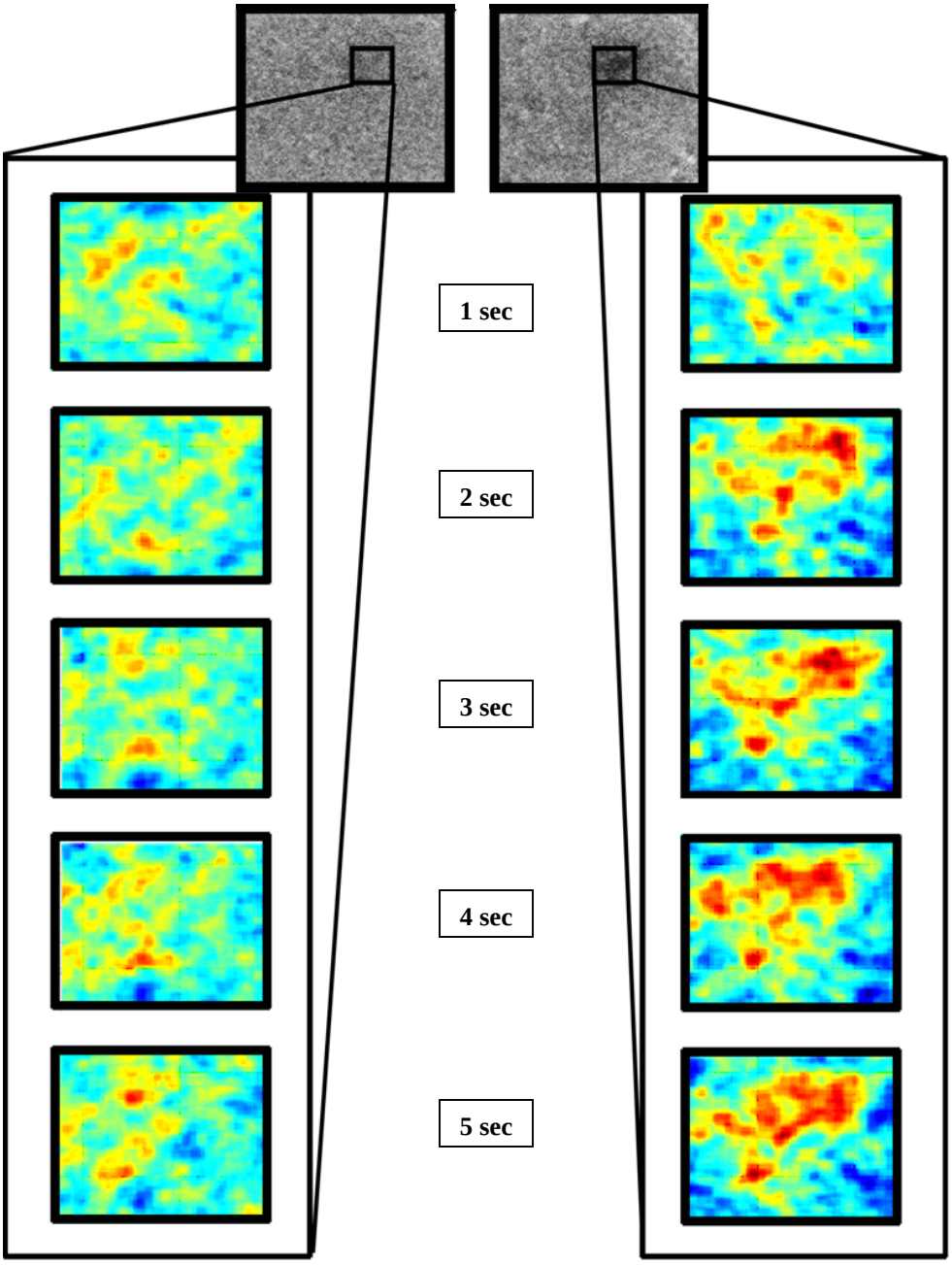

Figure 4. OIS images of short (0.5sec) and long (5sec) duration stimuli, respectively, with 2x2mm boxels surrounding the ROIs. Enlarged images of the ROI of the spatiotemporal patterns evoked by flutter vibrotactile stimuli (25Hz 200μm) applied on the thenar in 1 subject. Images shown are for 0.5sec (left panel) and 5sec (right panel) stimulus durations from 1-5 seconds after stimulus onset. Notice that the spatial pattern that is evoked 1sec after stimulus onset for the 5sec stimulus condition only becomes more distinct and prominent as time progresses, and the magnitude of the evoked response increases in those distinct regions. However, for the short stimulus duration (0.5sec), there is no distinct organized spatial pattern that is evoked by the stimulus.

In order to further assess the differences in the evoked spatial patterns as well as response characteristics between short and long duration stimuli, the cortical response in the 2x2mm ROI for the long duration stimulus was used as a template to assess the areas where maximal activation occurred. Figure 5 shows a filtered and thresholded image of the 2x2mm ROI region, top and bottom panels, respectively. The OIS images collected at 4-6sec after stimulus onset were summed, filtered, and thresholded so that the ROI was separated into two areas, the "highlighted" region which contains areas with activation in the top 10% (shaded black in the bottom image), and the "non-highlighted" region (white area in the bottom image) which contains the rest of the ROI not included in the highlighted region (figure 5). OIS images collected at 4-6sec after stimulus onset were chosen to be used in the analyses, because distinct regions that maximally respond to the stimulus have already formed a "steady-state" and organized spatial pattern that contains little variation in the evoked spatial pattern from 4-6 seconds after stimulus onset. This observation is similar to and already established concept of cortical response funneling, where the magnitude of response in the activated group of macrocolumns only becomes more defined over the course of the stimulus.

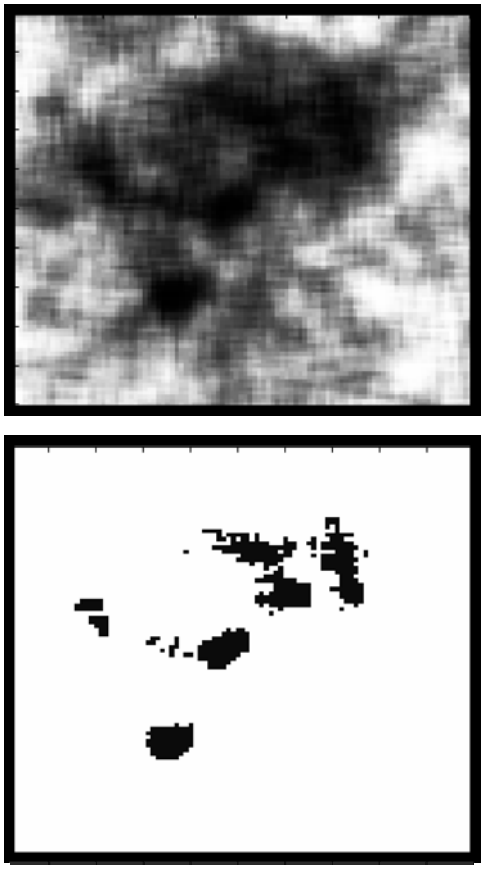

Figure 5. Filtered and thresholded OIS images of the 2x2mm ROI region obtained from the long duration stimulus condition, top and bottom panel, respectively. The ROI was separated into two areas for use in comparison analysis, the "highlighted" (shaded black in bottom panel) and "non-highlighted" regions (white area in bottom panel). "Highlighted" regions are regions which have activation in the top 10%.

Figure 6 contains plots of absorbance values that were obtained in the highlighted regions and non-highlighted regions of the ROI for both short and long duration stimuli. Notice that for the short duration stimulus, the absorbance values were similar for both highlighted and non-highlighted regions. This finding is highly significant because it reveals that cortical activation evoked by short duration stimuli are more evenly distributed, and that on average, the ROI contains no specific regions that significantly contribute to the overall magnitude of the evoked cortical response. In contrast, the

absorbance values in the highlighted region obtained from the long duration stimulus were significantly greater than the non-highlighted region, strengthening the idea that the evoked cortical response is strongly dependent on the emergent spatial pattern found only with long duration stimulus (i.e. repetitive stimulation). Figure 7 is an averaged plot (n=5) of absorbance values obtained in the highlighted and non-highlighted regions for both long and short duration stimuli. Notice that the same trends holds true for all subjects, where the absorbance values for short duration stimuli are similar for both highlighted and non-highlighted regions, whereas long duration stimuli have absorbance values that are significantly greater in the highlighted region than in the non-highlighted region.

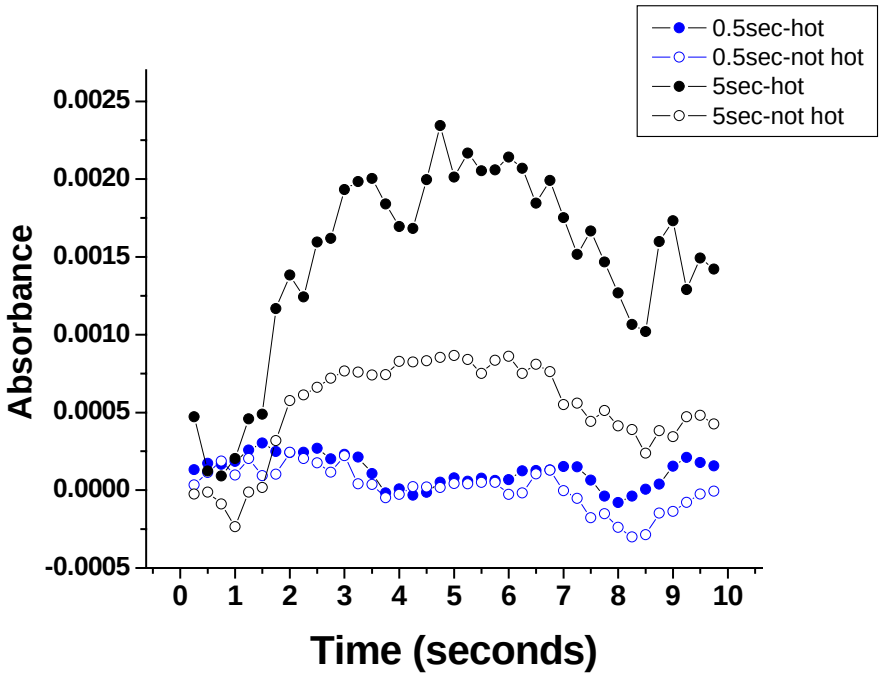

Figure 6. Plots of absorbance values obtained in "highlighted" and "non-highlighted" regions of both long (5sec) and short (0.5sec) duration stimuli. Notice that there is no significant difference in the absorbance values between the highlighted and non-highlighted regions for a short duration stimulus. However, for the long duration stimulus, the absorbance values in the highlighted region were significantly greater than the absorbance values in the non-highlighted region.

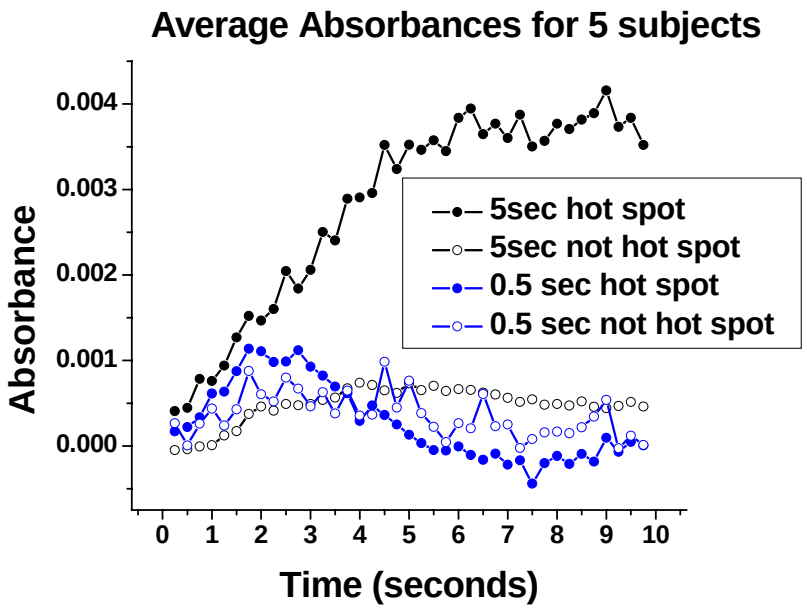

Figure 7. Averaged absorbance plots obtained in "highlighted" and "non-highlighted" regions of both long (5sec) and short (0.5sec) duration stimuli in 5subjects. Notice that for all subjects, there was no significant difference in the absorbance values between the highlighted and non-highlighted region for short duration stimuli. However, for the long duration stimuli, the absorbance values in the highlighted region were significantly greater than the absorbance values in the non-highlighted region in all subjects.

The effects of varying stimulus durations (0.5, 1, 2, and 5sec) on evoked cortical response in relation to evoked spatial patterns were also assessed. The hypothesis was that distinct and organized evoked cortical spatial patterns were only an emergent property of long stimulus durations, (i.e. stimulus durations >750msec). Figure 8 is a set of graphs of absorbance values obtained for both highlighted and non-highlighted regions. Notice that the absorbance values for both highlighted and non-highlighted regions are similar with stimulus duration of 0.5sec, which means that there are no distinct regions in the ROI that responds strongly to the applied stimulus. However, note that for a stimulus duration of 1sec, since the absorbance values obtained in the highlighted region of the ROI is significantly greater (almost double) than the absorbance values obtained in the

non-highlighted region, it can be concluded that distinct regions with increased cortical activity (i.e. evoked spatial pattern) that responds strongly to the stimulus have emerged. Additionally, the magnitude of the cortical response in this evoked spatial pattern ("highlighted" region) increases with increasing stimulus duration, and the overall response in the non-highlighted region tends to remain insensitive to changes in stimulus duration.

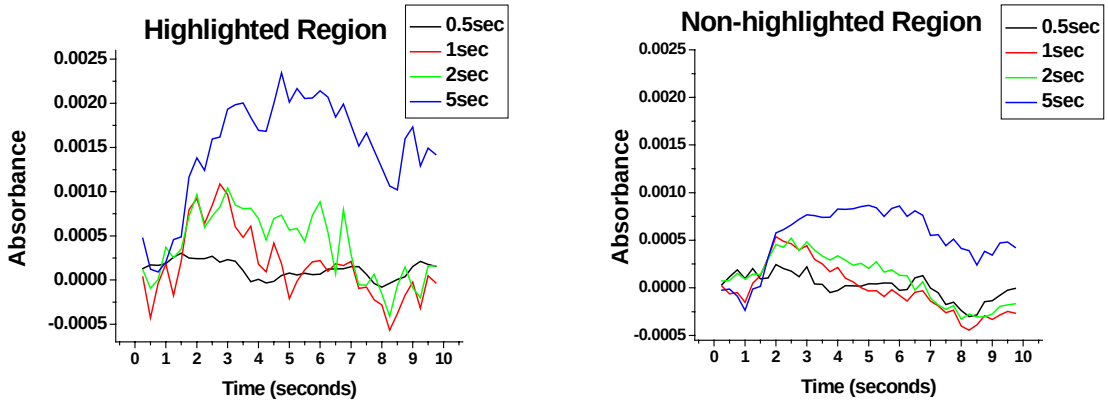

Figure 8. Absorbance values are plotted for both highlighted (left graph) and non-highlighted (right graph) regions for varying stimulus durations (0.5, 1, 2, and 5sec). Notice that absorbance values in the highlighted and non-highlighted regions are similar with the 0.5sec stimulus duration. However, even when the stimulus duration is 1sec, the absorbance values obtained in the highlighted region is already significantly greater than the absorbance values in the non-highlighted region. Note that the absorbance values in the highlighted region increase in magnitude with increasing stimulus duration, but the absorbance values in the non-highlighted region tend to be less sensitive to changes in stimulus durations.

The relative power spectra using 2-D Fourier Transforms were obtained to further characterize and quantify the differences in the evoked spatial patterns with regards to changes in stimulus duration (Figure 9). The relative power spectra for both short (0.5sec) and long (5sec) stimulus durations are plotted on the above graphs, respectively. The

relative power spectra of the control condition, (i.e. no stimulus), is plotted on the top row of graphs for both short and long stimulus durations. The relative power spectra at 2, 4, and 6sec after stimulus onset are plotted on second, third, and fourth row of the graphs, respectively. The prominent peak frequency for the control condition is marked with black vertical lines for both short and long stimulus conditions on the graphs, at 25cycles/mm (40.0μm period). With a long duration stimulus (5sec), there is an increase in the low frequency spectra from the control condition, where the prominent peak frequency decreases and is maintained at 17cycles/mm (58.8μm period). However, with the short duration stimulus, initially, the prominent peak frequency decreases to 14 cycles/mm (71.4μm period), but the frequency spectra almost immediately shifts towards higher spectral frequency by 4sec after stimulus onset, at 22cycles/mm (45.5μm period). The reasoning in the abrupt shift in the peak power spectra from lower frequency to higher frequencies for short duration stimuli is due to the lack of spatial organization or the formation of spatial patterns. Notice that at 6sec after stimulus onset, the spectral frequency for the short duration stimulus has almost returned to the peak spectral frequency of the control condition, but for the long duration stimulus, the peak spectral frequency is maintained at 17cycles/mm. From spectral frequency analysis, the data can be interpreted to show that the relative power for short duration response is greater than that of the long duration response, due to the lack of spatial organization in the cortical response.

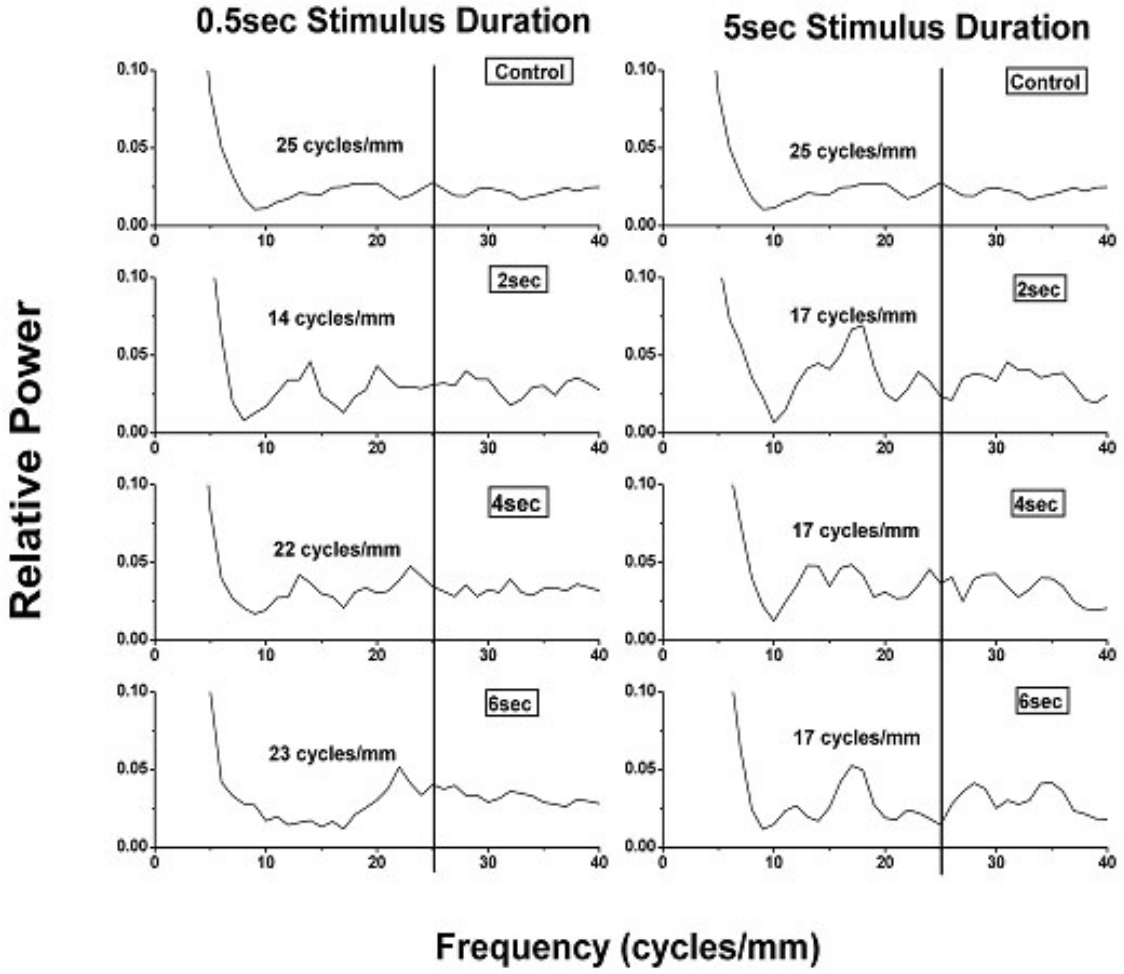

Figure 9. 2-D Fourier transforms of the ROI for both short (0.5sec) and long (5sec) stimulus durations. The relative frequencies were obtained for a control condition (i.e. no stimulus) and at 2, 4, and 6 seconds after stimulus onset. Notice that the prominent peak frequency of the short duration response initially decreases to lower spectral frequencies, but the peak spectral frequency immediately returns to higher spectral frequencies, similar to the peak spectral frequency of the control condition. However, with the long duration stimulus, the peak spectral frequency decreases to lower frequencies, and is maintained due to cortical spatial organization.

The conclusion that evoked spatial patterns are an emergent property, and that these evoked spatial patterns can only be found with long stimulus durations (>750msec), can prove to be relevant in the further understanding of tactile discrimination and how tactile information is processed cortically. With longer stimulus durations (>750msec) and with increasing stimulus amplitudes, regions that respond maximally in the region of

interest (ROI) will drive down the activity of its neighboring columns, therefore enhancing its evoked response to the stimulus. These evoked OIS spatial patterns will then become more distinct as stimulus duration increases, and will emerge much sooner with stronger stimulus amplitudes. The formation of these organized and "fixed" spatial patterns through repetitive stimulation could be one form of cortical processing or mechanism that could account for improvements in tactile discrimination, resulting in decreased psychophysical thresholds.

Section III

Different Modes of Long Duration Stimuli will evoke *different* but *reproducible* Cortical Response Patterns.

If stimulus position remained unchanged, globally, evoked cortical spatial patterns appear very similar. In chapter 3, it has previously been revealed that these evoked cortical patterns are stimulus dependent. However, how do these evoked cortical spatial patterns differ with varying stimulus parameters (i.e. frequency), and are the evoked minicolumnar patterns reproducible? Differences in stimulus frequency (20, 25, and 30Hz) were altered in order to determine the baseline quantitative differences in the cortical response patterns, (figure 10). In figure 10, summed OIS images at 4-6sec after stimulus onset were acquired from flutter vibrotactile stimulation of the thenar using varying stimulus frequencies (25, 30, or 35 Hz 200μm stimulus, respectively). Black boxels encompasses the ROI in each OIS image. Notice that the evoked macrocolumnar patterns are spatially similar regardless of the change in stimulus frequency.

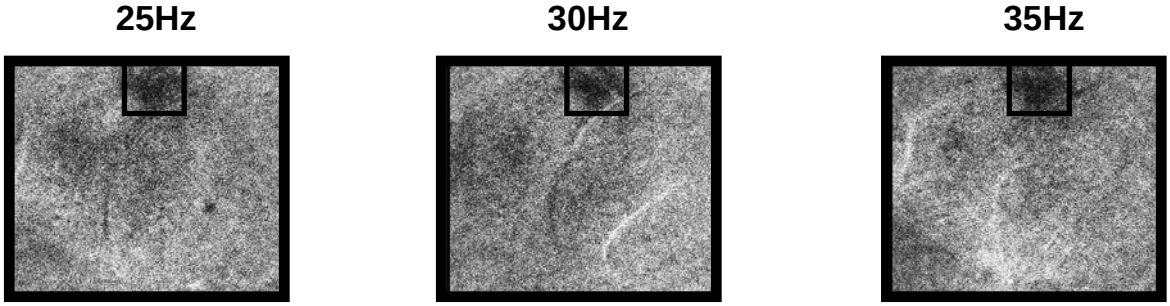

Figure 10. OIS images of the evoked responses are shown using 5sec 200μm vibrotactile stimuli with varying stimulus frequencies (25, 30, and 35Hz), respectively, in the flutter range. Stimulus was applied on the thenar of a subject. Note that all stimulus frequencies evoked similar global spatial patterns and had similar ROI.

However, enlarged images of the ROI revealed that even though the same groups of macrocolumns are activated regardless of stimulus frequency, the evoked minicolumnar patterns are very different. Figure 11 shows enlarged views from OIS images (top panel) of the ROI (indicated by a 2x2mm black boxel) activated with a 200μm 25, 30, or 35 Hz stimulus, respectively. The enlarged images were thresholded so that only regions that are activated in the top 10% are shaded black (bottom panel). Note that each frequency has evokes minicolumnar patterns that are discrete.

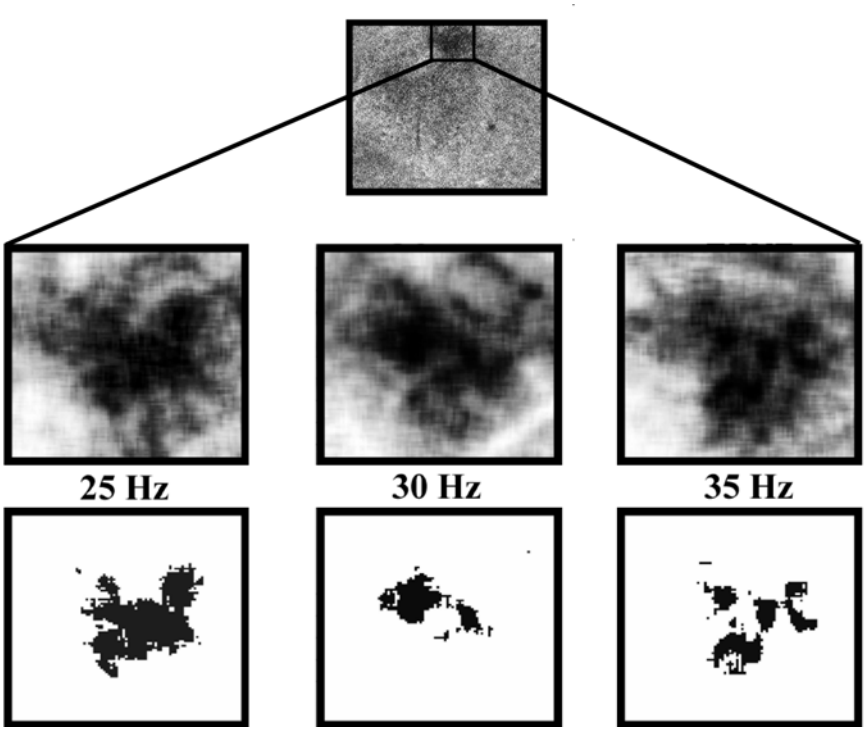

Figure 11. Enlarged images of the 2x2mm ROI evoked by 200μm vibrotactile stimuli with frequencies of 25, 30, and 35Hz. ROI is indicated by a black boxel in the OIS image at the top panel. Note that each frequency evokes minicolumnar patterns that are discrete.

Not only are the evoked minicolumnar patterns discrete for each stimulus frequency, but these evoked cortical spatial patterns are reproducible as well, further implying that each stimulus parameter has a specific spatial "code or pattern" that is learned and stimulus specific. With a repetitive stimulus, the cortex has the ability to learn what that stimulus is specifically, by spatially shaping its response to that particular stimulus, and is able to "recall" that spatial response pattern when the stimulus is reapplied. Figure 12 is another example of how even though the evoked global spatial patterns are similar, by examining the cortical response patterns more closely, the spatial patterns evoked by two different stimulus frequencies varied only by the alteration of the evoked minicolumnar patterns. Black 2x2mm boxels on the OIS images indicate the ROI

(first column). Enlarged images of the 2x2mm ROI (second column) obtained from OIS images reveal the differences in the evoked minicolumnar patterns from a 25Hz (top panel) or 20Hz (bottom panel) 200µm 5sec vibrotactile stimulus. The enlarged ROI images were then thresholded (showing only regions with top 10% activation) for both stimulus frequencies (25Hz in gray; 20Hz in red), and superimposed on top of one another (far right image). A gray arrow indicates the region ("region 1") where a 25Hz stimulus evoked a greater response than the 20Hz stimulus, and a red arrow indicates the region ("region 2") where the evoked response was greater with the 20Hz stimulus in comparison to the 25Hz stimulus.

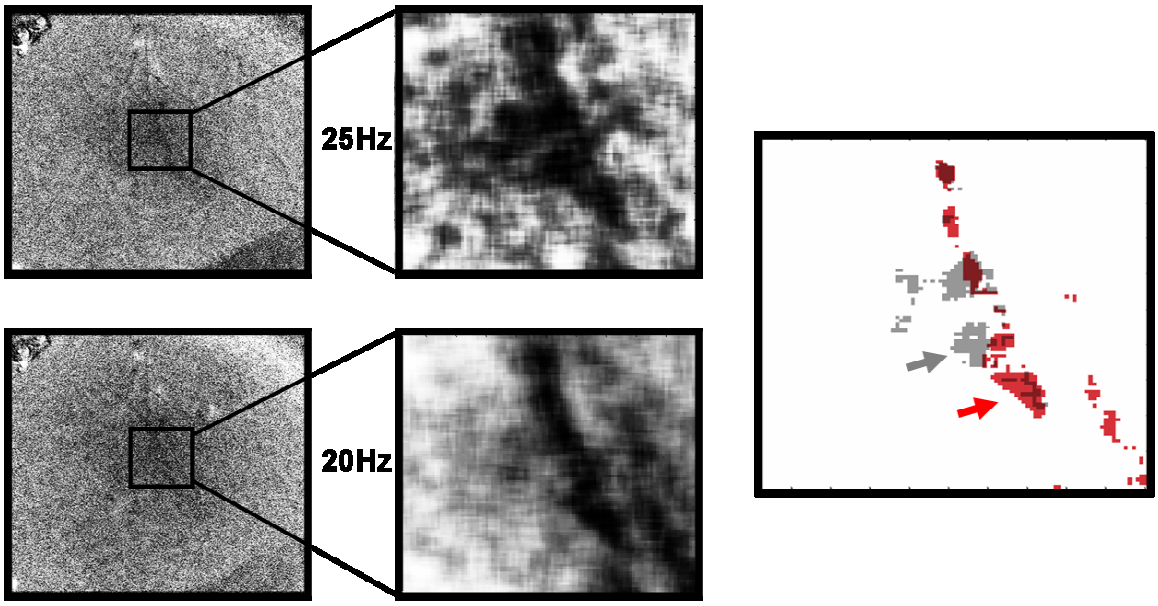

Figure 12. OIS images obtained from either a 25 or 20 Hz 200µm 5sec vibrotactile stimulus (left panel). A 2x2mm black boxel indicated the ROI. Second panel shows enlarged views of the ROI. Far right image shows thresholded images showing regions with top 10% activation superimposed on top of one another for both 25Hz (red) and 20Hz (gray) stimuli. Red arrow indicates where the evoked response from the 25Hz stimulus was greater than the 20Hz stimulus, and the gray arrow indicates the region where the evoked response was greater for the 20Hz stimulus than the 25Hz stimulus.

Since the differences were found not globally, but in the evoked minicolumnar patterns, absorbance values were obtained at the regions which were found to be greater for one stimulus frequency over the other. When the cortical response in one region is increased, another region in the evoked minicolumnar pattern will decrease. The absorbance values obtained in "region 1" and "region 2" from cortical responses of both 25Hz and 20Hz stimulus are plotted on the far left and right graph, respectively, of figure 13. Small figures on the bottom right had corner of the graphs indicates where the regions were in the ROI. Notice that response in region 1 was greater for the 25Hz stimulus, and the response in region 2 was greater for the 20Hz stimulus. Just by altering the minicolumnar pattern minimally, the cortex was able distinguish between the two different stimulus frequencies.

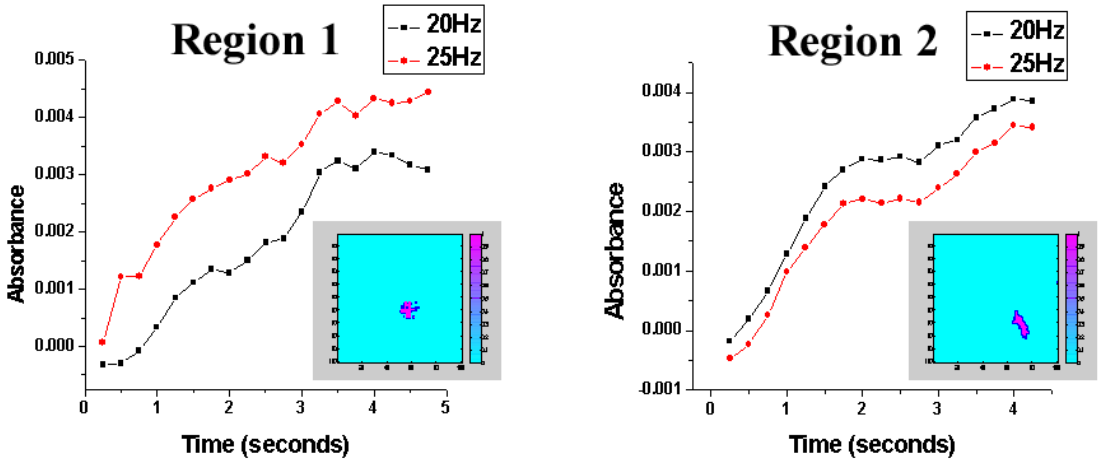

Figure 13. Absorbance values obtained in "region 1" and "region 2" (indicated by figures on bottom right had corner of graphs), were plotted on the above graphs for both 25Hz and 20Hz vibrotactile stimuli. Cortical responses were evoked with either a 5sec 200µm 25Hz or 20Hz stimulus. Notice that "region 1" is an area where the cortical response was greater for the 25Hz stimulus than the 20Hz stimulus, and "region 2" shows the region where the cortical response was greater for the 20Hz stimulus than the 25Hz stimulus.

Furthermore, when the 25Hz 200µm 5sec vibrotactile stimulus was applied during two separate sets of experimental trials the cortex was able to reproduce the evoked spatial pattern observed from the first set of experimental trials, shown in figure 14. Enlarged images of the ROI (indicated with a 2x2mm black boxel) from the OIS images were obtained and thresholded to show only regions with top 10% activation (second and third columns, respectively). The thresholded images from both experimental trials were superimposed over one another. Notice how the evoked spatial patterns in both cases are essentially the same. Just from inspection of the enlarged OIS images, the differences are difficult to distinguish.

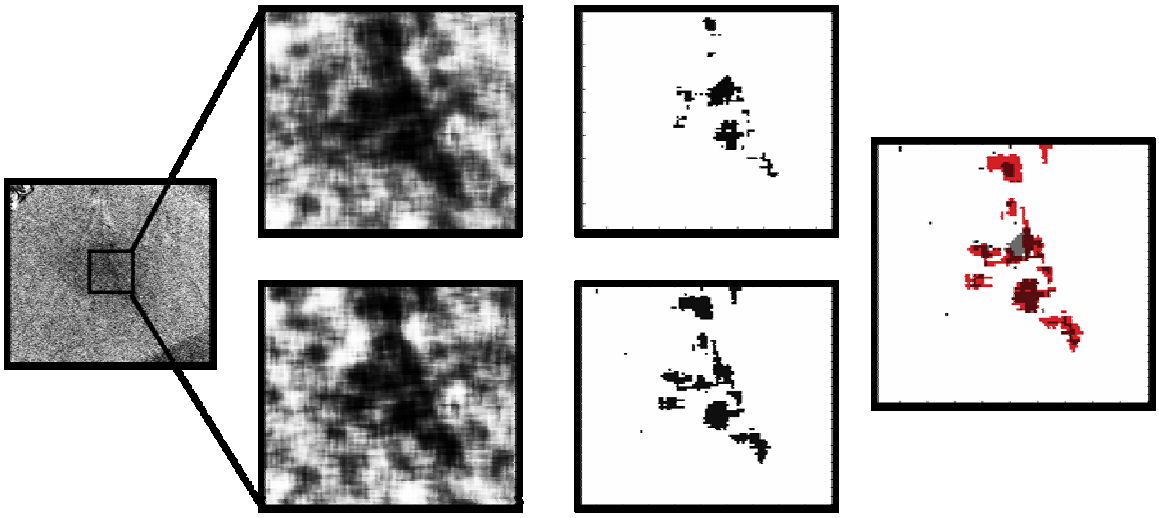

Figure 14. Enlarged views from OIS images are shown in the second column of images. All images were obtained from two separate sets of experimental trials using a 25Hz 200µm 5sec vibrotactile stimulus. A 2x2mm black boxel from the far left OIS image indicates the ROI. Third column of images are thresholded OIS images of the enlarged views, showing only regions with top 10% activation. These thresholded images are then superimposed on top of one another and shown in the far right image. Note the strong similarity between the evoked spatial response patterns obtained during separate experimental trials.

The cortex has now been shown to be capable of reproducing these evoked spatial patterns across experimental trials. The fact that these evoked spatial patterns are stimulus specific is relevant to the further understanding of how a person can determine what the perceived stimulus is, and how to discriminate between stimuli. These observed findings could reveal some insight into the mechanisms with which perceived tactile discrimination occurs.

Section IV

Effects of pre-exposure to a skin stimulus on the minicolumnar pattern of a subsequent skin stimulus

In order to determine the impact that short term sensory history has on subsequent novel stimuli, the effect of an adapting stimulus (i.e. long duration stimulus) on a novel stimulus was examined. The changes that were observed in the SI cortical response were hypothesized to correlate with the perceptual changes that are caused by the same stimulus conditions in human psychophysical studies. An adapting stimulus will evoke a discrete minicolumnar pattern in SI, and when a second, novel stimulus ("test stimulus") is applied at the same skin position (which differs in frequency, but not significantly, from the adapting stimulus), the evoked global spatial pattern will remain unchanged, but changes in the minicolumnar patterns will occur over time, and the evoked minicolumnar patterns will begin resembling the minicolumnar patterns specific to the novel stimulus. Human psychophysical studies have shown that, in the presence of an adapting stimulus,

thresholds to stimuli similar to the adapting stimulus increases but ability to discriminate between similar stimuli increases. Such psychophysical findings have been reported for a subject's ability to discriminate amplitude and frequency of a stimulus (Hollins *et al*, 1990).

Long stimulus durations (>0.5sec) have been shown to evoke spatial patterns that are discrete and well defined. A possible mechanism to why psychophysical thresholds are elevated is that since the adapting stimulus and the test stimulus both spatially activate the same groups of macrocolumns, the same sets of neurons have already been activated, and a stimulus that is not significantly different from the adapting stimulus will not significantly change the evoked minicolumnar pattern resulting in increased discrimination thresholds. Improvement in tactile discrimination may also occur due to the fact that the evoked spatial pattern from the adapting stimulus has already emerged and has become "primed". However, if the cortex does not have ample time between the adapting stimulus and the test stimulus to return to baseline cortical activity, the evoked spatial pattern from the adapting stimulus will be maintained by the cortex, therefore reducing the time it takes for the test stimulus to evoke and shape its minicolumnar pattern, resulting in improved discrimination.

Figure 15 shows an example of how the cortex was able to maintain the evoked spatial pattern from a 5sec 25Hz 200μm adapting stimulus before a 5sec 20Hz 200μm test stimulus was applied after a 1sec interstimulus interval. The OIS image at the top of the figure has a 2x2mm black boxel surrounding the ROI where the enlarged images in the second row were obtained. Third row of images are thresholded images of the enlarged images of the ROI where regions with top 10% activation are shown. Notice

that the evoked spatial patterns in the second row of images for both the adapting stimulus and the test stimulus are similar. Even as early as 2 seconds after the test stimulus is applied, the evoked minicolumnar pattern already resembles the evoked minicolumnar pattern of the 20Hz 200μm vibrotactile stimulus obtained from earlier trials (refer to figure 12 for evoked spatial patterns with respect to either a 25Hz or 20Hz 200μm vibrotactile stimulus from earlier trials). A red circle encompasses the region that responded to the 25Hz stimulus more strongly that the evoked response from the 20Hz stimulus. After the test stimulus has been applied, note the decrease in the evoked cortical response in this region. Notice that the evoked spatial patterns obtained from 3-5sec after stimulus onset from the 25Hz adapting stimulus and the resulting evoked minicolumnar pattern from the 20Hz test stimulus (2sec after test stimulus onset) resembles the evoked spatial patterns from earlier experimental trials seen in figure 12.

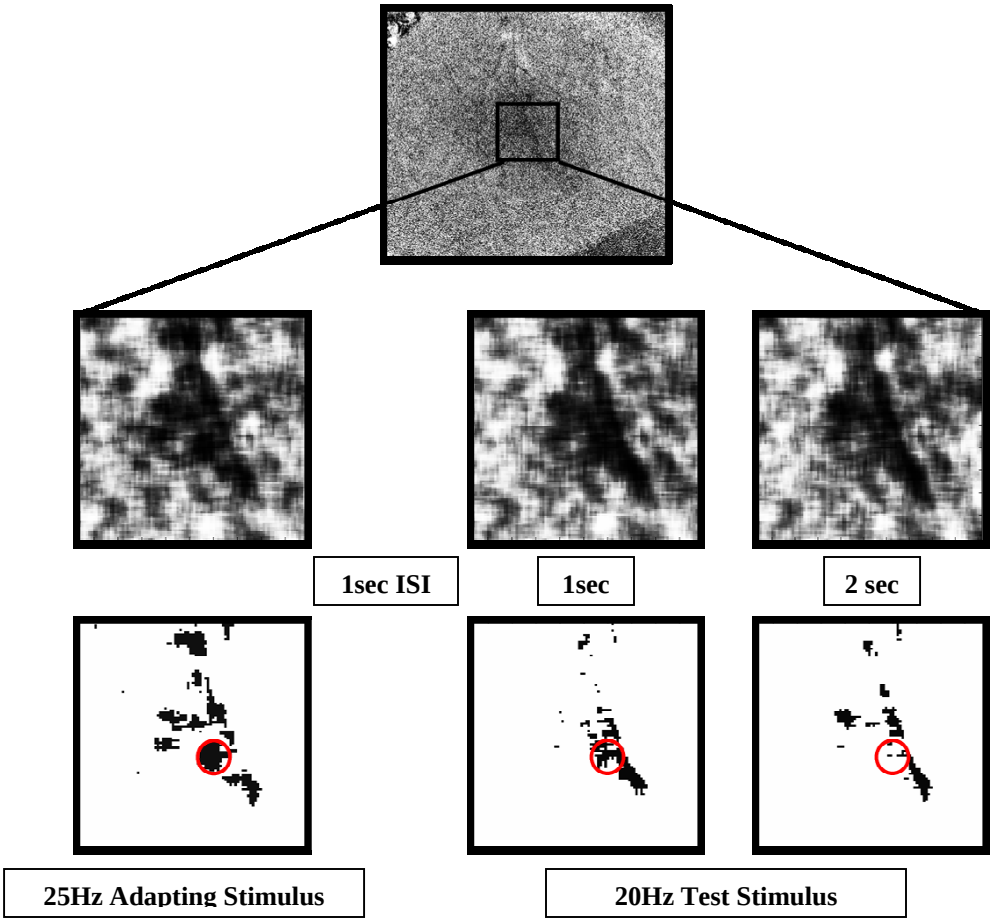

Figure 15. OIS images obtained from a 5sec 25Hz 200µm adapting stimulus followed by a 5sec 20Hz 200µm test stimulus, with a 1sec ISI. A 2x2mm black boxel on the top OIS image indicates the ROI where enlarged images shown in the second row were obtained. Third row of images were obtained by thresholding the ROI to show regions with activation in the top 10%. First column of images of the enlarged ROI were obtained at 3-5sec after the adapting stimulus was applied, and the second and third column of the enlarged images were obtained after the 20Hz test stimulus was applied for 1sec and 2sec, respectively. Note that as early as 1 sec after the test stimulus has been applied, the evoked minicolumnar pattern already begins to resemble the minicolumnar pattern evoked by a 20Hz 200µm vibrotactile stimulus obtained in previous trials (see figure 12). A red circle encompasses "region 1" (region where the evoked response was greater for the 25Hz stimulus than the 20Hz stimulus). Notice that the evoked response in region 1 decreases after the test stimulus has been applied.

In order to further assess the changes in the cortical response after the test stimulus has been applied, absorbance values were obtained from "region 1" and "region

2" (plotted on graphs, figure 16). Notice that the absorbance values in the region that was strongly activated by the 20Hz test stimulus increases ("region 2") after the test stimulus was applied, and the absorbance values in the region that was strongly activated by the 25Hz adapting stimulus decreases ("region 1"). This finding is indicative of the role that minicolumnar response patterns have, in which the cortex uses as a mechanism to discriminate between two different stimuli. Again, the cortex is also able to reproduce the evoked minicolumnar patterns, even after it has already adapted to a particular stimulus. As long as the adapting stimulus and the test stimulus are similar, it will be able to temporally reproduce the evoked minicolumnar pattern of the test stimulus quicker than if the test stimulus had been applied solely.

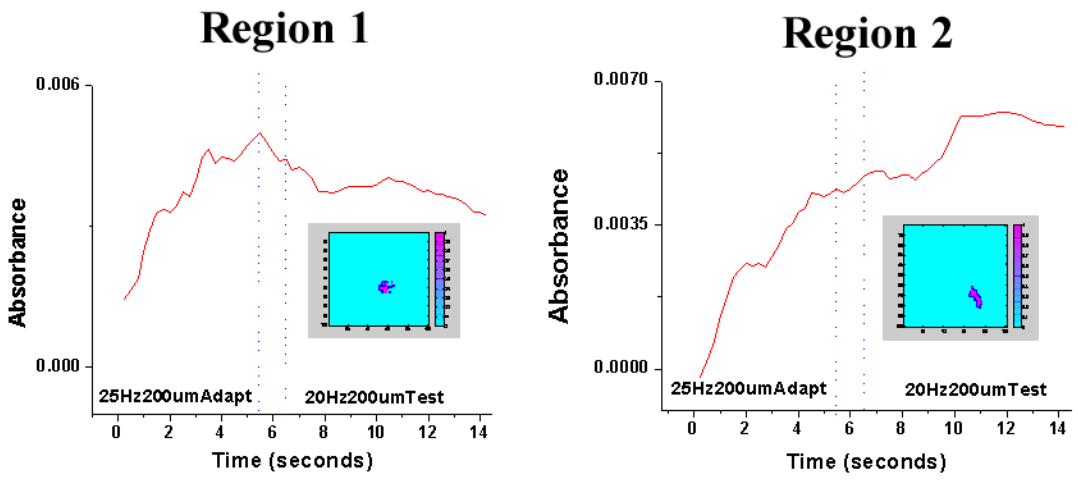

Figure 16. Absorbance values obtained in both "region 1" and "region 2" are plotted on the above absorbance graphs, respectively. The first dotted vertical line represents where the 5sec 25Hz adapting stimulus was removed, and the second dotted vertical line represents when the 5sec 20Hz test stimulus was applied. Notice that the absorbance values in region 1 decreases after the 20Hz test stimulus has been applied. In contrast to region 1, the absorbance values in region 2 increases in response to the 20Hz stimulus.

However, if the test stimulus was significantly different from the adapting stimulus, then the test stimulus will disrupt the evoked spatial pattern of the adapting stimulus, and this robust change in the evoked spatial pattern will lead to an unorganized cortical response pattern, which could possibly cause both tactile discrimination and psychophysical thresholds for the test stimulus to decrease.

In addition, long stimulus durations will cause neurons to adapt and show entrainment, and neuronal populations will become more synchronous. Therefore, it can be suggested that evoked "fixed" spatial patterns are necessary for tactile discrimination. If the test stimulus applied after the adapting stimulus was similar to the adapting stimulus, then entrainment will be expected to occur faster temporally, and discrimination thresholds will decrease. However, if the test stimulus was significantly different from the adapting stimulus, then entrainment will be disrupted, and discrimination thresholds for the test stimulus will be increased.

Prior psychophysical studies have also shown that threshold elevation relies on the relationship between the vibrotactile frequencies of the adapting and test stimuli (Wedell, 1938). Adaptation was found to lower the detection threshold for a stimulus that is different from that of adapting stimulus, therefore enhancing discrimination. Hollins and co-workers (Hollins *et al*., 1990) predicted that for a given adapting frequency, the amount of threshold elevation produced was a systematically increasing function of the amplitude of the adapting stimulus. Finally, improvement in discrimination was found to occur when the amplitude and frequency of the test stimulus and the adapting stimulus were comparable (Goble and Hollins, 1993; Delemos and Hollins, 1996). The current cortical response characteristics observed thus far, tries to correlate cortical

response to the psychophysical findings. The data provides a more in depth characterization of minicolumnar response to tactile stimuli, and was aimed to further understanding the mechanisms of perceived tactile discrimination.

Chapter 5

CONTRALATERAL EFFECTS ON IPSILATERAL RESPONSE IN SI

This chapter shows an example of a published method for comparing activity in the ROI using high resolution pattern analyses. It is also the first time it has been shown that spatial patterns of minicolumnar activity play an important role in information processing. Many believed that information processing was only due to temporal coding, and also that there were no bilateral effects to the evoked tactile response. However, as shown in this chapter, some minicolumns change their activity when an ipsilateral stimulus is applied in conjunction to a contralateral stimulus. Some cells were found to only have contralateral RFs, while some cells have bilateral RFs. Most of the content in this chapter has been published in "Ipsilateral input modifies the SI response to contralateral skin flutter" in "*Journal of Neuroscience*" (Tommerdahl et al, 2006).

Chapter Abstract

We recorded the optical intrinsic signal (OIS) response of squirrel monkey SI cortex to 25Hz vibrotactile ("flutter") stimulation applied independently to the thenar eminence on each hand, and also to bilateral (simultaneous) stimulation of both thenars. The following observations were obtained in every subject (n=5): (1) ipsilateral stimulation was accompanied by an increase in absorbance within the SI hand region substantially smaller than the absorbance increase evoked by contralateral stimulation; (2) the absorbance increase evoked by simultaneous bilateral stimulation was smaller (by ~30%) than that evoked by contralateral stimulation; (3) the spatiointensive pattern of the SI response to bilateral flutter was distinctly different than the pattern that accompanied contralateral flutter stimulation – with contralateral flutter the center of the responding region of SI underwent a large increase in absorbance, whereas absorbance decreased in the surrounding region; in contrast, during bilateral flutter absorbance decreased (relative to that evoked by contralateral flutter) in the central region of SI, but increased in the surround. The results raise the possibility that somatosensory perceptual experiences specific to bimanual tactile object exploration derive, at least in part, from the unique spatiointensive activity pattern evoked in SI when the stimulus makes contact with both hands. It is suggested that modulatory influences evoked by ipsilateral thenar flutter stimulation reach SI via a 2-stage pathway involving interhemispheric (callosal) connections between information processing levels higher than SI, and subsequently via intrahemispheric (corticocortical) projections to the SI hand region.

Introduction

The activity a stimulus evokes in skin mechanoreceptive afferents is projected at short latency, and with great security to neurons in the middle laminae of primary somatosensory cortex (SI) in the contralateral hemisphere. Additionally, imaging and neurophysiological studies (Lipton *et al*., 2006; Iwamura *et al*., 2001 – in monkeys; Hlushchuk *et al*., 2006; Nihashi *et al*., 2005; Kanno *et al*., 2003; Korvenoja *et al*., 1999; Allison *et al*., 1989a,b – in humans) have described modifications of SI (area 3b) activity in response to input evoked either by mechanical stimulation of an ipsilateral skin site or electrical stimulation of an ipsilateral peripheral nerve. Human investigations have shown that ipsilateral input can modify the SI response to a subsequent contralateral stimulus. Schnitzler *et al*. (1995), using magnetoencephalography (MEG), reported that concurrent tactile stimulation of the ipsilateral hand *enhances* SI's response to stimulation of the contralateral median nerve. Conversely, (i) Korvenoja *et al*. (1995) reported that the SI activation (detected using MEG) evoked by contralateral median nerve stimulation is *suppressed* during ipsilateral hand movement, (ii) fMRI studies in both monkeys (Lipton *et al*., 2006) and humans (Hluschuk *et al*., 2006) showed that an ipsilateral skin stimulus evokes CNS actions that partially *suppress* the SI response to a contralateral stimulus, (iii) destruction of SI in one hemisphere (rats) was shown to be accompanied by the appearance (in the opposite SI) of neurons with bilateral receptive fields (interpreted to indicate that SI activity exerts a suppressive influence on SI neurons in the opposite hemisphere – Pluto *et al*., 2005), and (iv) low-frequency transcranial magnetic stimulation of sensorimotor cortex (TMS, in humans – Pal *et al*., 2005) was found to reduce excitability in the opposite hemisphere. Viewed collectively, these findings raise

the possibility that the SI hand region's response to a tactile stimulus (and thus the stimulus-evoked perceptual experience) may be subject to modulatory influences arising from the ipsilateral hand.

The concept of the SI (especially area 3b) hand region as a processor of tactile information arising exclusively in contralateral skin mechanoreceptors has coexisted with the idea that fusion of tactile information from the two hands occurs at a relatively early stage of cortical information processing. Casual observation makes it evident that concurrent and/or sequential tactile stimulation of the hands is the frequent result of subject-initiated motor behaviors (e.g., bimanual tactile exploration), and experimentation has shown that such stimulation underlies perceptual capacities of considerable adaptive value. Examples are the abilities to: (1) categorize and discriminate tactile patterns that engage both hands (Craig and Qian, 1997; Craig, 1985); (2) detect and discriminate the direction and velocity of stimuli that move sequentially or simultaneously over the two hands (Essick and Whitsel, 1988); and (3) compare the frequencies of vibrotactile stimuli applied to bilateral sites on the distal fore- or hindlimbs (Harris *et al*., 2001).

This study used the OIS imaging method to evaluate the impact of ipsilateral stimulation on SI tactile information processing. More specifically, we determined the effects of 25 Hz vibrotactile ("flutter") stimulation of the ipsilateral thenar eminence on the SI response to an identical stimulus applied contralaterally. The results suggest that the effect of ipsilateral input to tactile information processing in the SI hand region is substantial, and provide clues about the underlying neural mechanisms.

Methods

Subjects & preparation. Adult squirrel monkeys (males and females; n = 5) were subjects. All surgical procedures were carried out under deep general anesthesia (1 – 4 % halothane in a 50/50 mixture of oxygen and nitrous oxide). After induction of general anesthesia the trachea was intubated with a soft tube; a polyethylene cannula was inserted in the femoral vein to allow administration of drugs and fluids (5 % dextrose and 0.9 % NaCl). A 1.5 cm diameter opening was made in the skull overlying SI cortex, a chamber was mounted to the skull over the opening with dental acrylic, and the dura overlying SI was incised and removed. Following completion of the surgical procedures all wound margins were infiltrated with long-lasting local anesthetic, skin and muscle incisions were closed with sutures, dressed with topical local anesthetic and bandaged.

1-3 hours prior to the image data acquisition phase of the experiment the subject was immobilized by i.v. infusion of Norcuron (vecuronium; 15 μg/kg/hr) and ventilated with a gas mixture (a 50/50 mix of oxygen and nitrous oxide; supplemented with 0.1 - 1.0 % halothane when necessary) delivered via a positive pressure respirator. Respirator rate and volume were adjusted to maintain end-tidal CO_2 between 3.0 - 4.0 %; EEG and autonomic signs (slow wave content; heart rate, etc.) monitored continuously and titrated (by adjustments of the anesthetic gas mixture) to maintain levels consistent with general anesthesia. Rectal temperature was maintained (using a heating pad) at 37.5 ° C. Euthanasia was achieved by intravenous injection of pentobarbital (45 mg/kg) and by intracardial perfusion with saline followed by fixative (10% formalin). Following the perfusion a tissue block was removed that contained the cortical region from which images were obtained and placed in fixative. After adequate fixation each cortical tissue

block was serially sectioned and the sections mounted and stained to demonstrate cortical cytoarchitecture.

All experimental procedures were reviewed and approved in advance by an institutional committee and are in full compliance with current NIH policy on animal welfare.

Stimuli and stimulus protocols. Precisely controlled sinusoidal vertical skin displacement stimulation (25Hz, 200 μm, stimulus duration 5sec, interstimulus interval 60sec - "skin flutter") was delivered using two servocontrolled transducers (Cantek Enterprises, Canonsburg, PA). The probe of each stimulator was advanced (using micropositioners) so that in the absence of stimulation the probe of each stimulator indented the skin by 500 microns - i.e. each stimulator probe was advanced 500 μm from the point at which it made initial contact with the skin. Skin contact was detected and signaled by the force transducer and readout circuitry of each servocontroller.

The flutter stimuli were delivered (1) independently to each member of a pair of mirror-symmetric ipsilateral and contralateral skin sites, and (2) simultaneously to the two sites (bilateral stimulation). Stimulus sites were located on the center of the thenar eminence. The sinusoidal contralateral and ipsilateral components of each bilateral flutter stimulus always were in-phase and synchronized so that the two stimuli started and stopped at the same time. The contralateral, ipsilateral, and bilateral skin flutter stimuli were delivered in the same run, and interleaved on a trial-by-trial basis.

OIS imaging. The imaging system consisted of a computer-interfaced CCD camera (Quantix 540; Roper Scentific), light source, guide and filters required for near-infrared (833 nm) illumination of the cortical surface, a focusing device, and a recording

chamber capped by an optical window (for additional details concerning procedures and apparatus see (Tommerdahl *et al*., 1999a; Tommerdahl *et al*., 1999b). Images of the exposed cortical surface were acquired 200 ms before stimulus onset (‘‘reference images’’) and continuously thereafter for 22 s after stimulus onset (‘‘poststimulus images’’) at a rate of one image every 0.9 –1.4 s. Exposure time for each image was 200 ms. Difference images were generated by subtracting each pre-stimulus image from its corresponding post-stimulus image. Averaged OIS difference images typically show regions of both increased light absorption (decreased reflectance) and decreased light absorption (increased reflectance) believed widely (Grinvald, 1985; Grinvald *et al*., 1991) to be accompanied by neuronal activation and inhibition, respectively. Use of near-infrared illumination minimizes the contributions to OIS images of the changes in cerebral cortical blood flow and flow/volume that normally accompany neuronal activation, and thus reflects the spatial location of stimulus-evoked changes in neuronal activity more accurately than do images obtained at lower wavelengths (Ba *et al*., 2002). Every difference image was examined prior to generation of summary graphics or statistical analyses. Any image containing random high amplitude noise was eliminated, and the remaining images obtained under a given stimulus condition (never fewer than 15; all obtained during the same run) were averaged to improve the signal-to-noise ratio of the response to that stimulus. Image analysis was carried out using custom routines written in Matlab.

Histological procedures/identification of cytoarchitectural boundaries. Following adequate fixation the tissue block containing the imaged cortical region was cryoprotected, frozen, sectioned serially at 30μm, and the sections stained with cresyl fast

violet. The boundaries between adjacent cytoarchitectonic areas were identified by scanning individual sagittal sections separated by no more than 300 μm and were plotted at high resolution using a microscope with a drawing tube attachment. The resulting plots were used to reconstruct a two-dimensional surface map of the cytoarchitectonic boundaries within the region studied. As the final step, the cytoarchitectonic boundaries were mapped onto the images of the stimulus-evoked intrinsic signal obtained from the same subject, using fiducial points (made by postmortem applications of India ink or by needle stabs) as well as morphological landmarks (e.g., blood vessels and sulci evident both in the optical images and in histological sections). Locations of cytoarchitectonic boundaries were identified using established criteria (Powell and Mountcastle, 1959a; Powell and Mountcastle, 1959b; Jones and Porter, 1980).

Results

The response of SI in the right hemisphere to vibrotactile stimulation of a site on each hand (center of thenar eminence) was studied in 5 squirrel monkeys. The goal in each experiment/subject was to assess the influence, if any, of ipsilateral stimulation on the response evoked from the mirror-symmetric contralateral skin site.

The patterns of absorbance change recorded in the hand representational region of SI in 2 of the 5 subjects are shown in Figure 1. The grayscale average difference images in the top and 3rd rows of Figure 1 show not only the response of the SI hand region to each of the three conditions of skin flutter stimulation (i.e., “contralateral, bilateral, ipsilateral”), but also the spatiointensive pattern of absorbance values recorded in the same SI region in the absence of intentional stimulation (“control”). Visual inspection of

these grayscale images reveal that in both exemplary subjects (1) the magnitude of the response to contralateral flutter exceeds by far the response to flutter stimulation of the mirror-symmetric ipsilateral skin site, whereas (2) although differences between the responses to contralateral vs. bilateral skin flutter can be discerned, they are relatively subtle.

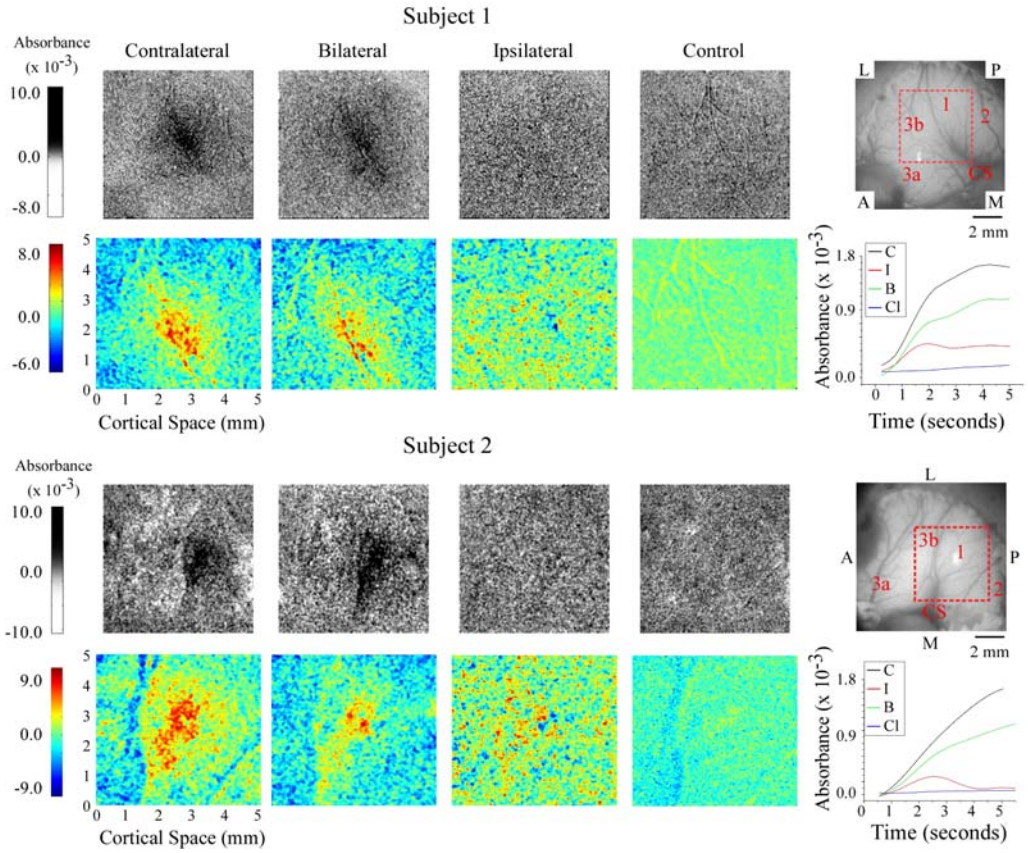

Figure 1. OIS response evoked by flutter stimulation of the thenar eminence in two subjects. *1st & 3rd Row*: Averaged difference images for responses evoked by contralateral, bilateral, and ipsilateral stimuli as well as the no-stimulus control. Orientation of images is indicated in the reference image at the right; P (posterior), A (anterior), M (medial) and L (lateral). *2nd & 4th row*: Selected regions (ROI is defined in image at far right of 1st & 3rd row) from absorbance images for each subject. Absorbance time courses are plotted and color-coded for each stimulus condition at far right; time courses were calculated within a 2mm diameter area centered on the region that maximally responded to contralateral stimulation.

Color maps of the responding region within each average difference image (ROI; the 5 x 5 mm region centered on the maximal response evoked by the contralateral stimulus – outlined in red in the image of the cortical surface shown at right of the top and 3rd rows in Figure 1) make evident the differences between the responses of SI of each subject to the 3 conditions of skin flutter stimulation. First, under the bilateral condition not only is the average response weaker than that evoked by contralateral skin flutter (for each subject compare 1st and 2nd color maps from left), but it also is spatially less extensive. Second, although the response to ipsilateral flutter is located in the same SI region that responds to contralateral flutter, the spatial distribution of absorbance values evoked by the ipsilateral stimulus is distinctly different from that (i) evoked from the contralateral site and (ii) obtained in the absence of stimulation (the no-stimulus condition) – i.e., in each subject ipsilateral flutter evoked a unique and spatially inhomogeneous pattern of absorbance values within the ROI. For both of the subjects whose data are illustrated in Figure 1 the average across-ROI increase in absorbance evoked by ipsilateral flutter is substantially smaller than the average across-ROI absorbance increase evoked by contralateral flutter, at numerous loci within the ROI the absorbance values attained during ipsilateral skin flutter exceed by far the values measured at the same locations in the absence of stimulation (compare 3rd and 4th color maps from left in 2nd and 4th rows in Figure 1).

The absorbance *vs.* time plots at the right of Figure 1 (2nd and 4th rows from top) show the time course of the response of SI to each of the four conditions (points on each curve show absorbance values at successive time intervals averaged across the 2mm diameter region that responded maximally to contralateral stimulation; see Simons *et al.* ,

2005 for methodological details). Such plots quantitatively confirm the impression (gained from visual inspection of the grayscale difference images in Figure 1) that the response of SI of each subject to bilateral skin flutter was substantially weaker than the response to contralateral flutter. In addition, the plots demonstrate that the SI responses (absorbance increases) to contralateral *vs.* bilateral skin flutter follow a very similar time course.

The across-subject consistency of the observations was evaluated by determining the average across-subject (n=5) absorbance value associated with each condition (summary graph in Figure 2). The fact that the contralateral-only stimulus condition evoked the strongest response in every subject permitted convenient normalization of the values of the absorbance increase obtained from each subject – i.e., the absorbance values obtained from each subject under the ipsilateral and the bilateral stimulus conditions were expressed in terms of the absorbance value obtained from the same subject under the contralateral stimulus condition (as a consequence, standard error for the response to the contralateral stimulus condition = 0). Surprisingly, the bar graph in Figure 2 reveals that while the average across-subject response to ipsilateral stimulation is only slightly greater than the across-subject average response observed in the absence of stimulation, the average response to bilateral flutter stimulation is ~35% smaller than the average response to contralateral skin flutter. In every subject the absorbance increase evoked in SI by bilateral flutter was smaller than the response to contralateral flutter. The data were evaluated statistically to determine if the average (across-subject) SI response evoked by bilateral stimulation differed significantly from the corresponding response to contralateral stimulation (i.e., if the across-subject bilateral/contralateral response ratio

was <1 at 5 sec after stimulus onset). Analysis of variance showed that the average across-subject bilateral/contralateral SI response ratio was between 0.55 and 0.80 ($p < 0.001$; H_o was that the ratio = 1).

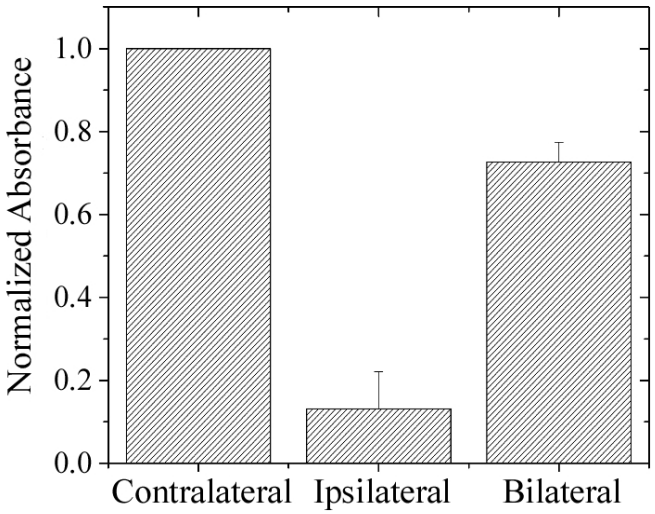

Figure 2. Barplot showing average across-subject (n=5) absorbance change (increase; normalized) in SI hand region. Measurements obtained at 5sec after stimulus onset. Note that although all 3 stimulus conditions (contralateral, ipsilateral and bilateral) evoked an absorbance increase, the response under the bilateral stimulus condition is ~35% less than that evoked by contralateral-only stimulation.

Figure 3 compares the responses evoked in SI of another subject by contralateral (Panel A) and bilateral (Panel B) stimulation. The image (color map) in Panel C was generated by computing the difference between the average difference images obtained under the 2 conditions (i.e., by subtracting the contralateral image from the bilateral image). Panel C reveals that in this subject a region located centrally within the imaged region in SI responded more vigorously to contralateral stimulation than to bilateral stimulation (indicated by red pixels) and, in contrast, the region surrounding the vigorously responding central region responded more vigorously to bilateral than to

contralateral skin flutter (indicated by blue pixels). This center-surround relationship between the territories that responded differentially to contralateral *vs.* bilateral flutter stimulation also is demonstrated by the distance *vs.* difference in absorbance plot (Panel D) obtained by radial histogram analysis of the color map in Panel C. The origin of the X-axis (distance=0) of the plot in Panel D corresponds to the center of the response evoked by contralateral stimulation in Panel A (point at center of the circle in Panel C). Accordingly, the plot in Panel D shows that the difference between the absorbance increases detected at the same location in the imaged field under the 2 stimulus conditions (bilateral minus contralateral; $D_{ABSORBANCE}$) varies systematically with increasing radial distance (in mm) from the center of the ROI. In other words, $D_{ABSORBANCE}$ is negative (the response to contralateral stimulation > the response to bilateral stimulation) at distances < 2.5 mm from the center of the ROI, but is positive (the response to contralateral stimulation < the response to bilateral stimulation) in regions located >2.5mm from the center of the ROI).

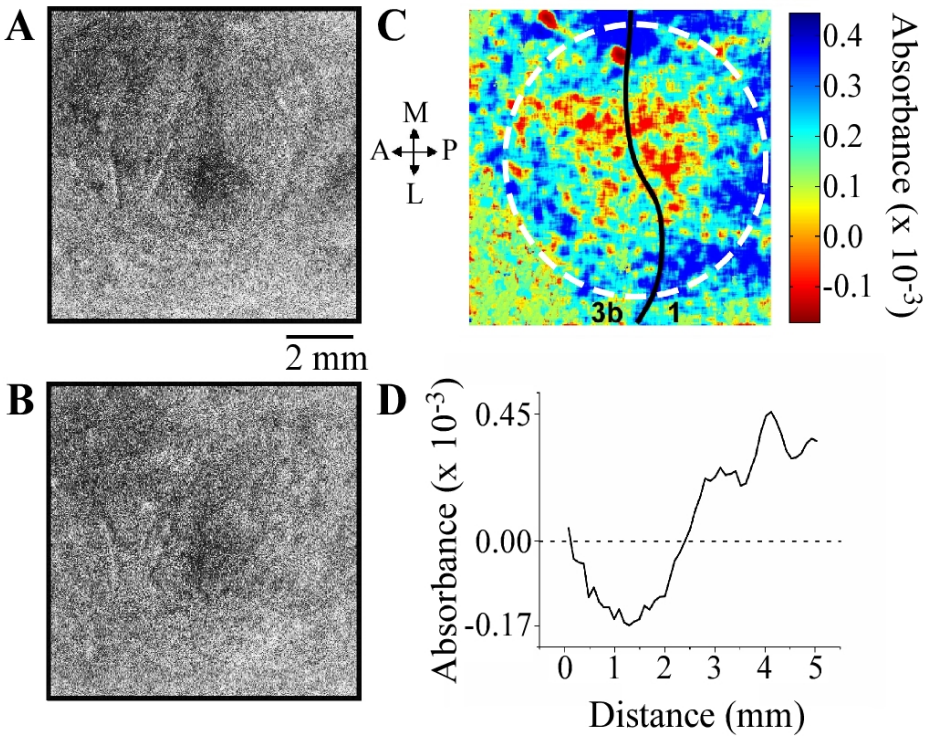

Figure 3. Comparison of SI hand region responses to contralateral vs. bilateral stimulation of the thenar eminence. **A.** Contralateral response to skin flutter. **B.** Response to the flutter stimulus applied bilaterally. **C.** Color map showing $D_{ABSORBANCE}$ values obtaining by subtracting image A from image B. Red pixels show central region (region in vicinity of point 0) where response evoked by contralateral-only stimulation exceeded the response to bilateral stimulation; blue pixels identify a surrounding region in which response to bilateral flutter exceeded the response to contralateral flutter. **D.** Result of radial histogram analysis of color map in Panel C. Distance=0mm is the origin of the plot (i.e., the central point in the circular region in image C- identified by dotted white line). $D_{ABSORBANCE}$ values less than 0 (negative) indicate that the response at that location during contra-only stimulation was greater than the response measured at that same location during bilateral stimulation; similarly, $D_{ABSORBANCE}$ values greater than 0 (positive) indicate that at that location the response evoked by bilateral stimulation exceeded the response to contralateral stimulation.

Figure 4 shows average across-subject (n=5) distance *vs.* $D_{ABSORBANCE}$ plot obtained by radial histogram analysis of the responses of each of the 5 subjects to contralateral vs. bilateral skin flutter stimulation. Clearly, Figure 4 confirms that the SI hand region generates a different response to bilateral stimulation than it does to contralateral

stimulation. In particular: (1) in the "center" region that extends ~1 mm from the center of the region that responds maximally to contralateral flutter, the response to bilateral flutter is less than that evoked by contralateral flutter, and (2) at distances between 2.0 and at least 5.0 mm from the center of the ROI ("the surround") the response to bilateral flutter exceeds the response to contralateral flutter.

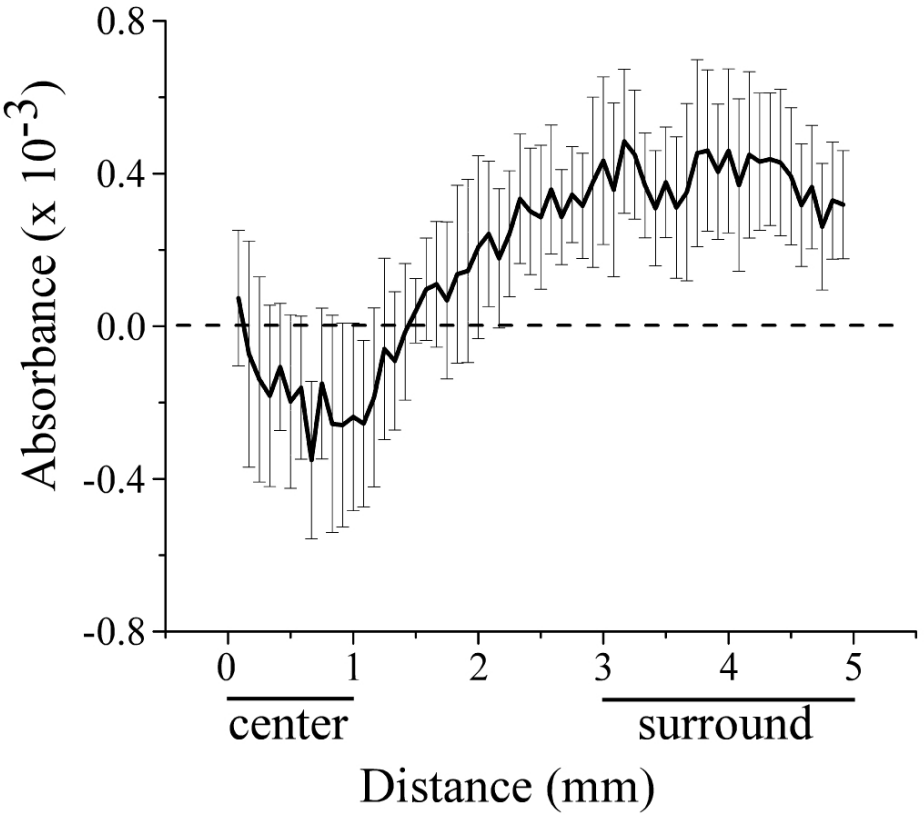

Figure 4. Average across-subject (n=5) $D_{ABSORBANCE}$ vs. distance plot generated using radial histogram analysis. Note that across-subject average $D_{ABSORBANCE}$ values in the vicinity of the center of the ROI are negative, indicating that in this region the response to stimulation of the contralateral thenar was greater than the response to bilateral thenar stimulation. In contrast, positive $D_{ABSORBANCE}$ values were obtained in the surrounding territory (the "surround" occupies the region located at radial distances between 3 and 5 mm from point 0). Horizontal bars below abscissa indicate locations of regions within the ROI identified as "center" vs. "surround".

Figure 5 compares the average across-subject responses (normalized absorbance changes) evoked by contralateral vs. bilateral flutter stimulation in the above-defined "center" *vs.* "surround" areas within the ROI in all 5 subjects. Although both the center and surround regions responded to ipsilateral flutter with a relatively weak absorbance increase, the response of the same regions to contralateral flutter was very different. In fact, the average across-subject response evoked in the surround region by contralateral flutter was a decrease in absorbance (the OIS sign of stimulus-evoked neuronal inhibition; Simons *et al*., 2005). In contrast, under both the bilateral and ipsilateral stimulus conditions absorbance increased in the surround region, although the increase was smaller under the ipsilateral condition. Statistical analysis revealed that the responses of the center and surround regions were significantly different for the contralateral ($p<0.001$; t-test) and bilateral ($p=0.078$) conditions. The responses in the center and surround of the ROI that were evoked by ipsilateral stimulation were not significantly different ($p=0.634$). However, the response evoked in the surround by the contralateral stimulus was significantly different from that evoked by bilateral stimulation ($p=0.001$).

To examine the spatial distribution of the modulatory effect of ipsilateral stimulation on the response of SI to simultaneous stimulation of the contralateral thenar we evaluated the central 2 x 2 mm boxel of the SI region that responded maximally to contralateral stimulation at higher resolution. The images in Figure 6 show the absorbance patterns evoked in this 2 x 2 mm region in 2 subjects by contralateral flutter stimulation (image pair in left column) and by simultaneous stimulation of both thenar sites (image pair in 2nd column from left). The highlighted (red) areas in each image in the 3rd column from the left indicate the sectors within this 2 x 2 mm region that were maximally activated

(sectors involving the upper 10% of the activated pixels are shown in red) under the contralateral stimulus condition. The plots in the 2nd column from the right reveal that for each subject the average time course of the absorbance change (increase) within the maximally driven region is virtually identical under the two stimulus conditions. In striking contrast, the plots in the right column show that the two stimulus conditions evoke very different absorbance changes in the territory outside the region that responds maximally to contralateral stimulation. Clearly, therefore, the latter plots reveal that differences in SI activation that occur under the contralateral and bilateral stimulus conditions occur primarily in the SI region non-maximally activated by flutter stimulation of the contralateral thenar. Across all subjects (n=5), the percent decrease change between the contralateral and bilateral conditions in the maximally driven region of SI was 2.5 ± 1% (ns), whereas the percent decrease observed in the non-maximally activated region was 41 ± 6% ($p<0.005$).

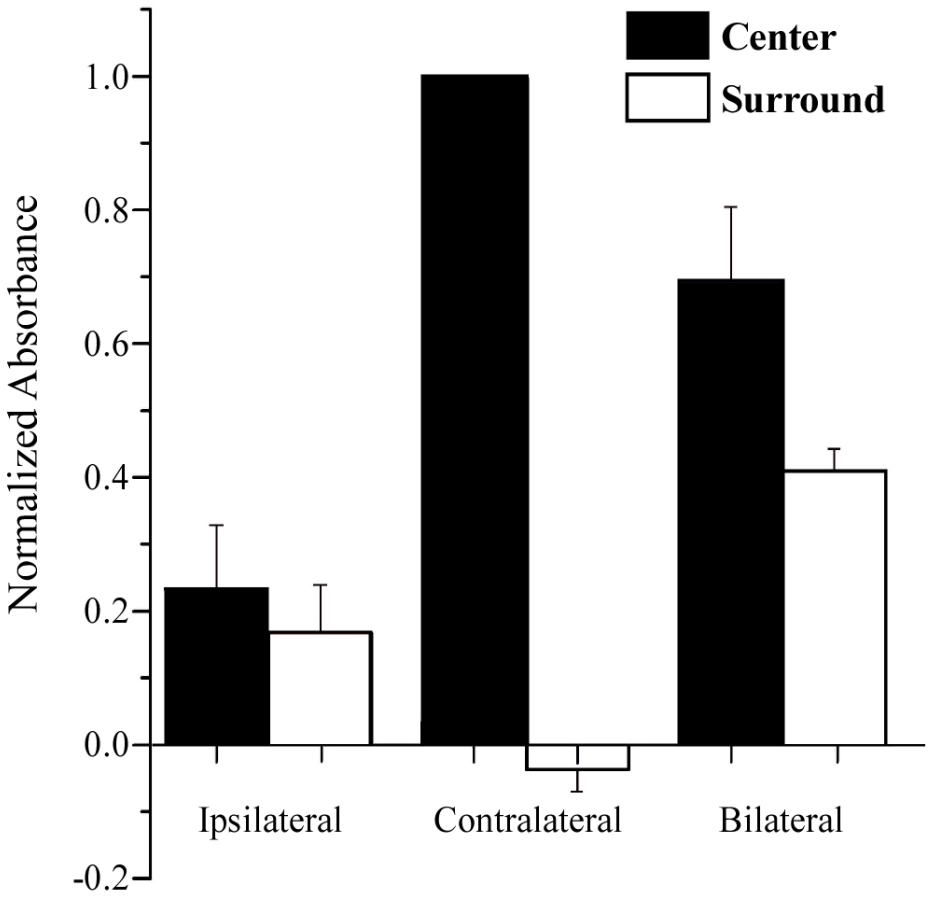

Figure 5. Bargraph showing average across-subject results (n=5). Filled bars indicate average across-subject absorbance values (normalized) for each stimulus condition measured within the maximally responding central region (radius = 1mm; cf. Figure 4) at 5 sec after stimulus onset. A positive value of normalized absorbance indicates that absorbance increased above that measured in the same region in the absence of stimulation. Note that response to bilateral flutter is approximately 30% less than the response to contralateral flutter. Open bars indicate average across-subject absorbance values obtained under the same conditions, but within the surround (defined in Figure 4). Under one condition (contralateral stimulation) average across-subject absorbance in the surround decreased below that measured in the absence of stimulation. The difference between the responses evoked in the center and surround for the ipsilateral condition is not statistically significant.

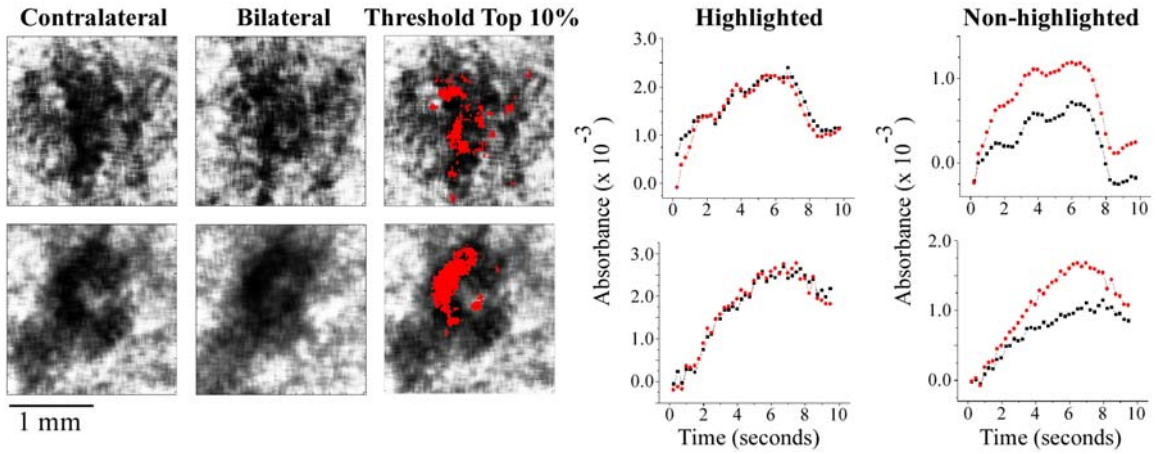

Figure 6. Within-ROI analysis for 2 subjects. Images in each row show the OIS response in the central 2 x 2 mm for one subject. Region maximally activated by contralateral stimulation (threshold set at maximal 10% of absorbance values) is indicated with red overlay. Plots in 2 columns on right: absorbance vs. time plots for highlighted region (red pixels) and non-highlighted region (all non-red pixels) in the 2x2mm ROI. Note that in the highlighted region similar absorbance values were obtained under the two stimulus conditions (plots in 2nd column from right), but in the non-highlighted region the response evoked by bilateral stimulation is, at all but the earliest times after stimulus onset, less than the response to contralateral flutter.

To obtain information about the specificity of the modulatory effect of ipsilateral input on the SI response to contralateral stimulation, we investigated in one subject the effect of changing the location of the ipsilateral stimulus. This subject's data showed that when the ipsilateral component of the bilateral stimulus was shifted to the tip of digit 2 (the contralateral stimulus was delivered to the thenar) a response reduction occurred that was indistinguishable from that observed when mirror-symmetric sites on the thenar were stimulated simultaneously. However, when the ipsilateral stimulus was shifted to the medial pad on the foot (as before, the contralateral stimulus was delivered to the thenar eminence on the hand), the response evoked within the SI hand region by simultaneous bilateral flutter did not differ significantly from that evoked by flutter stimulation applied independently to the contralateral thenar.

Discussion

It is established that a non-noxious mechanical skin stimulus activates via a short-latency, high-security neural transmission path, neurons in the middle layers of SI in the contralateral hemisphere (Mountcastle, 1984). Furthermore, much of the current literature reflects the long-held idea that gentle mechanical stimulation of the skin of the hand either has either no or, at most, a negligible influence on neurons in areas 3b and 1 of the SI hand representational region in the ipsilateral hemisphere.

The findings reported in this study are incompatible with the widely accepted idea that areas 3b and 1 in the SI hand region are insensitive to mechanical events on the ipsilateral hand. First, they provide unambiguous evidence that a skin flutter stimulus to the ipsilateral thenar eminence of the squirrel monkey evokes a statistically significant optical response (OIS; an absorbance increase) within the same SI territory that in prior combined OIS-neurophysiological studies (Shoham and Grinvald, 2001; Whitsel *et al*., 2001; Tommerdahl *et al*., 2002; Whitsel *et al*., 2003) was shown to undergo increased single neuron spike discharge activity in response to flutter stimulation of the contralateral hand. Second, our experiments demonstrate that simultaneous bilateral stimulation of both the ipsilateral and contralateral hand sites evokes an SI response significantly smaller and spatially less coherent than the response evoked in the same SI region by stimulation of only a site on the contralateral hand – a finding that strongly suggests that input from the ipsilateral hand can modify the ability of SI to process information about the status of mechanoreceptors in the skin of the contralateral hand.

The above-described modulatory effect of ipsilateral input on the SI response to stimulation of the contralateral hand, together with (1) reports by others of neurons with

ipsilateral receptive fields in SI of non-human primates (see Iwamura *et al*., 2002 for review), (2) demonstrations of short-latency activation of human SI in response to electrical stimulation of the ipsilateral median nerve (Allison *et al*., 1989a; Allison *et al*., 1989b; Allison *et al*., 1992; Korvenoja *et al*., 1995; Nihashi *et al*., 2005), and (3) the recent discovery that unilaterally applied flutter stimulation of the hand evokes short-latency neuromagnetic activity in both the contralateral and ipsilateral SI of conscious humans (Tan *et al*., 2004) demonstrates not only that the SI hand representational region receives substantial ipsilateral input but, in addition, shows that ipsilateral input evoked by gentle mechanical skin stimulation can alter the SI response to contralateral flutter stimulation.

Insofar as the perceptual meaning of our finding that ipsilateral input alters the SI hand region's optical response to skin flutter is concerned, observations reported in published human psychophysical studies are highly suggestive – those observations clearly indicate that input from a skin region on one hand can significantly alter one's perception of a tactile stimulus to the opposite hand. Importantly, while some of the published psychophysical findings indicate that concurrent input from mirror-symmetric sites on the two hands can enhance tactile perceptual performance above that obtained with unilateral stimulation, other studies indicate that tactile input from the two hands can lead to perceptual performance inferior to that observed when the stimulus is applied unilaterally. As examples of the former, (i) Lappin and Foulke (1973) observed that when a subject scans the pattern using two fingers on opposite hands, braille cell perception improves over that achieved unilaterally; (ii) Craig (1985) reported that a subject's ability to correctly identify a split tactile pattern (dot array) is substantially greater when the two

halves of the pattern are presented simultaneously to two fingers on opposite hands (relative to the performance achieved when the two halves are delivered to two fingers - neighboring or non-neighboring - on the same hand); and (iii) Essick and Whitsel found that human subjects' accuracy of perceived direction of tactile motion on the hands improves greatly over that obtained with unilateral stimulation when the bilateral stimuli (the sites on the 2 hands were mirror-symmetric) move across the 2 sites at the same time, in the same direction, and at the same velocity. Essick and Whitsel also reported that whenever the physical properties of the brushing stimulus applied to one hand differed in some way (e.g., in direction, velocity, relative timing) from those of the stimulus to the opposite hand, the subject's ability to accurately report direction of bilaterally applied stimulus motion declined, often reaching performance levels well below those achieved when each moving stimulus was applied unilaterally (Essick and Whitsel, 1988). Furthermore, a recent human psychophysical study found that vibrotactile stimulation of an unattended hand reduces tactile spatial acuity (as measured using a 2-point discrimination paradigm) on the attended hand by as much as 35% (Tannan *et al*., 2005). That same study also found that two-point discrimination improves substantially when a small-amplitude high-frequency vibration is superimposed on both of the probes used to present the two-point stimulus, but worsens during the delivery of high-frequency stimulation of the mirror-symmetric site on the opposite hand. Taken together, these observations strongly suggest that multiple factors (e.g., positional, temporal, and modal correspondence between the two stimuli) may determine the sign and magnitude of the influence of input from one hand on how a stimulus to the other hand is perceived.

How does input that arises in the mechanoreceptors of the skin of the ipsilateral hand access the SI hand region? While the available evidence does not enable this question to be answered definitively, the observations obtained in multiple neuroanatomical tracing studies (for review see Jones, 1986) make it clear that the modulatory influence exerted on the SI hand representational region evoked by stimulation of the ipsilateral hand is not mediated directly via interhemispheric connections that cross the midline in the corpus callosum. Indeed, the fact that a distinguishing feature of the SI hand area is its *lack* of direct interhemispheric connections forces the conclusion that the modulatory influence on SI of ipsilateral hand stimulation detected in the present study is mediated by a 2-stage path: a route that initially involves the extensive interhemispheric (callosal) connections that directly link higher-level (integrative) areas in the two hemispheres, and subsequently involves intrahemispheric connections from those higher-level areas to the SI hand region in the same hemisphere. A recent study, using cats as subjects, made simultaneous observations of activity evoked in SI and SII under conditions of ipsilateral, contralateral, and bilateral mechanical skin stimulation very similar to those reported in this paper (Tommerdahl *et al*., 2005a; 2005b). The data obtained in that study indicated that while different regions of SII were activated under the different conditions of stimulation, there was significant correlation (both positive and negative) between the stimulus-evoked activities in SII and SI, and the sign of the correlation was stimulus-dependent. Thus, there is indirect evidence that SII, which receives extensive interhemispheric projections, may be the source of the modulatory influence that is exerted on SI during stimulation of the ipsilateral hand. The fact that the modulatory influence is only crudely somatotopic (i.e.,

the effect is evident even when the ipsilateral stimulus is delivered to a site in the general vicinity of the mirror-symmetric site – see Figure 5) is regarded as consistent with the suggestion that the influence derives from SII – because the receptive fields of SII neurons are large relative those of neurons in SI.

The evidence presented in this paper leads the authors to suggest that although the distal limb regions of SI are relatively acallosal, this should not (as is frequently done) be interpreted to indicate that these SI regions are free of influences arising from the ipsilateral body. The extraordinary ability of primates to use the two hands cooperatively to explore and discriminate the features of tactile objects shows not only that fusion of sensory input from both hands occurs within the CNS, but that it underlies essential behaviors. With this in mind, therefore, the absence of direct callosal connections should not be viewed to indicate that an SI region does not receive significant influences from the ipsilateral body. Instead, absence of callosal connections in the distal limb regions of SI may be a reflection of (1) the extraordinary flexibility/mobility of the primate hands (i.e., the ability to substantially alter the positional relationships between distal forelimb skin regions in the accomplishment of tactile object exploration and feature extraction – in contrast, the positional relationship between skin regions on opposite sides of the midline at the level of the proximal limbs/trunk is relatively fixed), and (2) the need for the participation of higher-level cortical areas in fusing the elaborate time-, position-, and modality-dependent somatosensory experiences gained via bimanual tactile exploration.

Future direction of research

When a single vibrotactile stimulus is applied to the skin with a certain amplitude and frequency, the cortex has neurons that will: 1) maximally respond to that stimulus, 2) respond to any stimulus, or 3) be suppressed. It has already been shown in chapter 4 that if the stimulus is applied long enough, the cortex associates that stimulus with a certain evoked spatial pattern that allows the cortex to distinguish that stimulus from another. Neurons that also share common RFs will be activated together, evoking a similar macrocolumnar pattern, and differing only in its evoked minicolumnar pattern.

The extension of the current research will be to assess the impact of multi-site, multi-modal vibrotactile stimuli on cortico-cortico interactions. The initial step would be to include a second stimulus, and see how varying the magnitude, stimulus position, stimulus order, and frequency of the second stimulus would alter the evoked minicolumnar pattern of the first stimulus, and vice versa. For example, if both stimuli were perceived to constantly be of equal magnitude, applied at the same time, and were separated only by 6mm on the skin, by changing the stimulus frequency of the second stimulus, possible outcomes are 1) the resulting evoked minicolumnar patterns of both ROIs will resemble an evoked spatial pattern of a stimulus frequency that was somewhere in between both stimuli, 2) the evoked minicolumnar pattern of the stimulus with the lower frequency will be more influenced by the stimulus with a higher frequency resulting in an evoked minicolumnar pattern that resembles one evoked by a

stimulus of a higher frequency, or 3) no change in the evoked minicolumnar patterns, and the patterns at each ROI resemble those evoked by single stimulus.

There are many questions that have yet to be studied about how the cortex is able to extract features from a stimulus. It is first important to learn and understand the basic science of how the brain "discriminates" in the somatosensory cortex, as well as in vision and audition. How does the cortex process the information for each of the senses, and how are they processed similarly or differently? The gained knowledge and understanding can then be built upon, and the goal is to determine how the cortex, as a whole, integrates the information obtained from all the senses.

References

Abbott L, Nelson S (2000) Synaptic plasticity: taming the beast. Nature Neuroscience 3:1178-1183.

Abeles M, Goldstein MH Jr (1970) Functional architecture in cat primary auditory cortex: columnar organization and organization according to depth. Journal of Neurophysiology 33:172-187.

Adorjan P, Schwabe L, Wenning G, Obermayer K (2002) Rapid adaptation to internal states as a coding strategy in visual cortex. NeuroReport 13:337-342.

Albus K (1975) A quantitative study of the projection area of the central and the paracentral visual field in area 17 of the cat, I: the spatial organization of the orientation domain. Experimental Brain research 24:181-202.

Allison T, McCarthy G, Wood C (1992) The relationship between human long-latency somatosensory evoked potentials recorded from the cortical surface and from the scalp. EEG Clinical Neurophysiology 84:301-314.

Allison T, McCarthy G, Wood C, Darcey T, Spencer D, Williamson P (1989a) Human cortical potentials evoked by stimulation of the median nerve. Journal of Neurophysiology 62:694-710.

Allison T, McCarthy G, Wood C, Williamson P, Spencer D (1989b) Human cortical potentials evoked by stimulation of the median nerve. II. Cytoarchitectonic areas generating long-latency activity. Journal of Neurophysiology 62:711-722.

Ba A, Guiou M, Pouratian N, Muthialu A, Rex D, Cannestra A, Chen J, Toga A (2002) Multiwavelength optical intrinsic signal imaging of cortical spreading depression. Journal of Neurophysiology Nov; 88:2726-2735.

Barlow H (1990) A theory about the functional role and synaptic mechanism of visual after-effects. In: Vision: Coding and Efficiency (Blakemore C, ed). Cambridge, UK: Cambridge University Press.

Bonhoeffer T, Grinvald A (1996) Optical imaging based on intrinsic signals: The methodology. In: Brain Mapping: The Methods (Toga AW, Mazziotia JC, eds), pp 55-97. New York.

Braun C, Hess H, Burkhardt M, Wuhle A, Preissl H (2005) The right hand knows what the left hand is feeling. Experimental Brain Research 366-373.

Bruno R, Khatri V, Land P, Simons D (2003) Thalamocortical angular tuning domains within individual barrels of rat somatosensory cortex. Journal of Neuroscience Oct; 23:9565-9574.

Burdett N, Menon D, Carpenter T, Jones J, Hall L (1995) Visualization of changes in regional cerebral blood flow (rCBF) produced by ketamine using long TE gradient-echo sequences: Preliminary results. Magnetic Resonance Imaging 13:549-553.

Burton H, Fabri M (1995) Ipsilateral intracortical connections of physiologically defined cutaneous representations in areas 3b and 1 of macaque monkeys: projections in the vicinity of the central sulcus. Journal of Comparative Neurology May; 355:508-538.

Buxhoeveden D, Switala A, Roy E, Casanova M (2000) Quantitative analysis of cell columns in the cerebral cortex. Journal of Neuroscience Methods Apr; 97:7-17.

Castro-Alamancos M (2004) Absence of Rapid Sensory Adaptation during Information Processing States. Neuron 41:455-464.

Chen LM, Friedman RM, Roe WA (2003) Optical imaging of a tactile illusion in area 3b of the primary somatosensory cortex. Science Oct 31; 302:881-885.

Chen LM, Friedman RM, Ramsden B, LaMotte R, Roe AW (2001) Fine-scale organization of SI (Area 3b) in the squirrel monkey revealed with intrinsic optical imaging. Journal of Neurophysiology Dec; 86:3011-3029.

Chiu JS, Tommerdahl M, Whitsel BL (2005) Stimulus-dependent spatial patterns of response in SI cortex. BMC Neuroscience Jul 19; 6:47.

Chubbuck J (1966) Small-motion biological stimulator. APL Technical Digest May-Jun:18-23.

Cohen L (1973) Changes in neuron structure during action potential propagation and synaptic transmission. Physiologcal Reviews Apr; 53:373-418.

Craig J (1985) Attending to two fingers: Two hands are better than one. Perception and Psychophysics 38:496-511.

Craig J, Qian X (1997) Tactile pattern perception by two fingers: Temporal interference and response competition. Perception & Psychophysics 59:252-265.

DeFelipe J, Farinas I (1992) The pyramidal neuron of the cerebral cortex: morphological and chemical characteristics of the synaptic inputs. Progress in Neurobiology 39:563-607.

DeFelipe J, Hendry MC, Jones EG (1989) Synapses of double bouquet cells in monkey cerebral cortex visualized by calbindin immunoreactivity. Brain Research 503:49-54.

Delemos K, Hollins M (1996) Adaptation-induced enhancement of vibrotactile amplitude discrimination: the role of adapting frequency. The Journal of the Acoustical Society of America Jan; 99:508-516.

Diamond M, Favorov O, Tommerdahl M, Kelly D, Whitsel B (1986) Organization of somatic sensory cortex: the detection of discrete topographic units and evidence for their integrative function. University of North Carolina, Chapel Hill Dissertation.

Doetsch G (2000) Patterns in the brain. Neuronal population coding in the somatosensory system. Physiol Behav 69:187-201.

Dragoi V, Turcu C, Sur M (2001) Stability of cortical responses and the statistics of natural scenes. Neuron 32:1181-1192.

Ebner T, Chen G (1995) Use of voltage-sensitive dyes and optical recordings in the central nervous system. Progress in Neurobiology Aug; 46:463-506.

Edelman GM (1978) Group selection and phasic reentrant signaling: A theory of higher brain function. In: Edelman GM, Mountcastle VB. *The Mindful Brain: Cortical Organization and the Group-Selective Theory of Higher Brain Function.* Cambridge, MA: MIT press; pp51-100.

Essick G, Whitsel B (1988) The capacity of human subjects to process directional information provided at two skin sites. Somatosensory & Motor Research 6: 1-20.

Favorov O, Diamond M (1990) Demonstration of discrete place-defined columns--segregates--in the cat SI. Journal of Comparative Neurology Aug 1; 298:97-112.

Favorov OV, Kelly DG (1994a) Minicolumnar organization within somatosensory cortical segregates, I: development of afferent connections. Cerebral Cortex 4:408-427.

Favorov OV, Kelly DG (1994b) Minicolumnar organization within somatosensory cortical segregates, II: emergent functional properties. Cerebral Cortex 4:428-442.

Favorov O, Kelly DG (1996) Local receptive field diversity within cortical neuronal populations. In: Franzen O, Johansson R, Terenius L, eds. *Somesthesis and the Neurobiology of the Somatosensory Cortex.* Basel: Birkhauser-Verlag; pp 395-408.

Favorov O, Whitsel B (1988a) Spatial organization of the peripheral input to area 1 cell columns: I. The detection of "segregates". Brain Research Reviews Jan-Mar; 472:25-42.

Favorov O, Whitsel B (1988b) Spatial organization of the peripheral input to area 1 cell columns: II. the forelimb representation achieved by a mosaic of segregates. Brain Research Reviews Jan-Mar; 472:43-56.

Fujibayashi T, Sugiura M, Yanagimoto M, Harada J, Goto Y (1994) Brain energy metabolism and blood flow during sevoflurane and halothane anesthesia: effects of hypocapnia and blood pressure fluctuations. ACTA Anaesthesiologica Scandinavica May; 38:413-418.

Gescheider G, Frisina R, Verrillo R (1979) Selective adaptation of vibrotactile thresholds. Sensory Process Mar; 3:37-48.

Ghazanfar A, Krupa D, Nicolelis M (2001) Role of cortical feedback in the receptive field structure and nonlinear response properties of somatosensory thalamic neurons. Experimental Brain Research 141:88-100.

Goble A, Hollins M (1993) Vibrotactile adaptation enhances amplitude discrimination. The Journal of the Acoustical Society of America Jan; 93:418-424.

Grinvald A (1985) Real-time optical mapping of neuronal activity: from single growth cones to the intact mammalian brain. Annual Review of Neuroscience 1985:263-305.

Grinvald A, Frostig R, Lieke E, Hildescheim R (1988) Optical imaging of neuronal activity. Physiology Reviews Oct; 68:1285-1365.

Grinvald A, Bonhoeffer T, Malonek D, Shoham D, Bartfeld E, Arierli A, Hildesheim R, Ratzlaff E (1991) Optical imaging of architecture and function in the living brain. In: Memory Organization and Locus of Change (Squire L, Weinberger N, Lynch G, McGaugh J, eds), pp 49-85. N.Y., Oxford Univ. Press.

Grinvald A, Lieke E, Frostig R, Hildesheim R (1994) Cortical point-spread function and long-range lateral interactions revealed by real-time optical imaging of macaque monkey primary visual cortex. Journal of Neuroscience May; 14:2545-2568.

Grinvald A, Bonhoeffer T, Malonek D, Shoham D, Bartfeld E, Arierli A, Hildesheim R, Ratzlaff E (1991) Optical imaging of architecture and function in the living brain. In: Memory Organization and Locus of Change (Squire L, Weinberger N, Lynch G, McGaugh J, eds), pp 49-85. N.Y.: Oxford Univ. Press.

Grinvald A, Shoham D, Glaser I, Vanzetta A, Shyoterman E, Slovin H, Wijnbergen C, Hildescheim R AA (1999) In-Vivo optical imaging of cortical architecture

and dynamics. In: Modern Techniques in Neuroscience Research. (Windhorst U, Johansson H, eds), pp 893-969. New York: Springer.

Haglund M, Ojemann G, Hochman D (1992) Optical imaging of epileptiform and functional activity in human cerebral cortex. Nature Aug; 358:668-671.

Harris J, Harris I, Diamond M. (2001) The topography of tactile learning in humans. Journal of Neuroscience 21:1056-1061.

Hess A, Stiller D, Kaulisch T, Heil P, Scheich H (2000) New insights into the hemodynamic blood oxygenation level-dependent response through combination of functional magnetic resonance imaging and optical recording in gerbil barrel cortex. Journal of Neuroscience May; 20:3328-3338.

Hlushchuk, Y, and Hari, R. (2006) Transient suppression of ipsilateral SI cortex during tactile finger stimulation. Journal of Neuroscience May 24; 26(21): 5819-24.

Hollins M, Goble A, Whitsel B, Tommerdahl M (1990) Time course and action spectrum of vibrotactile adaptation. Somatosensory Motor Research 7:205-221.

Hubel DH, Wiesel TN (1974) Sequence regularity and geometry of orientation columns in the monkey striate cortex. Journal of Computational Neurology 158: 267-294.

Iwamura, Y, Taoka, M, and Atsushi, I. (2001) Bilateral activity and callosal connections in the somatosensory cortex. The Neuroscientist 7: 419-429.

Iwamura Y, Tanaka M, Iriki A, Taoka M, Toda T (2002) Processing of tactile and kinesthetic signals from bilateral sides of the body in the postcentral gyrus of awake monkeys. Behavioral Brain Research 135:185-190.

Jones EG (1975) Varieties and distribution of non-pyramidal cells in the somatic sensory cortex of the squirrel monkey. Journal of Computational Neurology 160:205-267.

Jones E (1986) Connectivity of the Primate Sensory-Motor Cortex. In: Cerebral Cortex: Sensory-Motor Areas and Aspects of Cortical Connectivity (Jones E, Peters A, eds). New York: Plenum Press.

Jones E, Porter R (1980) What is area 3a? Brain Research May: 1-43.

Jones E (2000) Cortical and subcortical contributions to activity-dependent plasticity in primate somatosensory cortex. Annual Reviews in Neuroscience 2000; 23:1-37.

Juliano S, Whitsel B (1987) A combined 2-deoxyglucose and neurophysiological study of primate somatosensory cortex. Journal of Comparative Neurology Sep; 263:4514-4525.

Kohn A, Movshon J (2004) Adaptation changes the direction tuning of macaque MT neurons. Nature Neuroscience Jul; 7:764-772.

Kohn A, Pinheiro A, Tommerdahl M, Whitsel B (1997) Optical imaging in vitro provides evidence for the minicolumnar nature of cortical response. Neuroreport Nov; 8:3513-3518.

Korvenoja A, Wikstrom H, Huttunen J, Virtanan J, Laine P, Aronen HJ, Seppalainen AM, Ilmoniemi RJ (1995) Activation of ipsilateral primary sensorimotor cortex by median nerve stimulation. Neuroreport 6: 2589-2593.

Lappin J, Foulke E (1973) Expanding the tactual field of view. Perception & Psychophysics 14:237-241.

Laughlin S, R dRvS, Anderson J (1998) The metabolic cost of neural information. Nature of Neuroscience May; 1:36-41.

Lieke E, Frostig R, Arieli A, Ts'o D, Hildesheim R, Grinvald A (1989) Optical imaging of cortical activity: real-time imaging using extrinsic dye-signals and high resolution imaging based on slow intrinsic signals. Annual Review of Physiology 51:543-559.

Lipton ML, Fu, K-M, Branch, CA, and Schroeder, CE. (2006) Ipsilateral hand input to area 3b revealed by converging hemodynamic and electrophysiological analyses in macaque monkeys. Journal of Neuroscience 26: 180-185.

Lu Z-L, Williamson S, Kaufman L (1992) Behavioral lifetime of human auditory sensory memory predicted by physiological measures. Science Dec; 258:1668-1670.

Lund JS (1984) Spiny stellate neurons. In: Jones EG, ed. Cellular Components of the Cerebral Cortex. New York: Plenum press; pp 255-308. Cerebral Cortex, vol 1.

MacVicar B, Hochman D (1991) Imaging of synaptically evoked intrinsic optical signals in hippocampal slices. Journal of Neuroscience May; 11:1458-1469.

McCasland JS, Woolsey TA (1988) High-resolution 2-deoxyglucose mapping of functional cortical columns in mouse barrel cortex. Journal of Comparative Neurology 278:555-569.

Merzenich MM, Sur M, Nelson RJ, Kaas JH (1981) Organization of the SI cortex: multiple cutaneous representations in areas 3b and 1 of the owl moneky. In: Woolsey CN, Ed. Cortical Sensory Organization, vol 1. Clifton, NJ: Humana Press; pp 47-66.

Metherate R, Tremblay N, Dykes R (1988a) The effects of acetylcholine on response properties of cat somatosensory cortical neurons. Journal of Neurophysiology Apr; 59:1231-1252.

Metherate R, Tremblay N, Dykes R (1988b) Transient and prolonged effects of acetylcholine on responsiveness of cat somatosensory cortical neurons. Journal of Neurophysiology Apr; 59:1253-1276.

Meyer E, Otero D (1985) Pharmacological and ionic characterizations of the muscarinic receptors modulating H3acetylcholine release from rat cortical synaptosomes. Journal of Neuroscience May; 5:1202-1207.

Montague PR, Gally JA, Elelman GM (1991) Spatial signaling in the development and function of neural connections. Cerebral Cortex 1:199-200.

Moore C (2004) Frequency-dependent processing in the vibrissa sensory system. Journal of Neurophysiology 91:2390-2399. Review.

Moore C, Nelson S, Sur M (1999) Dynamics of neuronal processing in rat somatosensory cortex. Trends in Neuroscience 22.

Mountcastle V (1978) An organizing principle of cerebral function: the unit module and the distributed system. In: The Mindful Brain (Mountcastle VB, Edelman GM, eds). Cambridge: MIT Press.

Mountcastle V (1984) Mechanoreceptive sensibility. In: Handbook of Physiology (Darian-Smith, ed). Bethesda, MD: American Physiological Society.

Mountcastle V (1988) Dynamic neuronal operations within the somatic sensory cortex. In: Neurobiology of Neocortex (Rakic P, Singer W, eds), pp 253-267. New York: Wiley.

Muller J, Metha A, Krauskopf J, Lennie P (1999) Rapid adaptation in visual cortex to the structure of images. Science Aug; 285:1405-1408.

Nihashi T, Naganawa S, Sato C, Kawai H, Nakamura T, Fukatsu H, Ishigaki T, Aoki I (2005) Contralateral and ipsilateral responses in primary somatosensory cortex following electrical median nerve stimulation - an fMRI study. Journal of Neurophysiology 116:842-848.

Pal PK, Hanajima, R, Gunraj, CA, Li, J-Y, Wagle-Shukla, A, Morgante, F, and Chen, R. (2005) Effect of low-frequency repetitive transcranial magnetic stimulation on interhemispheric inhibition. Journal of Neurophysiology 94: 1668-1675.

Pearson JC, Finkel LM, Edelman GM (1987) Plasticity in the organization of adult cerebral cortical maps: a computer simulation based on neuronal group selection. Journal of Neuroscience 7:4209-4223.

Peters A, Yilmaz E (1993) Neuronal organization in area 17 o f cat visual cortex. Cerebral Cortex 3:49-68.

Pluto CP, Chiaia, NL, Rhodes, RW, and Lane, RD. (2005) Reducing contralateral SI activity reveals hindlimb receptive fields in the SI forelimb-stump representation of neonatally amputated rats. Journal of Neurophysiology 94:1727-1732.

Powell T, Mountcastle V (1959a) The cytoarchitecture of the postcentral gyrus of the monkey Macaca mulatta. Bull Johns Hopkins Hosp Sep: 108-131.

Powell T, Mountcastle V (1959b) Some aspects of the functional organization of the cortex of the postcentral gyrus of the monkey: a correlation of findings obtained in a single unit analysis with cytoarchitecture. Bulletin of the Johns Hopkins Hospital Sep; 105:133-162.

Rakic P (1988) Specification of cerebral cortical areas. Science 241:170-176.

Rausell E, Bickford L, Manger P, Woods T, Jones E (1998) Extensive divergence and convergence in the thalamocortical projection to monkey somatosensory cortex. Journal of Neuroscience Jun; 18:4216-4232.

Schnitzler A, Salmelin R, Salenius S, Jousmaki V, Hari R (1995) Tactile information from the human hand reaches the ipsilateral primary somatosensory cortex. Neuroscience Letters 200:25-28.

Schuett S, Bonhoeffoer T, Hubener M (2001) Pairing-induced changes of orientation maps in cat visual cortex. Neuron 32: 325-337.

Schwindt P, Spain W, Foehring R, Chubb M, Crill W (1988b) Slow conductances in neurons from cat sensorimotor cortex in vitro and their role in conductances in neurons from cat sensorimotor cortex in vitro and their role in slow excitability changes. Journal of Neurophysiology Feb; 59:450-467.

Senft SL, Woolsey TA (1991) mouse barrel cortex viewed as Dirichlet domains. Cerebral Cortex 1:348-363.

Sheth B, Moore C, Sur M (1998) Temporal modulation of spatial borders in rat barrel cortex. Journal of Neurophysiology Jan; 79:464-470.

Shmuel A, Grinvald A (1996) Functional organization for direction of motion and its relationship to orientation maps in cat area 18. Journal of Neuroscience Nov; 16:6945-6964.

Shoham D, Grinvald A (2001) The cortical representation of the hand in macaque and human area s-i: high resolution optical imaging. Journal of Neuroscience Sep 1; 21:6820-6825.

Simons S, Tannan V, Chiu J, Favorov O, Whitsel B, Tommerdahl M (2005) Amplitude-dependency of response of SI cortex to vibrotactile stimulation. BMC Neuroscience 6(1):43.

Sretavan D, Dykes R (1983) The organization of two cutaneous submodalities in the forearm region of area 3b of cat somatosensory cortex. Journal of Comparative Neurology Feb; 213:381-398.

Staines WR, Graham SJ, Black SE, McIlroy WE (2002) Task-relevant modulation of contralateral and ipsilateral primary somatosensory cortex and the role of a prefrontal-cortical sensory gating system. NeuroImage 15:190-199.

Sur M, Wall J, Kaas J (1984) Modular distribution of neurons with slowly adapting and rapidly adapting responses in area 3b of somatosensory cortex in monkeys. Journal of Neurophysiology Apr; 51:724-744.

Sur M, Schummers J, Dragoi V (2002) Cortical plasticity: time for a change. Curr Biol 12:168-170. Review.

Tan H, Wuhle A, Braun C (2004) Unilaterally applied stimuli in a frequency discrimination task are represented bilaterally in primary somatosensory cortex. Neurol Clin Neurophysiol 83.

Tannan V, Dennis R, Tommerdahl M (2005) Stimulus-dependent changes in spatial acuity. Behavioral and Brain Functions Oct 10.

Tommerdahl, M, Chiu, J, Whitsel, BL, and Favorov, OV (2005) Minicolumnar patterns in the global cortical response to sensory stimulation. In: Neocortical modularity and the cell minicolumn (Casanova, M. F., ed.), Ch 8. Nova Scientific Publishers.

Tommerdahl M, Whitsel B, Cox E, Diamond M, Kelly D (1987) Analysis of the periodicities in somatosensory cortical activity patterns. Society for Neuroscience Abstracts 13:470.

Tommerdahl M (1989) Stimulus evoked activity patterns in somatosensory cortex: evidence for an opponent mechanism. The University of North Carolina at Chapel Hill Dissertation.

Tommerdahl M, Favorov O, Whitsel B, Nakhle B, Gonchar Y (1993) Minicolumnar activation patterns in cat and monkey SI cortex. Cerebral Cortex Sep-Oct; 3:399-411.

Tommerdahl M, Delemos K, Vierck CJ, Favorov O, Whitsel B (1996) Anterior parietal cortical response to tactile and skin-heating stimuli applied to the same skin site. Journal of Neurophysiology Jun; 75:2662-2670.

Tommerdahl M, Delemos K, Favorov O, Metz C, Whitsel B (1998) Response of anterior parietal cortex to different modes of same-site skin stimulation. Journal of Neurophysiology Dec; 80:3272-3283.

Tommerdahl M, Delemos KA, Whitsel BL, Favorov OV, Metz CB (1999a) Response of anterior parietal cortex to cutaneous flutter and vibration. Journal of Neurophysiology 82:16-33.

Tommerdahl M, Favorov O, Whitsel B (2002) Optical imaging of intrinsic signals in somatosensory cortex. Behavioral Brain Research Sep; 135:83-91.

Tommerdahl M, Favorov O, Chiu J, Whitsel B (2004) Optical intrinsic signal imaging of ipsilateral, contralateral, and bilateral forelimb inputs to cat SII. Society for Neuroscience abstracts 642.612.

Tommerdahl M, Simons SB, Chiu JS, Favorov OV, Whitsel BL (2006) Ipsilateral input modifies the SI response to contralateral skin flutter. Journal of Neuroscience May 31; 26(22):5970-5977.

Tommerdahl M, Whitsel BL, Favorov OV, Metz CB, O'Quinn BL (1999b) Responses of contralateral SI and SII in cat to same site cutaneous flutter versus vibration. Journal of Neurophysiology Oct: 1982-1992.

Verrillo R, Gescheider G (1977) Effect of prior stimulation on vibrotactile thresholds. Sensory Processes Aug; 1:292-300.

Wedell C, Cummings SJ (1938) Fatigue of the vibratory sense. Journal of Experimental Psychology: Animal Behavior Processes 22.

Whitsel B, Juliano S (1984) Imaging the responding neuronal population with 14C2DG: the somatosensory cerebral cortical signature of a tactile stimulus. In: Somatosensory Mechanisms (von Euler C, Franzen O, Lindblom U, Ottoson D, eds), pp 61-80. London: Macmillan.

Whitsel B, Kelly D (1988) Knowledge acquisition ("learning") by the somatosensory cortex. In: AAAS Selected Symposium (Davis JL, Newburgh RW, Wegman E, eds), pp 93-131. Boulder: Westview Press.

Whitsel B, Franzen O (1989) Dynamics of Information Processing in the Somatosensory Cortex. In: Brain and Reading (Euler C, Lundberg I, Lennerstrand G, eds), pp 129-137. London: Macmillan Press.

Whitsel B, Favorov O, Tommerdahl M, Diamond M, Juliano S, Kelly D (1989) Dynamic processes govern the somatosensory cortical response to natural stimulation. In: Sensory Processing in the Mammalian Brain (Lund JS, ed), pp 79-107. New York: Oxford Univ. Press.

Whitsel BL, Kelly EF, Xu M, Tommerdahl M, Quibrera M (2001) Frequency-dependent response of SI RA-class neurons to vibrotactile stimulation of the receptive field. Somatosensory and Motor Research: 263-285.

Whitsel BL, Kelly EF, Quibrera M, Tommerdahl M, Li Y, Favorov OV, Xu M, Metz CB (2003) Time-dependence of SI RA neuron response to cutaneous flutter stimulation. Somatosensory and Motor Research 20:45-69.

Woolsey T, Rovainen C, Cox S, Henegar M, Liang G, Moskalenko Y, Sui J, Wei L (1996) Neuronal units linked to microvascular modules in cerebral cortex: response elements for imaging the brain. Cerebral Cortex Sep-Oct; 6:647-660.

Xing J, Gerstein GL (1996) Networks with lateral connectivity, II: development of neuronal grouping and corresponding receptive field changes. Journal of Neurophysiology 75:200-216.